RUBENS JUNQUEIRA

HYDROLOGICAL BEHAVIOR AND DROUGHT ANALYSIS IN THE PANDEIROS RIVER BASIN, BRAZILIAN SAVANNA

LAVRAS-MG
2022

RUBENS JUNQUEIRA

HYDROLOGICAL BEHAVIOR AND DROUGHT ANALYSIS IN THE PANDEIROS RIVER BASIN, BRAZILIAN SAVANNA

Tese apresentada à Universidade Federal de Lavras, como parte das exigências do Programa de Pós-Graduação em Recursos Hídricos, área de concentração em Hidrologia, para a obtenção do título de Doutor.

Prof. Dr. Marcelo Ribeiro Viola
Orientador

LAVRAS-MG
2022

Ficha catalográfica elaborada pelo Sistema de Geração de Ficha Catalográfica da Biblioteca Universitária da UFLA, com dados informados pelo(a) próprio(a) autor(a).

Junqueira, Rubens.

Hydrological behavior and drought analysis in the Pandeiros river basin, Brazilian savanna / Rubens Junqueira. - 2022.

98 p.

Orientador(a): Marcelo Ribeiro Viola.

Tese (doutorado) - Universidade Federal de Lavras, 2022.

Bibliografia.

1. Modelagem hidrológica. 2. Retrospectiva hidrológica. 3. Seca histórica. I. Viola, Marcelo Ribeiro. II. Título.

RUBENS JUNQUEIRA

COMPORTAMENTO HIDROLÓGICO E ANÁLISE DE SECA NA BACIA HIDROGRÁFICA DO RIO PANDEIROS, SAVANA BRASILEIRA

HYDROLOGICAL BEHAVIOR AND DROUGHT ANALYSIS IN THE PANDEIROS RIVER BASIN, BRAZILIAN SAVANNA

Tese apresentada à Universidade Federal de Lavras, como parte das exigências do Programa de Pós-Graduação em Recursos Hídricos, área de concentração em Hidrologia, para a obtenção do título de Doutor.

APROVADA em 01 de abril de 2022
Dr. Carlos Rogério de Mello UFLA
Dr. Marcelo Vieira da Silva Filho UFLA
Dr. Donizete dos Reis Pereira UFV
Dr. Sly Wongchuig UGA

gov.br
Documento assinado digitalmente
MARCELO RIBEIRO VIOLA
Data: 25/04/2022 10:04:53-0300
Verifique em https://verificador.iti.br

Prof. Dr. Marcelo Ribeiro Viola
Orientador

LAVRAS-MG
2022

AGRADECIMENTOS

Em primeiro lugar, agradeço a Deus pela presença em todas as etapas da minha vida, me ajudando a vencer todos os obstáculos.

À minha família, pelo amor, incentivo e pelo amor incondicional em todos momentos, em especial para meus pais, cujo caráter definiu o tipo de pessoa que gostaria de ser.

Aos demais familiares, em especial aos meus avós, pelo amor e por todos os ensinamentos durante minha vida.

À minha noiva, Amanda, pelo amor e pelas palavras de carinho e incentivo durante todo o processo.

À Universidade Federal de Lavras (UFLA) e ao Programa de Pós-Graduação em Recursos Hídricos (PPGRH), pela formação acadêmica e desenvolvimento pessoal.

Ao meu orientador, Dr. Marcelo Ribeiro Viola, pelos ensinamentos, pela atenção e pela constante orientação durante todas as fases deste trabalho.

Aos membros da banca, Dr. Carlos Rogério de Mello, Dr. Marcelo Vieira da Silva Filho, Dr. Donizete dos Reis Pereira e Dr. Sly Wongchuig, pela disponibilidade e contribuição.

Aos colegas de pós-graduação, em especial André, Jhones, Jonas e Vanessa, pela amizade e os momentos de descontração.

A todos os funcionários e professores do PPGRH, que contribuíram de forma direta ou indireta para minha formação acadêmica.

À Coordenação de Aperfeiçoamento de Pessoal de Nível Superior (CAPES) pela concessão de bolsa de estudos (processo 88882.446869/2019-01), ao Conselho Nacional de Desenvolvimento Científico e Tecnológico (CNPq) pela concessão de bolsa produtividade em pesquisa ao orientador (processos 311191/2021-5 e 308947/2018-5) e ao projeto de pesquisa P&D ANEEL/CEMIG GT-611.

Muito obrigado!

RESUMO

Estudos hidrológicos são importantes para auxiliar a gestão de recursos hídricos em bacias hidrográficas, especialmente diante de eventos extremos, como as secas. No entanto, a disponibilidade de dados hidrometeorológicos observados no Brasil é baixa, o que dificulta o desenvolvimento de estudos hidrológicos consistentes. Diante disso, objetivou-se por meio deste trabalho: i) analisar as características e propagação da seca meteorológica para hidrológica e sua influência sobre o comportamento hidrológico na bacia hidrográfica do rio Pandeiros (BHRP), localizada no bioma Cerrado; ii) validar a precipitação utilizando dados do *Tropical Rainfall Measuring Mission Multi-Satellite Precipitation Analysis* (TMPA) e *Integrated Multi-satellitE Retrievals for Global Precipitation Measurement* (IMERG), bem como avaliar o desempenho e a incerteza da modelagem hidrológica com esses dados e com chuva observada; e iii) realizar a retrospectiva hidrológica (RH) utilizando dados de reanálise climática e analisar a ocorrência e características de secas históricas na bacia. Para isso, foram utilizados dados hidrometeorológicos observados, dados climáticos do *Climatic Research Unit* (CRU), dados pluviométricos estimados com base em satélites (TMPA e do IMERG) e de reanálise climática (conjunto de modelo atmosférico do século 20 - ERA-20CM, e o componente terrestre da 5ª geração da *European ReAnalysis* - ERA5-Land). Além disso, foram utilizados o Modelo Digital de Elevação e mapas de tipo e uso do solo. A modelagem hidrológica foi realizada com o *Soil and Water Assessment Tool* (SWAT). Foram utilizados ainda o *Standardized Precipitation Index* (SPI) e o *Standardized Streamflow Index* (SSI) para determinar a seca meteorológica e hidrológica, respectivamente. Na análise de propagação das secas, foi observado que a seca meteorológica gerou uma redução na recarga subterrânea, gerando a ocorrência da seca hidrológica mesmo após a normalização da precipitação. A propagação da seca apresentou maior correlação para uma defasagem de até seis meses do SPI em relação ao SSI, sendo que, para maiores defasagens foi observada uma menor influência da seca meteorológica sobre a hidrológica. Com relação à análise dos produtos de precipitação por satélite, tanto o IMERG como o TMPA superestimaram a precipitação observada. O IMERG apresentou melhor desempenho na validação da chuva e da vazão simulada com o modelo hidrológico, sendo considerado uma alternativa importante para estudos hidrológicos na BHRP. Dentre os produtos de reanálise climática, o ERA5-Land apresentou resultado satisfatório na estimativa da precipitação, da vazão simulada com o modelo hidrológico e da seca hidrológica na bacia, enquanto que os produtos derivados do ERA-20CM apresentaram desempenho insatisfatório em todas as análises. Dessa forma, o ERA5-Land foi utilizado para realizar a reanálise hidrológica de 1950 a 2018, bem como analisar a ocorrência e características das secas hidrológicas históricas na bacia, onde foi possível identificar que os anos de 1958/62, 1970/72, 1974/77, 2001/03 e 2012/18 foram aqueles com maior severidade e duração da seca no período analisado. Além disso, foi observado um aumento no número de meses secos e redução de meses úmidos nas últimas décadas, com 51,7% dos meses secos ocorrendo a partir de 1996. Portanto, o ERA5-Land é adequado para estudos hidrológicos que envolvam séries históricas longas na bacia.

Palavras-chave: Bioma Cerrado. Modelagem hidrológica. Precipitação. Retrospectiva hidrológica. Seca histórica.

ABSTRACT

Hydrological studies are important to assist the water resources management in watersheds, especially in the face of extreme events such as droughts. However, the availability of hydrometeorological observed data in Brazil is low, besides presenting several problems, such as gaps in historical series and irregular spatial distribution. Therefore, this study aimed to (i) analyze the characteristics and propagation of meteorological to hydrological drought and its influence on hydrological behavior in the Pandeiros river basin (PRB), located in the Cerrado biome; ii) to validate precipitation using Tropical Rainfall Measuring Mission Multi-Satellite Precipitation Analysis (TMPA) and Integrated Multi-satellitE Retrievals for Global Precipitation Measurement (IMERG) data, as well as to evaluate the performance and uncertainty of hydrological modeling with these data and with observed precipitation; and iii) to perform hydrological retrospective (RH) using climate reanalysis data and to analyze the occurrence and characteristics of historical droughts in the basin. For this, observed hydrometeorological data, climate data from the Climatic Research Unit (CRU), satellite-based estimated rainfall data (TMPA and from IMERG), and climate reanalysis (20th-century atmospheric model ensemble - ERA-20CM, and the land component of the 5th generation European ReAnalysis - ERA5-Land) were used. In addition, the Digital Elevation Model and maps of land type and land use were used. Hydrological modeling was performed with the Soil and Water Assessment Tool (SWAT). Standardized Precipitation Index (SPI) and Standardized Streamflow Index (SSI) were also used to determine meteorological and hydrological droughts, respectively. In the drought propagation analysis, the meteorological drought caused a reduction in groundwater recharge, generating the occurrence of hydrological drought even after the normalization of precipitation. The drought propagation presented a higher correlation for a lag of up to six months of the SPI in relation to the SSI, and for longer lags, a lower influence of the meteorological drought on the hydrological one was observed. With respect to the analysis of satellite precipitation products, both IMERG and TMPA overestimated the observed precipitation. IMERG showed better performance in validating the precipitation and streamflow simulated with the hydrological model and is considered an important alternative for hydrological studies in the BHRP. Among the climate reanalysis products, ERA5-Land showed satisfactory results in estimating precipitation, streamflow simulated with the hydrological model, and hydrological drought in the basin, while the products derived from ERA-20CM showed unsatisfactory performance in all analyses. Thus, ERA5-Land was used to perform hydrological reanalysis from 1950 to 2018, as well as analyze the occurrence and characteristics of historical hydrological droughts in the basin, where it was possible to identify that the years 1958/62, 1970/72, 1974/77, 2001/03, and 2012/18 were those with the greatest drought severity and duration in the analyzed period. In addition, an increase in the number of drought months and a reduction of wet months was observed in the last decades, with 51.7% of the dry months occurring from 1996 on. Therefore, ERA5-Land is suitable for hydrological studies involving long historical series in the basin.

Keywords: Cerrado biome. Hydrological modeling. Precipitation. Hydrological retrospective. Historical drought.

SUMÁRIO

PRIMEIRA PARTE – INTRODUÇÃO GERAL

1. INTRODUÇÃO

Estudos hidrológicos são importantes para auxiliar a gestão de recursos hídricos em bacias hidrográficas, especialmente diante de eventos extremos, como as secas. A seca é causada principalmente pela redução anormal da precipitação, podendo ser intensificada em períodos de elevada evapotranspiração (VAN LOON, 2015). Esse fenômeno tem impacto negativo sobre a produção agrícola, abastecimento de água urbano, produção hidrelétrica, meio ambiente, disponibilidade hídrica superficial e subterrânea, entre outros.

Entender e representar de forma adequada o processo de escoamento em bacias hidrográficas é fundamental para estudos envolvendo eventos extremos, bem como outras aplicações, como a previsão de vazões, qualidade da água, análise de cenários de intervenções, etc. (FAN; PONTES; PAIVA, 2014). Diante disso, os modelos hidrológicos de bacias hidrográficas, desenvolvidos para descrever quantitativamente os processos que integram o balanço hídrico de uma bacia (CALDEIRA et al., 2019), têm sido amplamente utilizados pela comunidade científica.

Segundo Devi, Ganasri e Dwarakish (2015), existem diversos modelos utilizados para analisar o impacto do clima e das propriedades do solo na hidrologia e recursos hídricos, cada um com características únicas. O *Soil and Water Assessment Tool* (SWAT) é um dos modelos hidrológicos mais utilizados atualmente, apresentando resultados satisfatórios em diversas áreas, como na retrospectiva hidrológica (AUERBACH et al., 2016), análise do impacto de mudanças climáticas (RODRIGUES et al., 2019), comparação entre diferentes produtos de precipitação (AMORIM et al., 2020; LE et al., 2020), etc.

Um dos principais problemas relacionados à modelagem hidrológica com o SWAT no Brasil é a disponibilidade de informações para descrever adequadamente a variabilidade espacial e temporal dos sistemas ambientais (BRESSIANI et al., 2015). Uma das principais variáveis de entrada dos modelos hidrológicos, os dados pluviométricos de superfície, apresentam diversas limitações no Brasil, tais como a baixa densidade da rede de postos de monitoramento, presença de falhas e a escassez de longas séries históricas. Com isso, a utilização da precipitação por satélite se tornou uma alternativa viável de informação pluviométrica, uma vez que esses produtos vêm apresentando desempenho satisfatório no Brasil (ALMEIDA et al., 2020; AMORIM et al., 2020; GADELHA et al., 2019), além de possuir adequadas resoluções espacial e temporal.

Uma outra alternativa que vem sendo adotada por pesquisadores é a utilização de dados de reanálise climática, que estima diversos parâmetros baseados em um reprocessamento consistente de observações meteorológicas (DEE et al., 2014). Esses produtos contêm longas e consistentes informações de variáveis meteorológicas, dentre elas a precipitação que, quando combinados aos modelos hidrológicos, permitem reproduzir séries hidrológicas de longo prazo, caracterizando a metodologia conhecida por retrospectiva hidrológica (CORREA et al., 2017).

Dessa forma, produtos de precipitação estimados por satélite e de reanálise climática podem ser importantes na gestão de recursos hídricos em bacias hidrográficas brasileiras com escasses de dados observados, como aquelas localizadas no bioma Cerrado (savana brasileira). Esse bioma ocupa cerca de 23,9% do território brasileiro (SOUZA et al., 2020) e apresenta uma das savanas com maior biodiversidade no mundo (SCHIASSI et al., 2018), sendo considerado um dos 25 *hotspots* globais de biodiversidade devido à concentração de espécies endêmicas e perda de habitat (MYERS et al., 2000). O Cerrado desempenha um papel fundamental na dinâmica dos recursos hídricos em diversas bacias, incluindo a bacia hidrográfica do rio São Francisco (BHRSF) (OLIVEIRA et al., 2014). No entanto, de acordo com Souza et al. (2020), esse bioma teve uma perda de vegetação igual a 346.000 km² de 1985 a 2017, o que representa 33,8% do total nacional nesse período.

A bacia hidrográfica do rio Pandeiros (BHRP) está completamente inserida no bioma Cerrado, sendo considerada Área de Proteção Ambiental (APA) para a preservação da paisagem natural e para a reprodução da ictiofauna no médio curso do rio São Francisco (SANTOS et al., 2015). O desenvolvimento de estudos hidrológicos nesta bacia é relevante para a gestão de recursos hídricos em função de sua importância ecológica, e também, devido à demanda de avaliação socioambiental sobre o descomissionamento da Pequena Central Hidrelétrica Pandeiros, que deixou de operar em 2008. Diante disso, nota-se a importância de desenvolver estudos que permitam conhecer o comportamento hidrológico da BHRP, bem como os impactos causados pela ocorrência de eventos extremos.

A presente tese está dividida em duas partes. A primeira apresenta uma abordagem geral, fornecendo bases teóricas e contribuições relevantes relacionadas ao tema. A segunda é composta por três artigos, sendo que o primeiro apresenta um estudo sobre o comportamento hidrológico da BHRP, bem como a relação das secas meteorológica e hidrológica e sua influência sobre a dinâmica da água na bacia. O segundo artigo buscou analisar a acurácia de dois produtos de precipitação por satélite com relação à precipitação observada, além de verificar a qualidade desses produtos aplicados à modelagem hidrológica. Por fim, no terceiro buscou-se validar dados de precipitação de dois produtos de reanálise climática e, por meio da

modelagem hidrológica, reconstruir séries de vazão de períodos anteriores ao início do monitoramento hidrológico com o objetivo de analisar a ocorrência de secas hidrológicas históricas.

2. REFERENCIAL TEÓRICO

2.1.Bioma Cerrado

O bioma Cerrado (savana brasileira) ocupa uma área de aproximadamente 2 milhões de km², o que representa 23,9% da área total do Brasil (SOUZA et al., 2020). Esse bioma é conhecido por apresentar uma das savanas com maior biodiversidade no mundo (SCHIASSI et al., 2018), constituindo constituindo um dos 25 *hotspots* globais de biodiversidade (MYERS et al., 2000). Apesar disso, apenas 2,2% de sua área está sob proteção legal (KLINK; MACHADO, 2005), um dos motivos dos quais fez com que o desmatamento nesse bioma representasse mais de um terço (33,8%) de toda área desmatada no Brasil no período de 1985 a 2017 (SOUZA et al., 2020).

Além de sua relevância ambiental, o Cerrado desempenha papel fundamental na dinâmica dos recursos hídricos na América do Sul, uma vez que distribui água doce para grandes bracias hidrográficas, como a do rio Tocantins-Araguaia, do rio Paraná e do rio São Francisco (OLIVEIRA et al., 2014), sendo esta última responsável por fornecer aproximadamente 70% da água superficial para a região Nordeste do Brasil (TORRES et al., 2012).

Pesquisas recentes apontam para uma tendência de redução da precipitação (CAMPOS; CHAVES, 2020) e da umidade relativa, bem como aumento da temperatura (HOFMANN et al., 2021) nas últimas décadas. Diante disso, estudos tem indicado um aumento na ocorrência e severidade das secas no bioma Cerrado nos últimos anos (CUARTAS et al., 2022; JUNQUEIRA et al., 2020b). Oliveira et al. (2014), utilizando produtos estimados por sensores remotos, concluíram que houve um aumento da evapotranspiração e redução no escoamento em regiões do Cerrado, afetando a disponibilidade hídrica para o abastecimento urbano, irrigação, navegação, etc.

De acordo com o *Sixth Assessment Report of the Intergovernmental Panel on Climate Change* (IPCC, 2021), existe uma tendência de redução da precipitação e aumento da temperatura em diversas regiões do Cerrado até o fim do século. Rodrigues et al. (2019) relatam um aumento na intensidade, duração e frequência das secas meteorológica e hidrológica na bacia hidrográfica do rio Sono, localizada no bioma Cerrado, até o final do século, podendo causar impactos negativos sobre as funções ecológicas do bioma, bem como redução na recarga dos aquíferos e da produção de energia hidrelétrica.

2.2.Variabilidade hidrológica e eventos de seca

A seca é um fenômeno natural causada por uma redução anormal na precipitação, no entanto, outros elementos meteorológicos, como a temperatura e ventos fortes, podem influenciar e intensificar sua ocorrência (WILHITE, 2016). De acordo com Vicente-Serrano et al. (2012), esse fenômeno apresenta um dos maiores riscos naturais, afetando diversos setores e gerando impacto sobre os recursos hídricos, agricultura e ecossistemas naturais.

A ocorrência da seca é mais difícil de ser identificada que outros fenômenos naturais devido aos diversos fatores que só são aparentes após uma longa deficiência na precipitação (VICENTE-SERRANO et al., 2012). Além disso, de acordo com a Organização Meteorológica Mundial (OMM, 2012), as secas são regionais em extensão e varia de acordo com as características climáticas de cada região, geralmente atingindo uma área maior que outros fenômenos naturais (HUANG et al., 2017).

A seca é um fenômeno complexo e pode ser definido de diversas formas (VAN LOON, 2015). Diante disso, Wilhite e Glantz (1985) dividiram esse fenômeno em quatro grupos principais: meteorológica (ou climatológica), agrícola, hidrológica e socioeconômica. De acordo com Van Loon (2015), a seca meteorológica refere-se a uma deficiência na precipitação, possivelmente combinada com um aumento na demanda evapotranspirométrica. A seca agrícola consiste em um déficit na umidade do solo, afetando a disponibilidade hídrica para a vegetação. A seca hidrológica está relacionada às anomalias negativas nas águas superficiais (rios, lagos, reservatórios, etc.) e subterrâneas. Por fim, a seca socioeconômica está associada aos impactos das outras secas sobre a sociedade e economia.

A seca hidrológica é afetada pela seca meteorológica, isto é, por uma baixa entrada de água no ciclo hidrológico (precipitação) e de elevadas saídas (evapotranspiração, por exemplo) (VAN LOON, 2015). Além disso, outras variáveis podem influenciar na relação entre as duas secas, como a topografia, litologia e vegetação (VICENTE-SERRANO et al., 2012). Huang et al. (2017) relatam ainda a influência de fenômenos climáticos de macroescala sobre a propagação da seca meteorológica para a hidrológica, como o El Niño-Oscilação Sul (ENOS).

A investigação da propagação da seca meteorológica para a hidrológica pode auxiliar na redução de seus danos (HUANG et al., 2017), tais como abastecimento de água urbana, produção agrícola, produção hidrelétrica, recreação e impactos sobre o ecossistema (VAN LOON, 2015). No entanto, devido à complexidade na interação entre essas secas, a maioria dos estudos sobre secas no Brasil tem focado apenas no componente meteorológico (JULIANI; OKAWA, 2017; PONTES FILHO et al., 2020; ROCHA JÚNIOR et al., 2020; TERASSI et al., 2018).

Junqueira et al. (2020) analisaram a interação entre a seca meteorológica e hidrológica na bacia hidrográfica do rio Tocantins em escala anual e sazonal, de acordo com o ano hidrológico e as estações do ano. Os autores observaram uma influência da seca meteorológica sobre a hidrológica, a qual persistiu por mais tempo devido à redução da recarga subterrânea. Cuartas et al. (2022) destacam que a seca hidrológica, expressa pelo SSFI, teve maior severidade na última década em comparação ao SPI em bacias localizadas em diferentes regiões do Brasil. Segundo os autores, essa diferença está associada ao aumento recente da temperatura média. De acordo com Jesus et al. (2020), em estudo realizado na bacia do rio Doce (sudeste do Brasil), houve maior influência da chuva no período úmido sobre a seca hidrológica durante todo ano. Segundo Van Loon (2015), uma seca no período chuvoso reduz o armazenamento e pode influenciar o escoamento durante a estiagem, potencializado ainda pela maior evapotranspiração comparada à chuva nesse período, processo comum em regiões de savana.

2.2.1. Índices de seca

Para ajudar a monitorar e quantificar a frequência, intensidade, duração e impactos causados pela seca no tempo e no espaço, recentemente foram desenvolvidos diversos índices de seca baseados em variáveis climáticas (BRITO et al., 2018). Esses índices permitem comparar a severidade das secas em diferentes regiões, independente das características climáticas locais (VICENTE-SERRANO et al., 2012).

Um dos principais índices de seca meteorológica, o *Standardized Precipitation Index* (SPI) (MCKEE; DOESKEN; KLEIST, 1993) destaca-se por sua eficiência e simplicidade na determinação da seca. Diante disso, a OMM (2012) recomenda esse índice como padrão para aqueles países que desejem monitorar esse fenômeno. No Brasil, o SPI tem sido bastante utilizado para determinar a ocorrência, intensidade e duração da seca em diferentes regiões, como no semiárido do Nordeste Brasileiro (AZEVEDO et al., 2018; BRITO et al., 2018), na bacia hidrográfica do rio Tocantins (JUNQUEIRA et al., 2020a; RODRIGUES et al., 2019) e na região Sudeste do Brasil (JESUS et al., 2020; NOBRE et al., 2016; SILVA; MELLO, 2021).

Com relação à seca hidrológica, um dos índices mais utilizados na literatura é o *Standardized Streamflow Index* (SSI), o qual permite comparar eventos de seca em diferentes regiões e épocas, em diversos regimes fluviométricos e em rios com características diferentes (ROSSATO et al., 2017; VICENTE-SERRANO et al., 2012). Como a caracterização da seca hidrológica é menos comum no Brasil, poucos trabalhos relevantes aplicaram esse índice em seus estudos, com destaque para Jesus et al. (2020) na bacia hidrográfica do rio Doce, onde foi

constatada a influência da seca meteorológica sobre a hidrológica mesmo após o término da primeira.

2.3.Modelagem hidrológica chuva-vazão

Um modelo consiste na representação de algum objeto ou sistema, de forma simplificada, com o objetivo de entende-lo e buscar respostas para diferentes entradas (TUCCI, 2005). Diante disso, os modelos hidrológicos podem ser definidos como um conjunto de equações que auxiliam na estimativa do escoamento como uma função de vários parâmetros característicos de cada bacia hidrográfica (DEVI; GANASRI; DWARAKISH, 2015).

De acordo com Caldeira et al. (2019), um modelo hidrológico do tipo chuva-vazão é utilizado para descrever quantitativamente, de forma simplificada, os processos associados ao balanço hídrico em uma bacia hidrográfica. Esses modelos podem ser utilizados na extensão de séries históricas, preenchimento de falhas, transposição paramétrica, análise de mudanças climáticas, alterações no uso do solo, produção e transporte de sedimentos, retrospectiva hidrológica, entre outras aplicações.

Segundo Tucci (2005), os modelos hidrológicos normalmente são classificados de acordo com o nível de discretização espacial (concentrado ou distribuído), quanto à sua formulação (empírico ou conceitual), em relação à escala temporal (contínuo ou discreto) e ao tipo de variável utilizada durante a modelagem (estocástico ou determinístico).

Nos modelos concentrados, toda bacia é tomada como uma unidade de captação única, desconsiderando a variabilidade espacial. Por outro lado, os modelos distribuídos consideram a variação espacial das variáveis e dos parâmetros (MORADKHANI; SOROOSHIAN, 2009).

Os modelos empíricos (caixa preta), segundo Devi, Ganasri e Dwarakish (2015), são definidos de acordo com os dados existentes, sem considerar as características e processos do sistema hidrológico. Um exemplo desse modelo são as hidrógrafas unitárias. Por outro lado, os modelos conceituais descrevem os processos hidrológicos dos componentes, sem a necessidade de embasamento físico, sendo necessário um grande número de registros hidrometeorológicos para sua calibração.

Além dos modelos empíricos e conceituais, Devi, Ganasri e Dwarakish (2015) destacam ainda os modelos fisicamente baseados, onde, além dos dados hidrometeorológicos, esse tipo de modelo requer outros dados de entrada, como a umidade do solo, topografia, dimensões do canal do rio, entre outros. Segundo os autores, esses modelos podem superar lacunas dos outros dois devido ao uso de parâmetros com interpretação física.

Com relação à escala temporal, o modelo é considerado continuo quando os fenômenos são contínuos no tempo, por outro lado, em modelos discretos, as mudanças de estado ocorrem em intervalos discretos (TUCCI, 2005). Na modelagem hidrológica, as variáveis são continuas, porém discretizadas em intervalos de tempo (por exemplo, a precipitação).

De acordo com Devi, Ganasri e Dwarakish (2015), os modelos determinísticos fornecem a mesma saída para um único conjunto de valores de entrada. Por outro lado, nos modelos estocásticos diferentes valores de saída podem ser produzidos para um único conjunto de entrada. A abordagem estocástica permite caracterizar as incertezas dos parâmetros ajustáveis do modelo e das previsões de saída (NG; EHEART; CAI, 2010).

Segundo Yapo, Gupta e Sorooshian (1998), para calibrar um modelo hidrológico, os parâmetros devem assumir valores para que o comportamento do modelo seja o mais próximo ao sistema real representado. Ainda de acordo com os citados autores, em alguns casos esses parâmetros podem ser determinados de forma direta, entretanto, grande parte dos parâmetros são representações conceituais de características da bacia hidrográfica, devendo ser calibrados para que a resposta final do modelo seja o mais próximo possível aos dados reais.

Caldeira et al. (2019) destacam que é importante que o modelo hidrológico seja o mais parcimonioso possível, ou seja, deve representar o comportamento do sistema utilizando a menor quantidade de parâmetros, evitando a superparametrização (*overparametrization*) e reduzindo as incertezas.

Para Devi, Ganasri e Dwarakish (2015), o modelo mais adequado é aquele que fornece os resultados mais próximos da realidade, utilizando o menor número de parâmetros e menor complexidade. Diante disso, foram desenvolvidos diversos modelos hidrológicos em diferentes partes do mundo, cada um com características distintas, por exemplo: o *Distributed Hydrology Soil Vegetation Model* - DHSVM (WIGMOSTA; VAIL; LETTENMAIER, 1994); o *Lavras Simulation of Hydrology* – LASH (BESKOW; MELLO; NORTON, 2011; CALDEIRA et al., 2019); e o SWAT (ARNOLD et al., 1998), o qual tem sido amplamente utilizado em estudos hidrológicos desenvolvidos em bacias hidrográficas no Brasil (BRESSIANI et al., 2015).

2.3.1. Soil and Water Assessment Tool - SWAT

O SWAT, segundo Arnold et al. (1998), é um modelo hidrológico do tipo chuva-vazão cuja motivação inicial foi desenvolver estudos relacionados a mudanças climáticas, gestão de recursos hídricos em regiões de clima árido, inundações e impactos fora do local de gestão do solo.

De acordo com Gassman et al. (2007), o SWAT é um modelo fisicamente baseado, opera em escala diária, computacionalmente eficiente e capaz de simular de forma contínua longos períodos de tempo. Nesse modelo, a bacia hidrográfica é dividida em múltiplas sub-bacias, que são posteriormente subdivididas em Unidades de Resposta Hidrológica (URHs) (GASSMAN et al., 2007). As URHs consistem em regiões com comportamento hidrológico semelhante, com mesma combinação de relevo, tipo e uso de solo (NEITSCH et al., 2011).

O SWAT foi desenvolvido para refletir corretamente as mudanças no uso do solo e na gestão agrícola sobre o escoamento do rio e a produção de sedimentos (ARNOLD et al., 1998). Para isso, segundo Neitsch et al. (2011), o ciclo hidrológico deve estar de acordo com a realidade da bacia hidrográfica.

No SWAT, a precipitação pode ser interceptada pelo dossel das plantas ou atingir a superfície do solo, onde ela pode infiltrar-se ou escoar superficialmente. A água proveniente do escoamento superficial move-se de forma rápida para o canal principal, enquanto que a parcela que infiltrou pode ficar retida no solo e, posteriormente, ser evapotranspirada, absorvida pelas plantas, escoar subsuperficialmente ou percolar para as camadas mais profundas, promovendo a recarga dos aquíferos livre e confinado, conforme representado na Figura 1 (NEITSCH et al., 2011).

Figura 1. Representação esquemática do ciclo hidrológico no SWAT.

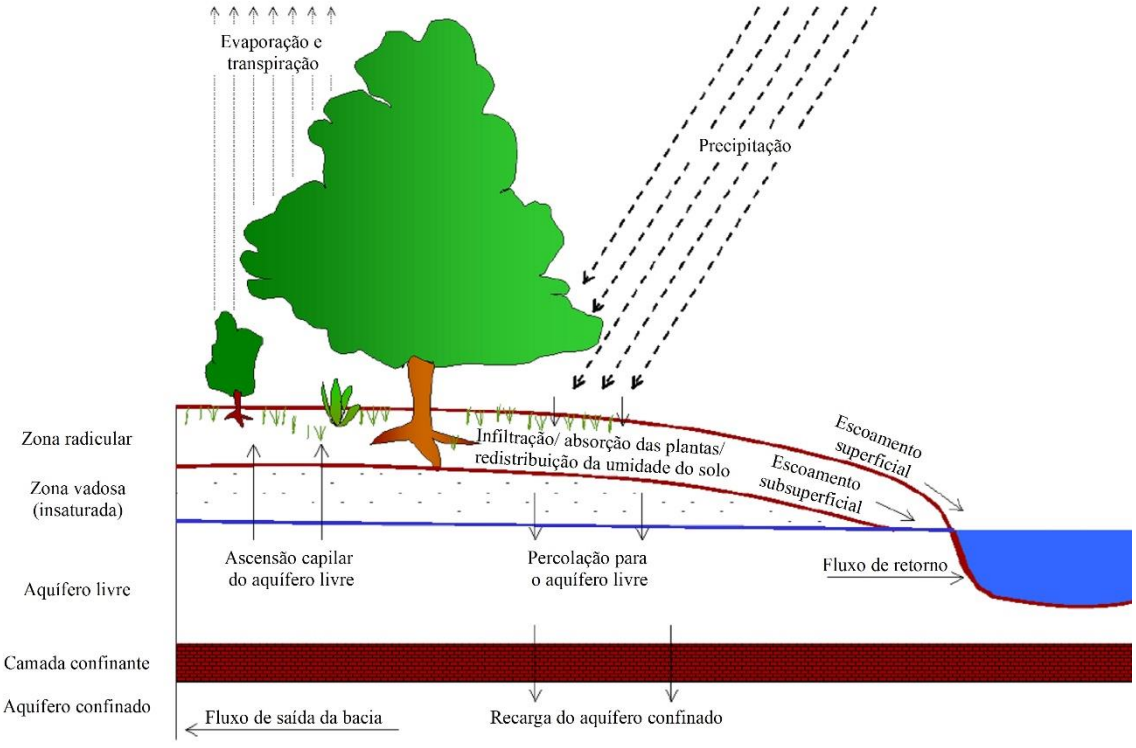

Fonte: Adaptado de Neitsch et al. (2011).

Após essa primeira fase, ocorre a propagação da água no canal principal pelo método de armazenamento variável (WILLIAMS, 1969) ou pelo método de Muskingum-Cunge (BRAKENSIEK, 1967; OVERTON, 1966). Além disso, o SWAT considera ainda o transporte de sedimentos, obtido pela Equação Universal de Perda de Solo Modificada – MUSLE (WILLIAMS, 1975); de nutrientes (nitrogênio e fósforo), os quais podem ser transportados por meio do escoamento superficial e subsuperficial; e de pesticida, modelado pela equação de GLEAMS (LEONARD; KNISEL; STILL, 1987; NEITSCH et al., 2011).

O SWAT é um dos modelos hidrológicos mais utilizados por pesquisadores devido à sua comprovada eficiência e versatilidade em diferentes bacias e comportamento climático distinto ao redor do mundo (AMORIM et al., 2020; GUSE; REUSSER; FOHRER, 2014; UNIYAL et al., 2019). No Brasil, grande parte dos estudos tem se concentrado apenas na capacidade do modelo em representar o ciclo hidrológico (BRESSIANI et al., 2015). No entanto, pesquisas aprofundadas utilizando o SWAT foram realizadas em diferentes regiões do Brasil, como Dias et al. (2018) no reservatório da usina hidrelétrica de Furnas e Meira Neto et al. (2018) na bacia do ribeirão da Onça.

Rodrigues et al. (2019) utilizaram o SWAT para analisar os impactos hidrológicos das mudanças climáticas até o final do século 21 em uma bacia localizada no bioma Cerrado. Além disso, foi feita análise da ocorrência e impactos das secas meteorológica e hidrológica na bacia. Os autores observaram uma redução no escoamento em todos os cenários. Ainda, houve aumento na duração, intensidade e frequência de ambas as secas para o cenário futuro, com uma duração maior da seca hidrológica sobre a meteorológica. Oliveira et al. (2017), por meio de simulação hidrológica com o SWAT, também projetaram uma redução nas vazões e, consequentemente, na produção hidrelétrica na região de cabeceira da bacia do rio Grande.

2.4.Precipitação por satélite

A precipitação é o principal componente do ciclo hidrológico e o mais importante dado de entrada de modelos hidrometeorológicos e estudos climáticos. A precisão desses estudos depende da qualidade da precipitação observada, principalmente com relação às suas características mais importantes, como a intensidade, duração e abrangência (SOROOSHIAN et al., 2011). Entretanto, de acordo com Islam (2018), a disponibilidade de dados pluviométricos observados de alta qualidade é limitada na maioria dos países em desenvolvimento.

Segundo Gadelha et al. (2019), a rede de monitoramento pluviométrica no Brasil possui alguns problemas, tais como baixa densidade e má distribuição espacial no território nacional, além de falhas nas séries históricas. Além disso, Hou et al. (2014) relatam que a medição direta

da precipitação por meio de pluviômetros apresenta problemas para representar a precipitação em áreas extensas devido à sua alta variabilidade espacial e temporal. A associação desses fatores faz com que a qualidade de estudos hidrológicos seja prejudicada.

As estimativas da precipitação por satélite com cobertura praticamente global e alta resolução temporal tem se tornado uma fonte alternativa de informação pluviométrica, principalmente em bacias pouco monitoradas (ISLAM, 2018). De acordo com Michaelides et al. (2009), o sensoriamento remoto desempenha um papel importante na complementação e aprimoramento do conhecimento sobre as características espaciais e temporais da precipitação. Diante disso, diversos pesquisadores tem aplicado esses produtos ao redor do mundo (AMORIM et al., 2020; GADELHA et al., 2019; ISLAM, 2018; LI et al., 2018).

Embora existam vários produtos disponíveis, deve-se atentar ao tipo de sensor utilizado devido às diferenças na precisão de medição. Sensores de infravermelho em satélites geoestacionários podem fornecer estimativas da precipitação em altas resoluções temporais (intervalos de até 15 minutos), no entanto, essas medidas estão relacionadas às características superiores das nuvens (albedo e temperatura), em vez de estarem diretamente relacionadas à precipitação. Por outro lado, os sensores de micro-ondas possuem maior precisão na medição da precipitação, uma vez que as assinaturas radiativas estão mais diretamente ligadas às partículas precipitantes, mas com resolução temporal inferior aos sensores de infravermelho (HOU et al., 2014; HUFFMAN et al., 2019).

2.4.1. Tropical Rainfall Measuring Mission (TRMM) Multi-Satellite Precipitation Analysis (TMPA)

O satélite *Tropical Rainfall Measuring Mission* (TRMM), desenvolvido em parceria pela *National Aeronautics and Space Administration* dos Estados Unidos (NASA) e *Japan Aerospace Exploration* (JAXA), foi o primeiro radar espacial projetado para capturar uma estrutura mais abrangente da chuva (FRANCHITO et al., 2009), tendo operado entre novembro de 1997 a abril de 2015. De acordo com Iguchi et al. (2000), esse satélite é não estacionário e orbita a 350 km acima da superfície, observando uma faixa de 220 km com 49 feixes a cada 0,6 segundos. O TRMM foi o primeiro satélite a permitir a captura da estrutura tridimensional de tempestades. As distribuições vertical e horizontal da chuva são importantes não apenas para investigar estruturas de tempestades, mas também modelos de circulação global (IGUCHI et al., 2000).

Segundo Kummerow e Barnes (1998), os principais instrumentos de medição de precipitação do TRMM são o Imageador de Micro-ondas (IM), o Radar de Precipitação (RP) e

o Sistema de Radiômetro Visível e Infravermelho (SRVI). O IM mede as radiações que são o produto final dos efeitos integrados da absorção eletromagnética, emissão e espalhamento através da nuvem de precipitação ao longo do caminho do sensor, com amplitude de frequência de 10 a 85,5 GHz. Por outro lado, os RPs fornecem uma estrutura tridimensional da precipitação, particularmente da distribuição vertical com base no tempo de atraso da potência de retorno em caso de precipitação, trabalhando a uma frequência de 13,8 GHz. O SRVI adiciona temperaturas e estruturas no topo da nuvem para complementar a descrição dos dois sensores de micro-ondas, agregando maior frequência temporal em relação a esses sensores (KUMMEROW; BARNES, 1998).

Um dos principais produtos gerados a partir do TRMM é o *TRMM Multi-Satellite Precipitation Analysis* (TMPA). Esse algoritmo foi projetado para combinar estimativas de precipitação de vários satélites, bem como medidores de precipitação na superfície, com resolução de três em três horas em 0,25º x 0,25º de latitude e longitude (HUFFMAN et al., 2006). Segundo Michaelides et al. (2009), o TMPA apresenta resultado razoável em escala mensal, no entanto, possui dificuldade ao estimar corretamente chuvas com intensidade leve e moderada em intervalos curtos.

Apesar do desempenho adequado da precipitação obtida por satélite em alguns locais e escalas temporais, são necessárias pesquisas aprofundadas para avaliar a qualidade e erros desse produto em diferentes regiões climáticas e estações do ano (SOROOSHIAN et al., 2011). Aires, Melo Neto e Mello (2016) encontraram uma correlação satisfatória entre a precipitação mensal estimada pelo TMPA e dados observados na bacia do rio Paraopeba, localizada na região de cabeceira do rio São Francisco.

Franchito et al. (2009) analisaram a adequabilidade da precipitação sazonal estimada pelo TMPA em relação aos dados medidos em superfície em cinco regiões com regime climático diferente no Brasil. Os autores observaram uma estimativa adequada da precipitação por satélite no período de dezembro a fevereiro e março a maio. Entretanto, durante o período de junho a agosto e setembro a novembro, apenas as regiões da Amazônia Sul e Amazônia Sudeste, respectivamente, foram consideradas adequadas. De forma geral, o TMPA apresentou resultado confiável onde a precipitação é alta e erros mais elevados durante o período de estiagem. Amorim et al. (2020) relatam que o TMPA proporcionou desempenho superior à simulação hidrológica com o SWAT em relação à simulação realizada com dados de precipitação observada.

2.4.2. Integrated Multi-satellitE Retrievals for Global Precipitation Measurement (IMERG)

Baseado no sucesso do TRMM, a NASA e a JAXA lançaram em fevereiro de 2014 o *Global Precipitation Measurement* (GPM). O objetivo dessa missão foi fornecer observações de precipitação global e uniformemente calibradas a cada 2-4 horas (MICHAELIDES et al., 2009). O satélite transporta o primeiro radar de precipitação de dupla frequência espacial (DFE), operando nas bandas Ku e Ka (13 e 35 GHz, respectivamente), além de um gerador de imagens de micro-ondas multicanal de varrimento cônico, o GIM (HOU et al., 2014).

De acordo com Hou et al. (2014), o DFE mede a estrutura tridimensional da precipitação, enquanto o GIM é um radiômetro de micro-ondas passivo de varredura cônica com 13 canais que variam de 10 a 183 GHz. Essas frequências foram otimizadas para detectar precipitação intensa, moderada e leve. O DFE e o GIM refinam os algoritmos de recuperação a partir da construção de uma base de dados observacional única, quantificando as propriedades microfísicas das partículas precipitantes.

Segundo Hou et al. (2014), o GPM fornece produtos com maior cobertura espacial, resolução espaço-temporal e estimativa mais precisa e confiável da precipitação que o TRMM, principalmente na estimativa de precipitação leve. Além disso, o GPM fornece produtos em quatro níveis com base em diferentes algoritmos, entre eles o *Integrated Multi-satellitE Retrievals for GPM* (IMERG), disponível com alta resolução espacial (0,1 x 0,1º) e temporal (meia hora) dentro da latitude 60ºN-S.

O IMERG realiza a intercalibração, junção e interpolação de diversas estimativas da precipitação por micro-ondas e infravermelho calibrado por micro-ondas, análises de medidores de precipitação terrestre e, potencialmente, outros estimadores de precipitação em escalas precisas de tempo e espaço para as eras TRMM e GPM em todo o globo (HUFFMAN et al., 2019).

Por se tratar de um produto recente, são necessários mais estudos para analisar o comportamento desses produtos em diferentes regiões e para diferentes aplicações. Gadelha et al. (2019) avaliaram o desempenho espacial e temporal do IMERG no Brasil em relação aos dados medidos por pluviômetros entre janeiro e dezembro de 2016 em diferentes escalas temporais (diária, mensal e anual). De forma geral, os autores observaram que o IMERG apresentou uma boa capacidade em estimar a variabilidade espacial da precipitação no Brasil, entretanto, houve uma pequena superestimativa da precipitação em todas as escalas de tempo. Além disso, a estimativa mensal da precipitação apresentou melhor desempenho quando comparada aos dados diários.

Rozante et al. (2018) compararam a precipitação diária do IMERG e TMPA com dados observados em cinco regiões com regime pluviométricos diferentes no Brasil e outra para todo o país entre abril de 2014 e fevereiro de 2017. Os autores observaram comportamento semelhante entre os dois produtos, em que ambos superestimam a precipitação na maioria das regiões do Brasil; com exceção do litoral nordestino, onde houve subestimativa da chuva. No entanto, em todas as regiões analisadas, o IMERG apresentou melhor desempenho em comparação ao TMPA que, segundo os autores, é importante para modelagem hidrológica em pequenas bacias, uma vez que a resolução espacial do IMERG é superior.

2.5.Reanálise climática

A reanálise pode ser entendida como um reprocessamento consistente de observações meteorológicas, incluindo precipitação e temperatura, obtida usando sistemas modernos de modelagem numérica. Seu produto consiste em conjuntos de dados multidecadais, em grades, os quais estimam diversos parâmetros da superfície atmosférica, do oceano e da superfície terrestre, incluindo muitos que não são diretamente observados (DEE et al., 2014).

A reanálise se baseia em modelos para interpretar, relacionar e combinar diversas observações diferentes de múltiplas fontes. As equações de movimento e processos físicos são utilizadas para gerar produtos de dados que são espacialmente completos e fisicamente consistentes (DEE et al., 2014). Com isso, diversos estudos recentes utilizando diferentes fontes de reanálise climática foram desenvolvidos no Brasil (CORREA et al., 2017, 2019; PAZ et al., 2018; REBOITA et al., 2018) e no mundo (CURIO et al., 2019; UNIYAL et al., 2019).

A reanálise climática vem sendo produzida por diferentes organizações, tais como: *European Centre for Medium-Range Weather Forecasts* (ECMWF), *National Oceanic and Atmospheric Administration* dos Estados Unidos (NOAA) e NASA. Recentemente, foi criado o *Advancing Reanalysis* (reanalyses.org), uma página online que tem como objetivo auxiliar pesquisadores a obter, ler e analisar conjuntos de dados de reanálise gerados por diferentes organizações climáticas e meteorológicas. Além disso, permite aos usuários fornecer conteúdo e fazer comentários, tornando-o mais interativo. Outra plataforma na internet, a *Climate Analyzer* (climatereanalyzer.org), desenvolvida pelo *Climate Change Institute* da Universidade de Maine, permite acessar informações de reanálise e dados históricos de estações, além de fornecer acesso a modelos de previsão do tempo.

Apesar dos avanços recentes nos produtos de reanálise, Dee et al. (2014) destacam dois pontos que podem ser melhorados futuramente: i) maior extensão da série histórica, com o intuito de fornecer registros mais longos para estudos climáticos e validação de modelos

climáticos; ii) melhor representação das interações e *feedbacks* entre a atmosfera e outros componentes do sistema climático.

Diversos produtos de reanálise climática foram desenvolvidos nos últimos anos, entre os quais destacam-se o conjunto de modelo atmosférico do século 20 (ERA-20CM) e o componente terrestre da 5ª geração da *European ReAnalysis* (ERA5), denominado ERA5-Land, ambos desenvolvidos pelo ECMWF, os quais serão discutidos com maiores detalhes a seguir.

2.5.1. ERA-20CM

O ERA-20CM (HERSBACH et al., 2015) é um produto de reanálise climática global que fornece dados de diversas variáveis em um intervalo de até 3 horas a uma resolução espacial de 0,125° e resolução espectral T159 (aproximadamente 125 km). Segundo Hersbach et al. (2015), esse produto é uma variação dos componentes do modelo de previsão atmosférica e das ondas oceânicas do Cy38r1, com algumas adaptações para permitir adicionar dados do *Hadley Centre Global Sea Ice and Sea Surface Temperature* versão 2.1 (HadISST2.1) e as recomendações do *Coupled Model Intercomparison Project Phase 5* (CMIP5).

O HadISST2.1 consiste em um conjunto com multiplas realizações (mais de 1400) diárias de temperatura da superfície do mar e concentração de gelo marinho em uma grade regular de 0,25°. Para o desenvolvimento do ERA-20CM, foram selecionadas dez realizações do HadISST2.1 de forma aleatória, cada uma com a mesma probabilidade. A variação nas realizações desse produto reflete a incerteza nas fontes observacionais, bem como o ajuste de viés. Por sua vez, o CMIP5 recomenda a utilização de algumas forçantes radiativas, tais como forçante solar, gases do efeito estufa, ozônio e aerossóis, além da ocorrência de eventos de grande escala, como o ENOS e erupções vulcânicas (HERSBACH et al., 2015). Segundo Taylor, Stouffer e Meehl (2012), o CMIP5 fornece um conjunto de dados multimodelo de última geração para avançar no conhecimento sobre variabilidade climática e mudanças climáticas.

Nenhuma observação atmosférica é assimilada ao ERA-20CM, ou seja, é independente de observações sinóticas, sendo que toda informação observacional é incorporada nas condições de contorno e forçantes (GAO et al., 2016; HERSBACH et al., 2015). No entanto, esse produto é capaz de fornecer uma estimativa estatística do clima. Além disso, a elevação da temperatura terrestre está de acordo com o CRUTEM4, o qual é baseado em dados observados (HERSBACH et al., 2015).

Com relação à precipitação, diversos estudos tem comprovado a eficiência do ERA-20CM em diferentes regiões climáticas, como na China (GAO et al., 2016) e no Sahel, região

próxima ao deserto do Sahara (BERNTELL et al., 2018). Apesar disso, Kim e Han (2019) relatam que a aplicabilidade do ERA-20CM pode variar de acordo com a região, sendo necessários mais estudos sobre a eficiência desses dados.

2.5.2. ERA5-Land

O ERA5-Land é um conjunto de dados de reanálise derivado do ERA5 (MUÑOZ-SABATER et al., 2021), que por sua vez representa uma atualização do ERA-Interim, com melhorias nas resoluções horizontal, vertical e temporal, bem como um maior número de parâmetros de saída (HERSBACH et al., 2020). Além disso, o ERA5 e o ERA5-Land utilizam observações de mais de 200 instrumentos de satélite e dados observados (HERSBACH et al., 2020; MUÑOZ-SABATER et al., 2021). Segundo Muñoz-Sabater et al. (2021), a principal melhoria do ERA5-Land em relação ao ERA5 e ERA-Interim se deve à redução de escala dinâmica não-linear com entrada termodinâmica corrigida.

O ERA5-Land fornece uma visão consistente da evolução das variáveis terrestre de 1950 até a atualidade (com uma defasagem de aproximadamente 3 meses), a uma resolução espacial de 9 km e temporal de 1 hora. Essas resoluções tornam o ERA5-Land muito útil para diversos estudos hidrológicos, tais como previsão de enchentes ou secas (MUÑOZ-SABATER, 2019).

O núcleo do ERA5-Land é o modelo de superfície terrestre do ECMWF: o Carbon Hydrology-Tiled ECMWF Scheme for Surface Exchanges over Land (CHTESSEL) do ciclo do modelo Cy45r1 de 2018, uma versão mais recente que a do ERA5 e do ERA-20CM, por exemplo. O ERA5-Land não assimila observações diretamente; no entanto, observações atmosféricas, como temperatura e umidade do ar, velocidade do vento e pressão superficial, são adicionadas como forçante atmosféricas (MUÑOZ-SABATER et al., 2021). Segundo Muñoz-Sabater (2019, 2021), sem as restrições dessas forçantes, as estimativas baseadas em modelos podem se desviar da realidade.

Os componentes do ciclo hidrológico do ERA5-Land foram validados com base em dados observados e de satélite ao redor do mundo, apresentando, inclusive, resultados superiores ao ERA5 e ao ERA-Interim (MUÑOZ-SABATER et al., 2021). Kawohi (2019) avaliou dados de precipitação estimados por reanálise (ERA5 e ERA5-Land) e de satélite (IMERG) na região centro-norte do Brasil (0-20 °S e 40-60 °O) e na Alemanha. O autor observou um melhor desempenho com os dados de reanálise em relação ao IMERG na Alemanha; no entanto, o IMERG apresentou melhor representação da precipitação no Brasil que os produtos de reanálise. Apesar desses estudos, existe ainda uma grande lacuna sobre a

utilização de produtos de reanálise no Brasil, em especial o ERA5-Land, por se tratar de um produto recente, principalmente relacionado à aplicações hidrológicas.

2.6.Retrospectiva hidrológica

A partir da reanálise climática, surgiu um conceito voltado para a hidrologia, conhecido como Retrospectiva Hidrológica (RH), que pode ser entendida como um registro consistente e coerente de campos espaço-temporais de variáveis hidrológicas. Segundo Correa et al. (2017), a RH consiste na junção de dados de modelagem hidrológica e reanálise climática ou grandes conjuntos de dados pluviométricos. Essa metodologia foi desenvolvida para representar adequadamente o comportamento hidrológico do passado, permitindo analisar eventos extremos como as secas e enchentes.

Alfieri et al. (2020) utilizou dados de reanálise do ERA5 para simular vazões em bacias de grande e médio porte em todo planeta no período de 1980 a 2018. Os autores obtiveram resultados médios satisfatórios, com coeficiente de eficiência de Kling-Gupta igual a 0.67 e correlação de Pearson igual a 0.8. No entanto, o desempenho da simulação foi superior em áreas mais desenvolvidas, como Europa e América do Norte, onde a densidade de estações é maior.

No Brasil, Correa et al. (2017) realizaram a RH na bacia Amazônica utilizando oito base de dados globais de precipitação, sendo cinco de reanálise (ERA-Interim, ERA-20CM, CFSR, JAR-55 e NOAA V2c) e três de combinação entre reanálise climática e dados de satélite e/ou *in-situ* (CHIRPS v2.0, ERA-Interim Land e MSWEP), além de dados climáticos mensais do CRU CL 2.0. Os autores observaram que a maior parte dos eventos extremos na bacia foi capturado pela RH, o que indica que esses dados podem ser utilizados em regiões onde a disponibilidade de precipitação observada é baixa ou inexistente.

3. CONSIDERAÇÕES GERAIS

O bioma Cerrado é uma savana tropical com condições únicas no mundo e apresenta elevada importância ambiental, hidrológica, social e econômica para o Brasil; no entanto, vem sofrendo com o desmatamento acelerado nas últimas décadas. A BHRP está completamente inserida no Cerrado e apresenta a preservação de sua cobertura vegetal como uma de suas principais características, o que a torna uma bacia representativa do referido bioma. Dessa forma, estudos hidrológicos nessa bacia são importantes para melhorar o entendimento sobre o ciclo da água, o manejo dos recursos hídricos e do ecossistema da região.

O desenvolvimento de estudos hidrológicos consistentes é afetado por uma baixa densidade de postos pluviométricos no Cerrado, além de séries históricas geralmente curtas e com a presença de falhas. Nesse contexto, a estimativa da precipitação por satélites tem como vantagem sua elevada resolução espacial e temporal em relação aos dados observados, além de fornecer dados com elevada precisão em diferentes regiões climáticas. Por sua vez, a reanálise climática apresenta séries históricas longas de precipitação, disponíveis em alta resolução temporal e espacial; no entanto, são necessários mais estudos relevantes em diferentes regiões climáticas para avaliar sua precisão.

Esses produtos de precipitação, quando associados à modelagem hidrológica, permitem realizar simulações longas e consistentes sobre o comportamento da bacia hidrológica. Além disso, a análise da vazão simulada com os produtos de reanálise climática proporciona um melhor entendimento sobre a ocorrência e características das secas históricas na bacia, se tornando uma ferramenta útil para uma melhor gestão dos recursos hídricos durante a ocorrência de secas no presente e no futuro.

REFERÊNCIAS BIBLIOGRÁFICAS

AIRES, U. R. V.; MELO NETO, J. DE O.; MELLO, C. R. DE. Estimativas de precipitação pluvial derivadas do sensor TRMM para a bacia hidrográfica do rio Paraopeba. **Revista Scientia Agraria**, v. 17, n. 2, p. 57–66, 2016.

ALFIERI, L. et al. A global streamflow reanalysis for 1980–2018. **Journal of Hydrology X**, v. 6, n. July 2019, p. 100049, 2020.

ALMEIDA, K. N. et al. Performance analysis of TRMM satellite in precipitation estimation for the Itapemirim River basin, Espirito Santo state, Brazil. **Theoretical and Applied Climatology**, v. 2, n. 2012, 12 Mei 2020.

AMORIM, J. S. et al. Evaluation of Satellite Precipitation Products for Hydrological Modeling in the Brazilian Cerrado Biome. **Water**, v. 12, n. 2571, p. 1–19, 2020.

ARNOLD, J. G. et al. Large area hydrologic modeling and assessment part I: model development. **Journal of the American Water Resources Association**, v. 34, n. 1, p. 73–89, 1998.

AUERBACH, D. A. et al. Evaluating weather observations and the Climate Forecast System Reanalysis as inputs for hydrologic modelling in the tropics. **Hydrological Processes**, v. 30, n. 19, p. 3466–3477, 15 Sep 2016.

AZEVEDO, S. C. DE et al. Analysis of the 2012-2016 drought in the northeast Brazil and its impacts on the Sobradinho water reservoir. **Remote Sensing Letters**, v. 9, n. 5, p. 438–446, 2018.

BERNTELL, E. et al. Representation of Multidecadal Sahel Rainfall Variability in 20th Century Reanalyses. **Scientific Reports**, v. 8, n. 1, p. 6–13, 2018.

BESKOW, S.; MELLO, C. R. DE; NORTON, L. D. Development, sensitivity and uncertainty analysis of LASH model. **Scientia Agricola**, v. 68, n. 3, p. 265–274, 2011.

BRAKENSIEK, D. L. Kinematic Flood Routing. **Transactions of the ASABE**, v. 10, n. 3, p. 340–343, 1967.

BRESSIANI, D. D. A. et al. Review of Soil and Water Assessment Tool (SWAT) applications in Brazil: Challenges and prospects. **International Journal of Agricultural and Biological Engineering**, v. 8, n. 3, p. 9–35, 2015.

BRITO, S. S. B. et al. Frequency, duration and severity of drought in the Semiarid Northeast Brazil region. **International Journal of Climatology**, v. 38, n. 2, p. 517–529, 2018.

CALDEIRA, T. L. et al. LASH hydrological model: An analysis focused on spatial discretization. **Catena**, v. 173, p. 183–193, Feb 2019.

CAMPOS, J. DE O.; CHAVES, H. M. L. Trends and variabilities in the historical series of monthly and annual precipitation in cerrado biome in the period 1977-2010. **Revista Brasileira de Meteorologia**, v. 35, n. 1, p. 157–169, 2020.

CORREA, S. W. et al. Multi-decadal Hydrological Retrospective: Case study of Amazon floods and droughts. **Journal of Hydrology**, v. 549, p. 667–684, 2017.

CORREA, S. W. et al. Hydrological reanalysis across the 20th century: A case study of the Amazon Basin. **Journal of Hydrology**, v. 570, p. 755–773, 2019.

CUARTAS, L. A. et al. Recent Hydrological Droughts in Brazil and Their Impact on Hydropower Generation. **Water**, v. 14, n. 4, p. 601, 16 Feb 2022.

CURIO, J. et al. Climatology of Tibetan Plateau Vortices in Reanalysis Data and a High-Resolution Global Climate Model. **Journal of Climate**, v. 32, n. 6, p. 1933–1950, 2019.

DEE, D. P. et al. Toward a consistent reanalysis of the climate system. **Bulletin of the American Meteorological Society**, v. 95, n. 8, p. 1235–1248, 2014.

DEVI, G. K.; GANASRI, B. P.; DWARAKISH, G. S. A Review on Hydrological Models. **Aquatic Procedia**, v. 4, p. 1001–1007, 2015.

DIAS, V. DE S. et al. Historical streamflow series analysis applied to furnas HPP reservoir watershed using the SWAT model. **Water**, v. 10, n. 4, p. 1–13, 2018.

FAN, F. M.; PONTES, P. R. M.; PAIVA, R. C. D. DE. Avaliação de um método de propagação de cheias em rios com aproximação inercial das equações de Saint-Venant. **Revista Brasileira de Recursos Hídricos**, v. 19, n. 4, p. 137–147, 2014.

FRANCHITO, S. H. et al. Validation of TRMM precipitation radar monthly rainfall estimates over Brazil. **Journal of Geophysical Research: Atmospheres**, v. 114, p. 1–9, 2009.

GADELHA, A. N. et al. Grid box-level evaluation of IMERG over Brazil at various space and time scales. **Atmospheric Research**, v. 218, p. 231–244, 2019.

GAO, L. et al. A first evaluation of ERA-20CM over China. **Monthly Weather Review**, v. 144, n. 1, p. 45–57, 2016.

GASSMAN, P. W. et al. The soil and water assessment tool: historical development, applications, and future research directions. **Transactions of the ASABE**, v. 50, n. 4, p. 1211–1250, 2007.

GUSE, B.; REUSSER, D. E.; FOHRER, N. How to improve the representation of hydrological processes in SWAT for a lowland catchment – temporal analysis of parameter sensitivity and model performance. **Hydrological Processes**, v. 28, n. 4, p. 2651–2670, 2014.

HERSBACH, H. et al. ERA-20CM: a twentieth-century atmospheric model ensemble. **Quarterly Journal of the Royal Meteorological Society**, v. 141, n. 691, p. 2350–2375, 2015.

HERSBACH, H. et al. The ERA5 global reanalysis. **Quarterly Journal of the Royal Meteorological Society**, v. 146, n. 730, p. 1999–2049, 2020.

HOFMANN, G. S. et al. The Brazilian Cerrado is becoming hotter and drier. **Global Change Biology**, v. 27, n. 17, p. 4060–4073, 2021.

HOU, A. Y. et al. The global precipitation measurement mission. **Bulletin of the American Meteorological Society**, v. 95, n. 5, p. 701–722, 2014.

HUANG, S. et al. The propagation from meteorological to hydrological drought and its

potential influence factors. **Journal of Hydrology**, v. 547, p. 184–195, 2017.

HUFFMAN, G. J. et al. The TRMM Multisatellite Precipitation Analysis (TMPA): Quasi-Global, Multiyear, Combined-Sensor Precipitation Estimates at Fine Scales. **Journal of Hydrometeorology**, v. 8, n. 1, p. 38–55, 2006.

HUFFMAN, G. J. et al. **NASA Global Precipitation Measurement (GPM) Integrated Multi-satellitE Retrievals for GPM (IMERG)NASA/GSFC Code**, 2019.

IGUCHI, T. et al. Rain-Profiling Algorithm for the TRMM Precipitation Radar. **Journal of Applied Meteorology**, v. 39, n. 12, p. 2038–2052, 2000.

IPCC. **Summary for Policymakers. In: Climate Change 2021: The Physical Science Basis. Contribution of Working Group I to the Sixth Assessment Report of the Intergovernmental Panel on Climate Change**. [s.l.] Cambridge University Press, 2021.

ISLAM, M. A. Statistical comparison of satellite-retrieved precipitation products with rain gauge observations over Bangladesh. **International Journal of Remote Sensing**, v. 39, n. 9, p. 2906–2936, 3 Mei 2018.

JESUS, E. T. et al. Meteorological and hydrological drought from 1987 to 2017 in Doce River Basin, Southeastern Brazil. **Revista Brasileira de Recursos Hídricos**, v. 25, p. 1–12, 2020.

JULIANI, B. H. T.; OKAWA, C. M. P. Application of a standardized precipitation index for meteorological drought analysis of the semi-arid climate influence in Minas Gerais, Brazil. **Hydrology**, v. 4, n. 2, 2017.

JUNQUEIRA, R. et al. Drought severity indexes for the Tocantins River Basin, Brazil. **Theoretical and Applied Climatology**, 2020a.

JUNQUEIRA, R. et al. Drought severity indexes for the Tocantins River Basin, Brazil. **Theoretical and Applied Climatology**, v. 140, p. 1–17, 3 Mei 2020b.

KAWOHI, T. O. **Evaluation of ERA5, ERA5-Land, and IMERG-F precipitation with a particular focus on elevation-dependent variations**. [s.l.] Universität Hamburg, 2019.

KIM, D.-I.; HAN, D. Evaluation of ERA-20cm reanalysis dataset over South Korea. **Journal of Hydro-Environment Research**, v. 23, n. January, p. 10–24, 2019.

KLINK, C. A.; MACHADO, R. B. Conservation of the Brazilian Cerrado. **Conservation Biology**, v. 19, n. 3, p. 707–713, 2005.

KUMMEROW, C.; BARNES, W. The Tropical Rainfall Measuring Mission (TRMM) Sensor Package. **Journal of Atmospheric and Oceanic Technology**, v. 15, n. 3, p. 809–817, 1998.

LE, M. H. et al. Adequacy of Satellite-derived Precipitation Estimate for Hydrological Modeling in Vietnam Basins. **Journal of Hydrology**, v. 586, n. February, 2020.

LEONARD, R. A.; KNISEL, W. G.; STILL, D. A. GLEAMS: Groundwater Loading Effects of Agricultural Management Systems. **Transactions of the ASAE**, v. 30, n. 5, p. 1403–

1418, 1987.

LI, D. et al. Adequacy of TRMM satellite rainfall data in driving the SWAT modeling of Tiaoxi catchment (Taihu lake basin, China). **Journal of Hydrology**, v. 556, p. 1139–1152, 2018.

MCKEE, T. B.; DOESKEN, N. J.; KLEIST, J. The relationship of drought frequency and duration to time scales. **Proceedings of the 8th Conference on Applied Climatology**, v. 17, n. 22, p. 179–183, 1993.

MEIRA NETO, A. A. et al. Improving streamflow prediction using uncertainty analysis and Bayesian model averaging. **Journal of Hydrologic Engineering**, v. 23, n. 5, p. 1–9, 2018.

MICHAELIDES, S. et al. Precipitation: Measurement, remote sensing, climatology and modeling. **Atmospheric Research**, v. 94, n. 4, p. 512–533, 2009.

MORADKHANI, H.; SOROOSHIAN, S. General Review of Rainfall-Runoff Modeling: Model Calibration, Data Assimilation, and Uncertainty Analysis. In: SOROOSH, S. et al. (Reds.). . **Hydrological Modelling and the Water Cycle**. Berlin, Heidelberg: Springer Berlin Heidelberg, 2009. v. 63p. 1–24.

MUÑOZ-SABATER, J. **ERA5-Land hourly data from 1981 to presentCopernicus Climate Change Service (C3S) Climate Data Store (CDS)**, 2019. Disponível em: <https://cds.climate.copernicus.eu/cdsapp#!/dataset/10.24381/cds.e2161bac?tab=overview>. Acesso em: 14 jul. 2021

MUÑOZ-SABATER, J. **ERA5-Land hourly data from 1950 to 1980Copernicus Climate Change Service (C3S) Climate Data Store (CDS)**, 2021. Disponível em: <https://cds.climate.copernicus.eu/cdsapp#!/dataset/reanalysis-era5-land?tab=overview>

MUÑOZ-SABATER, J. et al. ERA5-Land: a state-of-the-art global reanalysis dataset for land applications. **Earth System Science Data**, v. 13, n. 9, p. 4349–4383, 7 Sep 2021.

MYERS, N. et al. Biodiversity hotspots for conservation priorities. **Nature**, v. 403, n. 6772, p. 853–858, Feb 2000.

NEITSCH, S. L. et al. **Soil & Water Assessment Tool Theoretical Documentation: Version 2009**. Texas: [s.n.].

NG, T. L.; EHEART, J. W.; CAI, X. M. Comparative Calibration of a Complex Hydrologic Model by Stochastic Methods GLUE and PEST. **Transactions of the ASABE**, v. 53, n. 6, p. 1773–1786, 2010.

NOBRE, C. A. et al. Some Characteristics and Impacts of the Drought and Water Crisis in Southeastern Brazil during 2014 and 2015. **Journal of Water Resource and Protection**, v. 8, n. 2, p. 252–262, 2016.

OLIVEIRA, P. T. S. et al. Trends in water balance components across the Brazilian Cerrado. **Water Resources Research**, v. 50, n. 9, p. 7100–7114, Sep 2014.

OLIVEIRA, V. A. et al. Assessment of climate change impacts on streamflow and hydropower potential in the headwater region of the Grande river basin, Southeastern Brazil.

International Journal of Climatology, v. 37, n. 15, p. 5005–5023, 1 Des 2017.

OMM - ORGANIZAÇÃO METEOROLÓGICA MUNDIAL. **Standardized Precipitation Index User Guide WMO-No. 1090**Geneva, SwitzerlandOMM, , 2012. Disponível em: <http://library.wmo.int/opac/index.php?lvl=notice_display&id=13682>

OVERTON, D. E. Muskingum flood routing of upland streamflow. **Journal of Hydrology**, v. 4, p. 185–200, 1966.

PAZ, Y. M. et al. Sensitivity analysis and calibration of the SWAT model for a basin in northeastern Brazil using observed and reanalysis climatic data. **Revista Brasileira de Geografia Física**, v. 11, n. 1, p. 371–389, 2018.

PONTES FILHO, J. D. et al. Copula-Based Multivariate Frequency Analysis of the 2012–2018 Drought in Northeast Brazil. **Water**, v. 12, n. 3, p. 834, 16 Mrt 2020.

REBOITA, M. S. et al. Previsão Climática Sazonal para o Brasil Obtida Através de Modelos Climáticos Globais e Regional. **Revista Brasileira de Meteorologia**, v. 33, n. 2, p. 207–224, 2018.

ROCHA JÚNIOR, R. L. et al. Bivariate assessment of drought return periods and frequency in brazilian northeast using joint distribution by copula method. **Geosciences (Switzerland)**, v. 10, n. 4, p. 135, 2020.

RODRIGUES, J. A. M. et al. Climate change impacts under representative concentration pathway scenarios on streamflow and droughts of basins in the Brazilian Cerrado biome. **International Journal of Climatology**, p. 1–16, 28 Okt 2019.

ROSSATO, L. et al. Impact of soil moisture over Palmer Drought Severity Index and its future projections in Brazil. **Revista Brasileira de Recursos Hídricos**, v. 22, 2017.

ROZANTE, J. R. et al. Evaluation of TRMM/GPM Blended Daily Products over Brazil. **Remote Sensing**, v. 10, n. 6, p. 1–17, 2018.

SANTOS, U. et al. Fish fauna of the Pandeiros River, a region of environmental protection for fish species in Minas Gerais state, Brazil. **Check List**, v. 11, n. 1, p. 1507, 1 Jan 2015.

SCHIASSI, M. C. E. V. et al. Fruits from the Brazilian Cerrado region: Physico-chemical characterization, bioactive compounds, antioxidant activities, and sensory evaluation. **Food Chemistry**, v. 245, p. 305–311, 2018.

SILVA, VI. O.; MELLO, C. R. Meteorological droughts in part of southeastern Brazil: Understanding the last 100 years. **Anais da Academia Brasileira de Ciências**, v. 93, n. suppl 4, p. 1–17, 2021.

SOROOSHIAN, S. et al. Advanced concepts on remote sensing of precipitation at multiple scales. **Bulletin of the American Meteorological Society**, v. 92, n. 10, p. 1353–1357, 2011.

SOUZA, C. M. et al. Reconstructing Three Decades of Land Use and Land Cover Changes in Brazilian Biomes with Landsat Archive and Earth Engine. **Remote Sensing**, v. 12,

n. 17, p. 2735, 25 Aug 2020.

TAYLOR, K. E.; STOUFFER, R. J.; MEEHL, G. A. An Overview of CMIP5 and the Experiment Design. **Bulletin of the American Meteorological Society**, v. 93, n. 4, p. 485–498, 1 Apr 2012.

TERASSI, P. M. DE B. et al. Variabilidade do Índice de Precipitação Padronizada na Região Norte do Estado do Paraná Associada aos Eventos de El Niño-Oscilação Sul. **Revista Brasileira de Meteorologia**, v. 33, n. 1, p. 11–25, Mrt 2018.

TORRES, M. D. O. et al. Economic impacts of regional water scarcity in the São Francisco river Basin, Brazil: An application of a linked hydro-economic model. **Environment and Development Economics**, v. 17, n. 2, p. 227–248, 2012.

TUCCI, C. E. M. **Modelos Hidrológicos**. 2. ed. Porto Alegre: UFRGS, 2005.

UNIYAL, B. et al. Simulation of regional irrigation requirement with SWAT in different agro-climatic zones driven by observed climate and two reanalysis datasets. **Science of The Total Environment**, v. 649, p. 846–865, 2019.

VAN LOON, A. F. Hydrological drought explained. **Wiley Interdisciplinary Reviews: Water**, v. 2, n. 4, p. 359–392, 2015.

VICENTE-SERRANO, S. M. et al. Accurate Computation of a Streamflow Drought Index. **Journal of Hydrologic Engineering**, v. 17, n. 2, p. 318–332, Feb 2012.

WIGMOSTA, M. S.; VAIL, L. W.; LETTENMAIER, D. P. A distributed hydrology-vegetation model for complex terrain. **Water Resources Research**, v. 30, n. 6, p. 1665–1679, 1994.

WILHITE, D. A. **Droughts: A Global Assesment**. London: [s.n.].

WILHITE, D. A.; GLANTZ, M. H. Understanding: the Drought Phenomenon: The Role of Definitions. **Water International**, v. 10, n. 3, p. 111–120, 22 Jan 1985.

WILLIAMS, J. R. Flood Routing With Variable Travel Time or Variable Storage Coefficients. **Transactions of the ASAE**, v. 12, n. 1, p. 100–103, 1969.

WILLIAMS, J. R. **Sediment-yield prediction with universal equation using runoff energy factor**. [s.l.] ARS-S, 1975.

YAPO, P. O.; GUPTA, H. V.; SOROOSHIAN, S. Multi-objective global optimization for hydrologic models. **Journal of Hydrology**, v. 204, p. 83–97, 1998.

SEGUNDA PARTE – ARTIGOS

ARTIGO 1 - Hydrological Response to Drought Occurrences in a Brazilian Savanna Basin

Rubens Junqueira, Marcelo R. Viola, Jhones da S. Amorim and Carlos R. de Mello

Programa de Pós-Graduação em Recursos Hídricos, Departamento de Recursos Hídricos, Universidade Federal de Lavras, Lavras 3037, Minas Gerais, Brazil; marcelo.viola@ufla.br (M.R.V.); jhonesamorim@gmail.com (J.d.S.A.); crmello@ufla.br (C.R.d.M.)

ABSTRACT

The Brazilian savanna is one of the world's 25 biodiversity hotspots. However, droughts can decrease water availability in this biome. This study aimed to analyze meteorological and hydrological droughts and their influence on the hydrological behavior in a Brazilian savanna basin. For that, hydrological indicators were calculated to analyze the hydrological behavior in the Pandeiros river basin (PRB). The Standardized Precipitation Index (SPI) and Standardized Streamflow Index (SSI) were calculated for the hydrological year and rainy season from 1977 to 2018. The propagation of the meteorological to hydrological drought was studied by means of the Pearson coefficient of correlation between the SSI and SPI with 0, 3, 6, 9, and 12-month lags. A longer meteorological drought was observed from 2014/15 to 2017/18 which caused a reduction in the groundwater recharge, besides potentially reducing the ecological functions of the Brazilian savanna. This drought was intensified by an increase in the average annual temperature, resulting in the increasing of evapotranspiration. Regarding drought propagation, there is no significant difference among the coefficients of correlation from 0 to 6-month lags. For the lags of 9 and 12 months, the correlation decreases, indicating a greater influence of the current rainy season than the past ones.

Keywords: extreme events; hydrological indicators; SPI; water resources management

1. INTRODUCTION

The Brazilian savanna (known as "Cerrado") is the second-largest biome in South America, covering an area of 2 million km^2. It is one of the world's 25 biodiversity hotspots due to the endemic species concentration and the high degree of threat (HUNKE et al., 2015; MYERS et al., 2000). Moreover, this biome plays an important role in providing water, maintaining its ecohydrological functionality for industry, agriculture, navigation, tourism, and hydroelectricity in several Brazilian and South American basins, including the São Francisco river basin (SFRB) (OLIVEIRA et al., 2014). Therefore, it is important to conduct hydrological studies for better assisting water resource management in the Brazilian savanna aiming to maintain its eco-hydrological services (RODRIGUES et al., 2016).

Hydrological indicators, such as the aquifer restitution rate (ARR) and the surface runoff rate (SRR), have been widely used to evaluate the hydrological behavior of Brazilian river basins (MELLO; VIOLA; BESKOW, 2010; RODRIGUES et al., 2016; SILVA et al., 2017). Nevertheless, during extreme events, for example, floods and droughts, the basin may present different behavior. Extreme drought events can abnormally reduce the streamflow, agricultural production, lake and reservoir levels, and groundwater recharge (VAN LOON, 2015).

Recently, several studies on drought have been developed in Brazil focused on meteorological droughts (JULIANI; OKAWA, 2017; PONTES FILHO et al., 2020; ROCHA JÚNIOR et al., 2020). According to Van Loon (2015), this drought is associated with a deficiency in precipitation, and possibly an increase in evapotranspiration. However, few studies have attempted to analyze the influence of meteorological drought on the streamflow (hydrological drought).

Although the origin of hydrological drought is commonly related to meteorological drought, other factors can influence it, highlighting lithology, vegetation, and human influence (VICENTE-SERRANO et al., 2012). Junqueira et al. (2020) reported a longer hydrological drought than meteorological ones from 2015 to 2017 due to the reduction in groundwater recharge in previous seasons in the Tocantins river basin, Brazil. As a result, the effects on irrigation, hydroelectricity, and urban supply were prolonged.

To analyze the occurrence, duration, and intensity of droughts, several indexes have been developed in recent years. The Standardized Precipitation Index (SPI) (MCKEE; DOESKEN; KLEIST, 1993) has been widely used in Brazil and worldwide (JESUS et al., 2020; JUNQUEIRA et al., 2020; SIENZ; BOTHE; FRAEDRICH, 2012; VICENTE-SERRANO et al., 2020). According to the World Meteorological Organization (WMO, 2012), this index is considered standard due to its accuracy and simplicity. Several indexes have emerged from the

SPI, such as the Standardized Streamflow Index (SSI) (VICENTE-SERRANO et al., 2012), a hydrological drought index with the same characteristics as the SPI. These indexes represent anomalies from a normal situation and allow for comparison in different regions (VAN LOON, 2015).

To calculate a standardized index, a Probability Distribution Function (PDF) is required. McKee, Doesken and Kleist (1993) applied the two parameters of Gamma distribution for SPI. Nevertheless, to be more accurate in estimating droughts, Vicente-Serrano et al. (2012) suggested it the most suitable PDF rather than adopting a single distribution for all situations. An inappropriate PDF may over- or underestimate the magnitude of the drought, as the extreme events are in the tail of the PDF (SIENZ; BOTHE; FRAEDRICH, 2012). Therefore, researchers have analyzed several PDFs to calculate standardized drought indexes and found different results worldwide (JAHANGIR; ABOLGHASEMI, 2019; PIEPER; DÜSTERHUS; BAEHR, 2020; VICENTE-SERRANO et al., 2012).

In this context, this study aimed to analyze the occurrence, intensity, duration, and propagation of meteorological to hydrological droughts and their influence on the hydrological behavior in a Brazilian savanna basin.

2. MATERIALS AND METHODS

2.1.Study Area

The Pandeiros river basin (PRB), located in the north Minas Gerais State, is inserted in the Brazilian savanna and has an area of 3220 km^2. Due to its ecological relevance for the Brazilian savanna and for the SFRB, the Pandeiros River Environmental Protection Area was created through State Law n° 11,901 to protect the native fish species, which represent 70% of the reproduction and development fish from the middle São Francisco River (NUNES et al., 2009; SANTOS et al., 2015). Figure 1 shows the PRB location, the streamflow and rain gauge stations, and the Digital Elevation Model (DEM) ALOS (Advanced Land Observing Satellite)

PALSAR (Phased Array L-band Synthetic Aperture Radar), with a spatial resolution of 12.5 m.

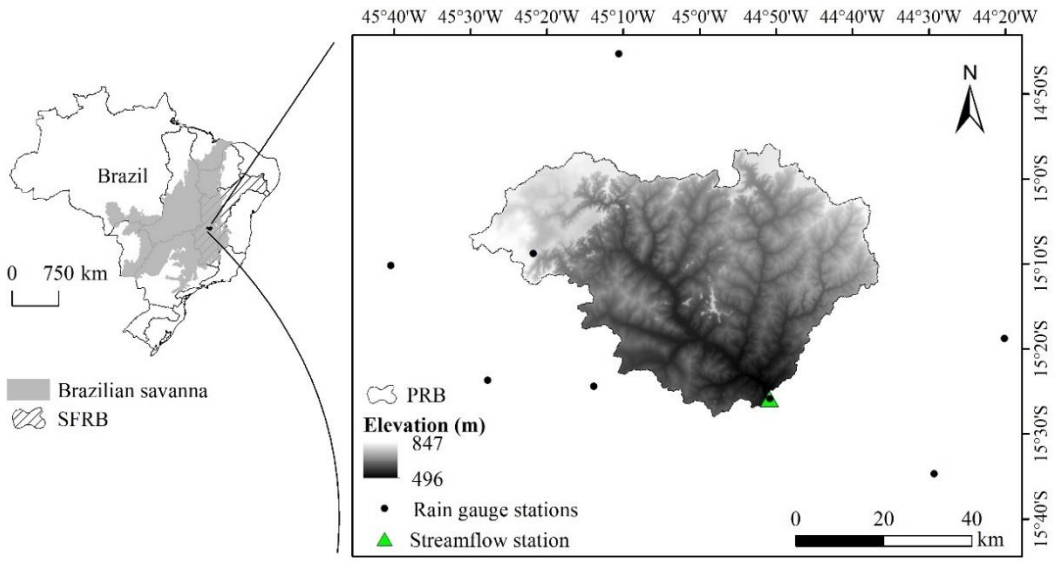

Figure 1. Locations of the PRB, streamflow and rain gauge stations, and DEM.

The elevation ranges from 496 to 847 m, with an average of 677 m. The climate, according to Köppen type-climate classification, is Aw (tropical with wet summers and dry winters) (ALVARES et al., 2013). The average precipitation for the hydrological year (October to September) is 1085 mm, of which 92% occurs during the rainy period (October to March).

The predominant soil in the PRB is the Latosol, which covers 88.3% of its area (FEAM, 2010), and the natural pasture, typical of the Brazilian savanna, is the land use predominant, covering 96.3% of the basin's area (IBGE, 2018).

2.2.Input Data

Daily streamflow and precipitation datasets were obtained from the Brazilian National Water Agency (ANA) from October 1977 to September 2018 (41 hydrological years), using only those with up to 10% of gaps, aiming to meet the data quality standards for carrying out drought analysis (JAHANGIR; ABOLGHASEMI, 2019). The double mass curve was used to analyze the homogeneity and consistency of the precipitation series (GAO et al., 2017). Then, gap filling was carried out on a monthly time scale using the Inverse Squared Distance Weighted method. The basin-scale precipitation was obtained using the area-weighted procedure with the eight rain gauge stations available (Figure 1) (GAO; LI, 2018).

2.3.Hydrological Behavior

2.3.1. Baseflow

To appraise the hydrological behavior of the PRB, the baseflow was taken using the recursive digital filters method, which divides the streamflow into direct surface runoff and baseflow (Equation (1)) (ECKHARDT, 2005).

$$y_k = f_k + b_k \quad (1)$$

where: *y* is the total streamflow ($m^3\ s^{-1}$); *f* is the direct surface runoff ($m^3\ s^{-1}$); *b* is the baseflow ($m^3\ s^{-1}$); and *k* is the time step (day).

For b_k calculation, the methodology proposed by Eckhardt (2005) for the general form of the recursive filter with one parameter is given by Equation (2).

$$b_k = \frac{(1 - BFI_{max}) \times a \times b_{k-1} + (1 - a) \times BFI_{max} \times y_k}{1 - a \times BFI_{max}} \quad (2)$$

where: BFI_{max} is the maximum value of the baseflow index that can be assumed equal to 0.8 as recommended by Eckhardt (2005) for perennial streams; and a corresponds to the groundwater recession constant (0.8925), dimensionless. This model assumes that the aquifer outflow is linearly proportional to its storage, which means an exponential recession of baseflow during the period without groundwater recharge (ECKHARDT, 2005).

2.3.2. Hydrological Indicators

The hydrological indicators adopted to study the hydrological behavior in the PRB are presented in Table 1.

Table 1. Hydrological indicators used in this study.

Hydrological Indicator	Abbreviation	Unit
Depletion coefficient	α	day^{-1}
Water depth stored in the aquifer at the end of the hydrological year	A_f	mm
Baseflow index	BFI	-
Aquifer restitution rate	ARR	%
Evapotranspiration rate	ETR	%
Surface runoff rate	SRR	%
Long-term streamflow	Q_{mean}	$m^3\ s^{-1}$
Minimum streamflow	Q_{min}	$m^3\ s^{-1}$
Maximum streamflow	Q_{max}	$m^3\ s^{-1}$
Minimum streamflow that occurs in 90% of the time	$Q_{90\%}$	$m^3\ s^{-1}$
Minimum streamflow that occurs in 95% of the time	$Q_{95\%}$	$m^3\ s^{-1}$
Minimum streamflow in seven consecutive days and a return period of 10 years	$Q_{7,10}$	$m^3\ s^{-1}$
Specific yield (SY) related to Q_{mean}, Q_{min}, Q_{max}, $Q_{90\%}$, $Q_{95\%}$, and $Q_{7,10}$	SY_{mean}, SY_{min}, SY_{max}, $SY_{90\%}$, $SY_{95\%}$, and $SY_{7,10}$, respectively	$L\ s^{-1}\ km^{-2}$

BFI is the long-term ratio between baseflow and total streamflow and the closer to 1 it is, the greater the contribution of baseflow to the streamflow. The ARR was obtained by the long-term ratio between baseflow and precipitation and indicates the precipitation rate that contributes to aquifer restitution. The evapotranspiration was calculated based on annual water balance (ET = precipitation − total streamflow, in mm), and then the ETR was calculated as ET divided by precipitation. The SRR consists of the long-term ratio between direct surface runoff (SR = total streamflow − baseflow) and precipitation. The α and A_f are described in Equations (3) and (4). According to Silva, Bacellar and Fernandes (2010), α values close to zero indicate higher natural regularization capacity.

$$Q_t = Q_0 \times e^{-\alpha.t} \tag{3}$$

$$A_f = \frac{Q_i \times 86.4}{\alpha \times A_b} \tag{4}$$

where Q_0 was the streamflow at the beginning of the recession, in $m^3 s^{-1}$; Q_t is the streamflow after t days of the beginning of the recession, in $m^3 s^{-1}$; Q_i is the streamflow at the end of the hydrological year, in $m^3 s^{-1}$; and A_b is the basin's area, in km^2.

The Q_{mean} was obtained from the average of the daily streamflow, while the Q_{min} and Q_{max} were obtained from the average of the minimum and maximum daily annual streamflow, respectively. To obtain $Q_{7,10}$, 10 PDFs fitted using the L-moments were analyzed (AMORIM et al., 2020): the 3-parameter log-normal (LN3), 3-parameter Pearson (PE3), the Gumbel extreme value, the Generalized Extreme Values (GEV), Gamma, Weibull, the 4-parameter Kappa, the 5-parameter Wakeby, the generalized logistic (GLO), and the generalized Pareto (GPA). The PDF was then selected based on the best fitting according to the Anderson–Darling (AD) test. The $Q_{90\%}$ and $Q_{95\%}$ were obtained based on the flow-duration curve. The SY is the result of the calculated streamflows ($Q_{90\%}$, $Q_{95\%}$, etc.) divided by the basin's area, which allows comparing them among different regions or sub-basins.

2.4.Meteorological and Hydrological Droughts

To analyze the occurrence, intensity, and duration of the droughts in the PRB, the SPI (MCKEE; DOESKEN; KLEIST, 1993) and SSI (VICENTE-SERRANO et al., 2012) were calculated by year, considering the hydrological year (October to September), and for half-year time scales, considering the rainy season (October to March).

For the SPI and SSI calculation, the basin-scale precipitation and streamflow series, respectively, were accumulated for the studied period and a PDF was fitted. Following that, they were transformed into a normal distribution, with mean and variance, respectively, equal to zero and one. The analysis of the most suitable PDF was performed in a similar way to the $Q_{7,10}$. This procedure, according to Vicente-Serrano et al. (2012), allows higher precision in obtaining drought indexes. Afterward, the indexes were classified following the WMO (2012) classification (Table 2).

Table 2. Classification for the SPI and SSI values.

Classification	Indexes Values	Probability (%)
Extremely dry (ED)	SPI and SSI ≤ −2.0	2.3
Severely dry (SD)	−2.0 < SPI and SSI ≤ −1.5	4.4
Moderately dry (MD)	−1.5 < SPI and SSI ≤ −1.0	9.2
Near normal (NN)	−1.0 < SPI and SSI < 1.0	68.2
Moderately wet (MW)	1.0 ≤ SPI and SSI < 1.5	9.2
Very wet (VW)	1.5 ≤ SPI and SSI < 2.0	4.4
Extremely wet (EW)	SPI and SSI ≥ 2.0	2.3

The Pearson correlation of the coefficient (r) with a statistical significance of 5% (α = 0.05) was used to analyze the correlation between the SPI and SSI on different time scales. In addition, to assess the propagation of meteorological to hydrological drought, the correlations between the 0, 3, 6, 9, and 12-month lags with both the SSI and SPI were performed on an annual scale.

3. RESULTS AND DISCUSSION

3.1.Hydrological Behavior

Figure 2A presents the average monthly precipitation, streamflow, and baseflow for the PRB. Surface runoff occurs predominantly in the rainy season, whereas in the dry season, it is the baseflow. The BFI indicator was equal to 0.80, which is a characteristic of perennial rivers (ECKHARDT, 2005), showing the importance of baseflow over the total streamflow in the studied basin. The ARR for the PRB was 14.9%, a high value when considering that 81.4% of the precipitation returns to the atmosphere by evapotranspiration (ETR). Besides, only 3.7% of the total precipitation is converted to surface runoff (SRR). The high ARR and low SRR values are associated with the predominance of Latosol, which is a deep soil with a high infiltration capacity (JUNQUEIRA JUNIOR et al., 2017), occurring in a flatter topography (average slope

of 5.9%). Moreover, the PRB is part of an environmental protection area and its vegetation has been preserved, which favors the soil-water infiltration and reduces direct surface runoff.

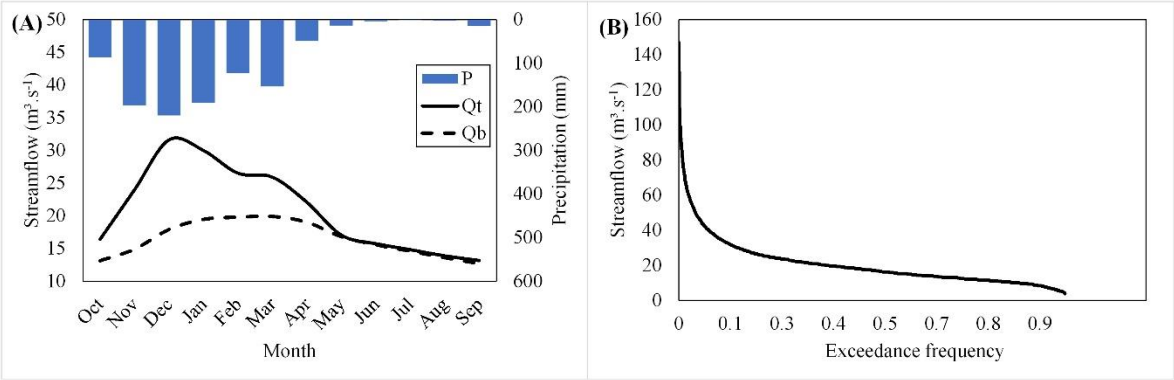

Figure 2. Hydrograph containing average monthly precipitation (P), total streamflow (Qt), and baseflow (Qb) (A); and permanent flow curve (B).

The SY_{mean} obtained for the PRB was 6.46 L s^{-1} km^{-2}, while the SY_{min} and SY_{max} were 3.6 and 24.8 L s^{-1} km^{-2}, respectively. These values are low when compared to others obtained for Brazilian savanna basins such as by Rodrigues et al. (2016) in the Manual Alves da Natividade river basin. However, the ETR obtained by Rodrigues et al. (2016) was 69.1%, lower than that obtained in the PRB (81.4%). Therefore, the high evapotranspiration contributed to the reduction of the streamflow in the PRB.

Regarding $Q_{7,10}$ (6.9 m^3 s^{-1}), for the streamflow that is used as a basis for granting water resources in the region, the PDF that presented the best fitting was Wakeby, with AD equal to 0.30. Amorim et al. (2020) found a similar result in the Mortes River, Southeastern Brazil, demonstrating the satisfactory performance of this PDF for the Q_7 series. The $SY_{7,10}$ was equal to 2.1 L s^{-1} km^{-2}, similar to that obtained by Silva et al. (2017) in the Minas Gerais State. According to the Euclydes, Ferreira and Faria Filho (2005) classification, the PRB has a high natural regularization capacity once $SY_{7,10}$ corresponds to 33% of SYmean, which follows the α value close to zero (0.0073). The α is close to that obtained by Freitas and Bacellar (2013) in sub-basins of the upper São Francisco River and by Junqueira et al. (2020) in the Tocantins river basin. From the flow-duration curve (Figure 2B), $Q_{90\%}$ and $Q_{95\%}$ was equal to 9.7 and 7.7 m^3 s^{-1}, respectively, which generated SY_{90} equal to 3.0 L s^{-1} km^{-2} and SY_{95} equal to 2.4 L s^{-1} km^{-2}, higher than $SY_{7,10}$.

3.2.Meteorological and Hydrological Droughts

Among the PDFs analyzed, Weibull presented a better fit in two historical series, whereas Wakeby showed better performance in six. Although McKee, Doesken and Kleist

(1993) have used Gamma for the SPI calculation, this PDF did not produce the best fit in either case. GPA presented unsatisfactory results for the basin-scale precipitation and streamflow series, not being approved in the AD test in both time scales. Table 3 presents the AD test results for the basin-scale precipitation and streamflow series for the hydrological years and rainy seasons obtained from each PDF.

Table 3. AD test results for the basin-scale precipitation and streamflow for the PRB.

PDF	Precipitation						Streamflow	
	Hy	**L3**	**L6**	**L9**	**L12**	**Rs**	**Hy**	**Rs**
Gumbel	0.929	0.874	0.690	0.886	0.249	0.527	0.348	0.462
Gamma	0.562	0.452	0.386	0.376	0.250	0.262	0.381	0.524
GEV	0.552	0.421	0.387	0.320	0.216	0.258	0.350	0.465
Kappa	0.537	0.398	0.368	0.318	0.217	0.243	0.359	0.520
GLO	0.612	0.492	0.456	0.359	0.244	0.341	0.423	0.567
GPA	-	-	-	-	-	-	-	-
Weibull	0.528 *	0.397 *	0.358	0.300	-	0.239	-	-
Wakeby	0.711	0.467	0.325 *	0.279 *	0.202 *	0.206 *	0.281 *	0.388 *
PE3	0.552	0.424	0.385	0.315	0.229	0.260	0.363	0.478
LN3	0.553	0.425	0.388	0.315	0.222	0.262	0.356	0.470

Note: * Best fit, Hy = Hydrological year, L3 = 3 months lag, L6 = 6 months lag, L9 = 9 months lag, L12 = 12 months lag, Rs = Rainy season.

The SPI and SSI results for the hydrological years and rainy seasons, calculated according to the most suitable PDF, can be observed in Figure 3. There is an agreement between the SPI values for the hydrological year and the rainy season (r = 0.96). A similar result is observed in the SSI, where r = 0.99. However, when comparing the SPI against the SSI at the two-time scales, the correlation decreases (r = 0.64). This is due to the complexity of the factors associated with the hydrological cycle in the basins, where the response to precipitation depends on factors such as vegetation, lithology, and topography (VICENTE-SERRANO et al., 2012).

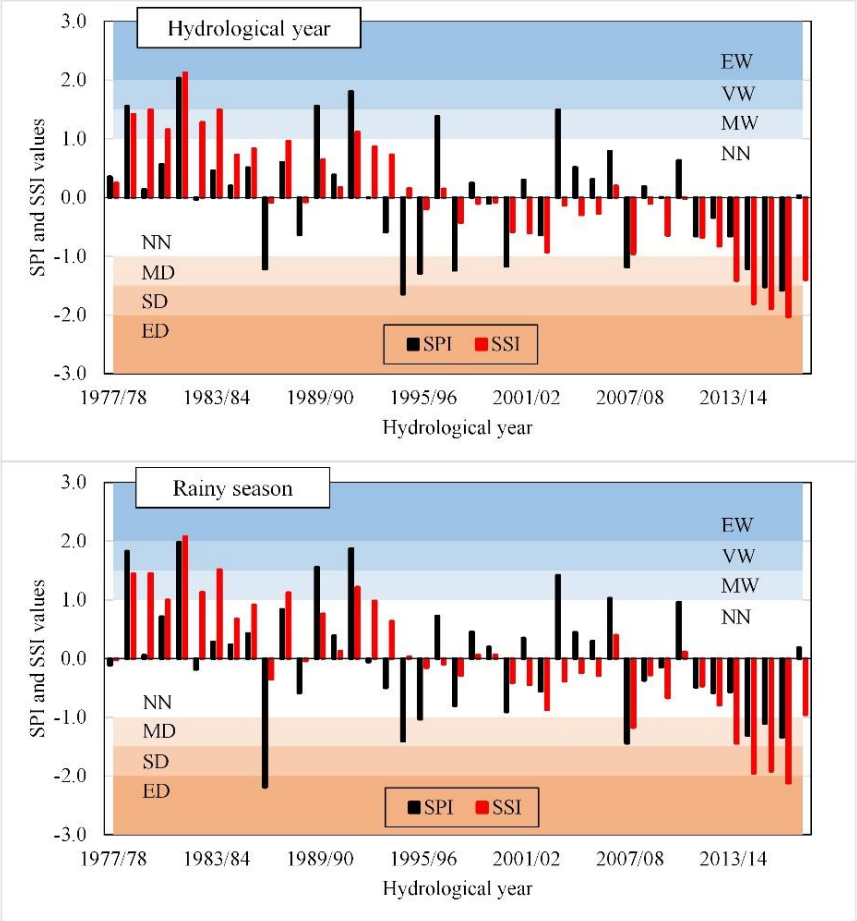

Figure 3. SPI and SSI results for hydrological years and rainy seasons in the PRB.

The most significant meteorological droughts occurred during the hydrological years of 1986/87, 1994/95, 1995/96, 1997/98, 2007/08, and between 2014/15 and 2016/17 in the PRB. Similar behavior was observed for the rainy season, however, with some differences concerning intensity. Although the dry season accounted for only 8% of annual precipitation, the total precipitation in this period for the hydrological year of 1986/87 was 171.1 mm, approximately twice the average (89.5 mm). Therefore, the attenuation of drought on a hydrological year scale may have occurred due to increased precipitation in the dry season.

As a result of some years with below-average precipitation, the hydrological years between 2013/14 to 2017/18 presented a long and intense hydrological drought. In these years, there was a high reduction in the long-term mean streamflow, from 20.8 $m^3\ s^{-1}$ in the whole period to 10.3 $m^3\ s^{-1}$ for the drought period (2013/14 to 2017/18), which is lower than the minimum streamflow for the entire studied period (11.5 $m^3\ s^{-1}$). Also, there was a significant reduction in ARR (14.9 to 9.2%), SRR (3.7 to 2.4%), SY_{mean} (6.5 to 3.2 L $s^{-1}\ km^{-2}$), SY_{min} (3.6 to 1.5 L $s^{-1}\ km^{-2}$), and SY_{max} (24.8 to 17.4 L $s^{-1}\ km^{-2}$).

Besides the reduction in precipitation, the increase in temperature and, consequently, in evapotranspiration, contributed to the hydrological drought intensification, as highlighted by Van Loon (2015) and Junqueira et al. (2020). According to data obtained from the Brazilian National Institute of Meteorology (INMET) using a weather station close to the basin (Januária station), the daily annual average temperature from 1977/78 to 2012/13 was 23.4 °C, however, from 2013/14 to 2017/18 there was an increase of 1.3 °C. Thus, the ETR in this period was equal to 88.4%, higher than the average observed in the studied period (81.4%).

Studies suggest an increase in the intensity and frequency of droughts by the end of the century worldwide due to atmospheric evaporative demand increases, reducing water availability, soil water storage, and agricultural production (DAI; ZHAO; CHEN, 2018; RODRIGUES et al., 2019; VICENTE-SERRANO et al., 2020). Yet, Santos et al. (2020) observed a reduction in the water table in the PRB wetlands, downstream of the streamflow gauge station of this study, due to a reduction in precipitation and an increase in temperature in recent years, affecting vegetation dynamics in the wetland.

During the period 2013/14 to 2017/18, similar events were found in other Brazilian regions such as the Doce river basin (JESUS et al., 2020), Tocantins river basin (JUNQUEIRA et al., 2020), Northeastern Brazil (MARENGO et al., 2018), Amazon (MARENGO et al., 2018), Paraná river basin (MELO et al., 2016), the metropolitan region of São Paulo (NOBRE et al., 2016), and Ceará State (PONTES FILHO et al., 2020), affecting the hydropower generation and urban supply. Besides, droughts can affect the ecological functions of the Brazilian savanna (RODRIGUES et al., 2019), as well as reduce the native fish species and increase exotic species (RAMÍREZ et al., 2018).

According to Azevedo et al. (2018), after a long period of drought, the Sobradinho hydropower plant reservoir, located in SFRB and responsible for almost 60% of the water resources in Northeastern Brazil, presented a reduction of up to 50% in surface water in 2015/16. In that year, hydropower generation was only 170 MW (its total installed power is 1050 MW).

Some researchers associate drought occurrence with anomalies in sea surface temperatures in the Pacific and the Atlantic Oceans (JUNQUEIRA et al., 2020; MARENGO et al., 2018; PONTES FILHO et al., 2020). Santos et al. (2019) reported that anomalies in the El Niño-Southern Oscillation (ENSO) phenomenon are related to the cycle of meteorological droughts in the region in which the PRB is located, however, the Pacific Decadal Oscillation (PDO) influence has not been identified as having a clear influence on drought events in this region. El Niño (positive phase of the ENSO) occurred during all the years in which there was

a meteorological drought in the PRB, except for 2007/08 and 2016/17, when the La Niña phenomenon (negative phase of the ENSO) took place for some months. Junqueira et al. (2020) and Marengo et al. (2018) also found the influence of the ENSO on the drought occurrences in the Tocantins river basin and Northeastern Brazil. According to Garreaud et al. (2009), although the PDO-related precipitation and temperature anomalies have the same behavior as the ENSO in South America, their effects seem to be less intense in the PRB region.

3.3.Drought Propagation

Table 4 presents the correlation results between the SSI and SPI with a lag of 0, 3, 6, 9, and 12 months, both on an annual scale. There is no difference between the r values from a 0 to 6-month lag. However, a higher correlation was obtained for the 3-month lag, indicating a lag in the propagation of the meteorological drought to the hydrological one. A similar result was found by Rodrigues et al. (2019) in sub-basins of the Tocantins River, where the correlation between the indices was higher in the period from 0 to 3 months.

Table 4. r results between the SSI and the SPI with a lag of 0, 3, 6, 9, and 12 months.

SPI Lags (Months)	0	3	6	9	12
r	0.64	0.65	0.64	0.47	0.39

Furthermore, the correlation is lower for 9 and 12-month lags, that is, changes in streamflow are more influenced by the current than the past rainy season. According to Van Loon (2015), rainfall deficit in the rainy season can influence following dry season conditions. In cases of longer meteorological drought, there may be a reduction in groundwater recharge, affecting the streamflow even after the meteorological conditions return to normal, as also reported by Jesus et al. (2020) in the Doce river basin and by Junqueira et al. (2020) in the Tocantins river basin. As an example, in the hydrological year 2017/18, the SPI was classified as near normal, however, the SSI was classified as moderately dry. This increase in precipitation from one year to the next attenuated the hydrological drought but was not enough to fill the recharge deficit from previous years.

According to Junqueira et al. (2020), baseflow depends on the precipitation/recharge rate in previous months, as well as on aquifer characteristics. As the streamflow in the PRB is strongly influenced by baseflow (BFI = 0.80), the deficiency in groundwater recharge has a prolonged effect on the streamflow. This deficiency is confirmed by the A_f values, where, from 2013/14 to 2017/18, the average was 21.1 mm, less than half the historical average (48.9 mm). The recharging deficiency increased during the drought until it reached its lowest value at the

end of 2016/17 (A_f = 16.3 mm). After the 2017/18 hydrological year, there was a slight recovery of water storage in the aquifer (A_f = 20.0 mm) due to the increase in precipitation, however, it remained below the historical average.

4. CONCLUSIONS

The SPI allowed us to identify the main droughts that hit the PRB (1986/87, 1994/95, 1995/96, 1997/98, 2000/01, 2007/08, 2014/15, 2015/16, and 2016/17). These events may be related to the occurrence of macro-scale climatic phenomena such as the ENSO, as observed in other Brazilian regions. Although the droughts observed in hydrological years presented a high correlation with the drought during the rainy season, the dry season can occasionally influence the drought intensity.

The hydrological drought from 2013/14 to 2017/18 occurred mainly due to a prolonged reduction in precipitation, reducing water availability, and affecting the fish reproduction in the PRB and SFRB and the ecological functions of the Brazilian savanna. In addition to the reduction in precipitation, the increase in temperature and, consequently, in evapotranspiration contributed to the intensification of the hydrological drought in the cited period.

Based on the hydrological indicators, a high influence of baseflow on the total streamflow (BFI = 0.8) and evapotranspiration (81.4% of the total precipitation) on the hydrological behavior of the PRB was observed. Moreover, the analysis of hydrological indicators highlighted the influence of droughts on groundwater recharge, evidenced by a reduction in A_f values.

The propagation of meteorological to hydrological drought occurred in shorter lags (0 to 6 months), with greater correlation in 3-month lag. However, for the lags of 9 and 12 months, the correlation decreased, indicating that changes in streamflow are more influenced by the current than previous rainy seasons.

REFERENCES

ALVARES, C. A. et al. Köppen's climate classification map for Brazil. **Meteorologische Zeitschrift**, v. 22, n. 6, p. 711–728, 2013.

AMORIM, J. DA S. et al. Streamflow regionalization for the Mortes River Basin upstream from the Funil Hydropower Plant, MG. **Ambiente e Água,** v. 15, n. 3, p. 1–11, 15 Mei 2020.

AZEVEDO, S. C. DE et al. Analysis of the 2012-2016 drought in the northeast Brazil and its impacts on the Sobradinho water reservoir. **Remote Sensing Letters**, v. 9, n. 5, p. 438–446, 2018.

BRAZILIAN INSTITUTE OF GEOGRAPHY AND STATISTICS (IBGE). **Mapa de Cobertura e Uso da Terra do Brasil 2010,** 2018. Disponível em: <https://www.ibge.gov.br/geociencias/informacoes-ambientais/cobertura-e-uso-da-terra/15831-cobertura-e-uso-da-terra-do-brasil.html?edicao=16023&t=sobre>

DAI, A.; ZHAO, T.; CHEN, J. Climate Change and Drought: a Precipitation and Evaporation Perspective. **Current Climate Change Reports**, v. 4, n. 3, p. 301–312, 2018.

ECKHARDT, K. How to construct recursive digital filters for baseflow separation. **Hydrological Processes**, v. 19, n. 2, p. 507–515, 2005.

EUCLYDES, H. P.; FERREIRA, P. A.; FARIA FILHO, R. F. **Atlas digital das águas de Minas**. 1st. ed. Viçosa: UFV, 2005.

FREITAS, S.; BACELLAR, L. Avaliação da Recarga de Aquíferos em Microbacias do Alto Rio das Velhas, Minas Gerais. **Revista Brasileira de Recursos Hídricos**, v. 18, n. 2, p. 31–38, 2013.

GAO, C.; LI, X. Precipitation thresholds of drought disaster for maize in areas in front of Bengbu Sluice, Huaihe River Basin, China. **Water (Switzerland)**, v. 10, n. 10, 2018.

GAO, P. et al. Use of double mass curves in hydrologic benefit evaluations. **Hydrological Processes**, v. 31, n. 26, p. 4639–4646, 2017.

GARREAUD, R. D. et al. Present-day South American climate. **Palaeogeography, Palaeoclimatology, Palaeoecology**, v. 281, n. 3–4, p. 180–195, 2009.

HUNKE, P. et al. The Brazilian Cerrado: Assessment of water and soil degradation in catchments under intensive agricultural use. **Ecohydrology**, v. 8, n. 6, p. 1154–1180, 2015.

JAHANGIR, M. H.; ABOLGHASEMI, M. Determining the most appropriate probability distribution function for calculate and compare the SPEI and SPI drought index in Tehran. **Desert Ecosystem Engineering Journal**, v. 8, n. 23, p. 1–16, 2019.

JESUS, E. T. et al. Meteorological and hydrological drought from 1987 to 2017 in Doce River Basin, Southeastern Brazil. **Revista Brasileira de Recursos Hídricos**, v. 25, p. 1–12, 2020.

JULIANI, B. H. T.; OKAWA, C. M. P. Application of a standardized precipitation index for meteorological drought analysis of the semi-arid climate influence in Minas Gerais, Brazil. **Hydrology**, v. 4, n. 2, 2017.

JUNQUEIRA JUNIOR, J. A. et al. Time-stability of soil water content (SWC) in an Atlantic Forest - Latosol site. **Geoderma**, v. 288, p. 64–78, 2017.

JUNQUEIRA, R. et al. Drought severity indexes for the Tocantins River Basin, Brazil. **Theoretical and Applied Climatology**, v. 140, p. 1–17, 3 Mei 2020.

MARENGO, J. A. et al. Climatic characteristics of the 2010-2016 drought in the semiarid northeast Brazil region. **Anais da Academia Brasileira de Ciencias**, v. 90, n. 2, p. 1973–1985, 2018.

MCKEE, T. B.; DOESKEN, N. J.; KLEIST, J. The relationship of drought frequency and duration to time scales. **Proceedings of the 8th Conference on Applied Climatology**, v. 17, n. 22, p. 179–183, 1993.

MELLO, C. R.; VIOLA, M. R.; BESKOW, S. Vazões máximas e mínimas na região do Alto Rio Grande, MG. **Ciência e Agrotecnologia**, v. 34, n. 2, p. 494–501, 2010.

MELO, D. C. D. et al. Reservoir storage and hydrologic responses to droughts in the Paraná River basin, south-eastern Brazil. **Hydrology and Earth System Sciences**, v. 20, n. 11, p. 4673–4688, 2016.

MINAS GERAIS STATE ENVIRONMENTAL FOUNDATION (FEAM). **Mapa de solos do Estado de Minas Gerais**, 2010.

MYERS, N. et al. Biodiversity hotspots for conservation priorities. **Nature**, v. 403, n. 6772, p. 853–858, Feb 2000.

NOBRE, C. A. et al. Some Characteristics and Impacts of the Drought and Water Crisis in Southeastern Brazil during 2014 and 2015. **Journal of Water Resource and Protection**, v. 8, n. 2, p. 252–262, 2016.

NUNES, Y. R. F. et al. Pandeiros: o Pantanal Mineiro. MG. **Biota**, v. 2, n. 2, p. 4–17, 2009.

OLIVEIRA, P. T. S. et al. Trends in water balance components across the Brazilian Cerrado. **Water Resources Research**, v. 50, n. 9, p. 7100–7114, Sep 2014.

PIEPER, P.; DÜSTERHUS, A.; BAEHR, J. Global and regional performances of SPI candidate distribution functions in observations and simulations. **Hydrology and Earth System Sciences Discussions**, n. January, p. 1–33, 2020.

PONTES FILHO, J. D. et al. Copula-Based Multivariate Frequency Analysis of the 2012–2018 Drought in Northeast Brazil. **Water**, v. 12, n. 3, p. 834, 16 Mrt 2020.

RAMÍREZ, A. et al. Drought facilitates species invasions in an urban stream: Results from a long-term study of tropical island fish assemblage structure**. Frontiers in Ecology and Evolution**, v. 6, p. 1–11, 2018.

ROCHA JÚNIOR, R. L. et al. Bivariate assessment of drought return periods and frequency in brazilian northeast using joint distribution by copula method. **Geosciences (Switzerland)**, v. 10, n. 4, p. 135, 2020.

RODRIGUES, J. A. M. et al. Indicadores hidrológicos para a gestão de recursos hídricos na bacia hidrográfica do rio Manuel Alves Da Natividade, Tocantins. **Scientia Agraria**, 2016.

RODRIGUES, J. A. M. et al. Climate change impacts under representative concentration pathway scenarios on streamflow and droughts of basins in the Brazilian Cerrado biome. **International Journal of Climatology**, p. 1–16, 28 Okt, 2019.

SANTOS, G. L. et al. Anthropogenic and climatic influences in the swamp environment of the Pandeiros River basin, Minas Gerais-Brazil. **Environmental Monitoring and Assessment**, v. 192, n. 4, 2020.

SANTOS, M. S. et al. Time-space characterization of droughts in the São Francisco river catchment using the Standard Precipitation Index and continuous wavelet transform. **Revista Brasileira de Recursos Hidricos**, v. 24, p. 1–12, 2019.

SANTOS, U. et al. Fish fauna of the Pandeiros River, a region of environmental protection for fish species in Minas Gerais state, Brazil. **Check List**, v. 11, n. 1, p. 1507, 1 Jan 2015.

SIENZ, F.; BOTHE, O.; FRAEDRICH, K. Monitoring and quantifying future climate projections of dryness and wetness extremes: SPI bias. **Hydrology and Earth System Sciences**, v. 16, n. 7, p. 2143–2157, 2012.

SILVA, L. A. et al. Minimum and reference discharges and specific yield for the state of Minas Gerais, Brazil. **Revista Brasileirade Ciencias Agrarias**, v. 12, n. 4, p. 543–549, 2017.

SILVA, R. F. G.; BACELLAR, L. DE A. P.; FERNANDES, K. N. Estimativa de parâmetros de aquíferos através do coeficiente de recessão em áreas de embasamento cristalino de Minas Gerais. **Rem: Revista Escola de Minas**, v. 63, n. 3, p. 465–471, Sep 2010.

VAN LOON, A. F. Hydrological drought explained. **Wiley Interdisciplinary Reviews: Water**, v. 2, n. 4, p. 359–392, 2015.

VICENTE-SERRANO, S. M. et al. Accurate Computation of a Streamflow Drought Index. **Journal of Hydrologic Engineering**, v. 17, n. 2, p. 318–332, Feb 2012.

VICENTE-SERRANO, S. M. et al. Global characterization of hydrological and meteorological droughts under future climate change: The importance of timescales, vegetation-CO2 feedbacks and changes to distribution functions. **International Journal of Climatology**, v. 40, n. 5, p. 2557–2567, 2020.

WMO - WORLD METEOROLOGICAL ORGANIZATION. **Standardized Precipitation Index User Guide.** WMO - No. 1090WMO-No. 1090 ©Geneva, SwitzerlandWMO, 2012. Disponível em: <http://library.wmo.int/opac/index.php?lvl=notice_display&id=13682>

ARTIGO 2 - Hydrological modeling using remote sensing precipitation data in a Brazilian savanna basin

Rubens Junqueira[1], Marcelo R. Viola[1], Jhones da S. Amorim[1], Carla Camargos[2], and Carlos R. de Mello[1]

[1]Departamento de Recursos Hídricos e Saneamento, Universidade Federal de Lavras, Lavras, Minas Gerais, Brazil. ORCID: 0000-0002-6104-5507, 0000-0002-3910-0987, 0000-0001-7012-9465, 0000-0002-6033-5342. E-mail: rubensjunqueira@live.com (corresponding author), marcelo.viola@ufla.br, jhonesamorim@gmail.com, crmello@ufla.br.

[2]Institute for Landscape Ecology and Resources Management (ILR), Research Centre for BioSystems, Land Use and Nutrition (iFZ), Justus Liebig University Giessen, Heinrich-Buff-Ring 26, 35392 Giessen, Germany. ORCID: 0000-0003-4117-2178. E-mail: carlacscamargos@gmail.com.

ABSTRACT

Precipitation is the main input for hydrological models. However, due to limitations of rain gauge stations, satellite precipitation estimates have become a good alternative to precipitation information. In this context, this study aimed to validate the precipitation data with Tropical Rainfall Measuring Mission Multisatellite Precipitation Analysis (TMPA) and Integrated Multi-satellitE Retrievals for Global Precipitation Measurement (IMERG) data, in addition to assessing the uncertainty and performance of the Soil and Water Assessment Tool (SWAT) using observed precipitation (OP), TMPA, and IMERG data. Statistical coefficients were used to validate TMPA and IMERG precipitation data. P-factor and r-factor were considered for the uncertainty analysis, while the Nash-Sutcliffe efficiency (NSE), its logarithmic version (LNSE), and the percent bias (PBIAS) were analyzed to characterize the model performance analysis in monthly time steps. There was an overestimation by TMPA and IMERG in the precipitation estimation, especially in the dry period. OP, TMPA, and IMERG setups presented satisfactory results for uncertainty and performance analysis in hydrological modeling. The IMERG setup generally showed better results than the TMPA setup, being a good alternative for hydrological modeling, especially in regions with scarce precipitation datasets.

Keywords: IMERG; SUFI-2; SWAT; TMPA; uncertainty analysis.

1. INTRODUCTION

The Brazilian savanna is one of the most biodiverse savannas worldwide (SCHIASSI et al., 2018), constituting one of the world's 25 biodiversity hotspots due to its concentration of endemic species, ecological function, natural wealth, and degree of threat (MYERS et al., 2000). This biome covers 23.92% of the Brazilian territory; however, it was responsible for 33.8% of the total vegetation loss in the country in the last three decades (SOUZA et al., 2020). Despite this, only 2.2% of its area (approximately 2 million km²) is under legal protection (KLINK; MACHADO, 2005).

The Brazilian savanna plays a fundamental role in water resource dynamics because it drains water that forms the largest basins in Brazil, including the São Francisco river basin (SFRB) (OLIVEIRA et al., 2014). This basin supplies 70% of the surface water to the northeast Brazilian region. Therefore, it is classified as one of the most complex basins in Brazil based on population density, natural resource base, economic activities, development levels, and ecosystem vulnerability, and is considered a spatial unit for planning and development in the country (TORRES et al., 2012). Thus, robust hydrological studies are required to support water resource management in this region which is fundamental for Brazilian sustainable development.

Hydrological models were developed to represent the hydrological cycle, which is indispensable for better water resource management strategies (MOKHTARI et al., 2016). Several hydrological models have been developed with specific characteristics (DEVI et al., 2015). These models quantitatively describe the processes that integrate the water balance in a basin and can be used for several purposes, such as assessing the climate and land-use changes impacts, real-time flood prediction, and hydraulic structure design (CALDEIRA et al., 2019).

The hydrological model outputs are sensitive to input data, especially precipitation (ABBASPOUR, 2015). However, according to data from the Brazilian National Water and Sanitation Agency (ANA), 2,332 rain gauge stations are registered on the Brazilian savanna, resulting in a network density of approximately 858 km² covered by only one station. This spatial representation is far from what is recommended by the World Meteorological Organization (WMO) for interior plains and undulating areas (575 km² per rain gauge stations) for climate study purposes (WMO, 2008).

In addition, most of these rain gauges have short historical series (less than 10 years), and additionally several gaps. Given this, convective precipitation events predominate in the Brazilian savanna which has high spatial variability (REBOITA et al., 2010), and the uncertainties of precipitation captured by rain gauge stations increase. Therefore, the

combination of these factors affects the reliability of input datasets and the predictions made by hydrological models.

According to Abbaspour (2015), future advances in hydrological modeling depend on progress in remote sensing data availability. The need for adequate spatially-distributed precipitation datasets has led to the development of several satellite precipitation products (ELGAMAL et al., 2017), such as the Tropical Rainfall Measuring Mission (TRMM) Multisatellite Precipitation Analysis (TMPA) (HUFFMAN et al., 2006) and the Integrated Multi-satellitE Retrievals for Global Precipitation Measurement (GPM) - IMERG (HUFFMAN; GEORGE et al., 2019). These products have provided accurate precipitation estimates in different regions worldwide (GADELHA et al., 2019, LI et al., 2018, ROZANTE et al., 2018, WANG et al., 2017), and a better representation of the hydrological processes in large basins.

TMPA is an algorithm that estimates precipitation every 3 hours from several modern satellite-borne precipitation-related sensors, especially TRMM, with a spatial resolution of 0.25º x 0.25º, covering approximately 80% of the Earth's surface between 50ºN-50ºS latitudes (HUFFMAN, et al., 2006, 2010). Similar to TMPA, IMERG precipitation estimates are calibrated to the TRMM/GPM single-or combined-sensor estimates considered to be the highest-quality (HUFFMAN et al., 2019). Also, IMERG has higher spatial (0.1º x 0.1º) and temporal resolutions (0.5 hours) than TMPA, in addition to covering a larger area of the globe (60ºN-60ºS).

Although TMPA and IMERG represent an advance in precipitation estimation, research using these data in hydrological studies in the Brazilian savanna and SFRB environments is still limited. Oliveira et al. (2014) found a significant correlation and low TMPA errors in estimating the precipitation in the Brazilian savanna on monthly and annual scales. This research presented relevant findings. Nevertheless, only the TMPA precipitation data was used to study a simplified water balance in the biome.

Considering the low density of observed precipitation (OP) data, gaps in the hydrological studies carried out in the Brazilian savanna and SFRB environments, as well as its ecological service for Brazilian sustainable development, this study aimed to: i) validate the precipitation data using TMPA and IMERG data; and ii) assess the uncertainty and performance of a hydrological model inputted with OP, TMPA, and IMERG data.

2. MATERIALS AND METHODS

2.1.Study area

The Pandeiros river basin (PRB) is entirely inserted in the Brazilian savanna and the SFRB and has an area of 3,220 km2. PRB is fundamental for the reproduction and development of several fish species of the São Francisco River midstream basin (NUNES et al., 2009). Due to its ecological relevance, the Pandeiros River Environmental Protection Area was created through State Law no. 11,901 in 1995 to protect the development and reproduction of native fish species (SANTOS et al., 2015).

Figure 1 shows the location of the PRB delimited from the "Usina do Pandeiros Montante" streamflow station, and the Digital Elevation Model (DEM) ALOS (Advanced Land Observing Satellite) PALSAR (Phased Array L-band Synthetic Aperture Radar), with a spatial resolution of 12.5 m x 12.5 m (https://asf.alaska.edu/data-sets/sar-data-sets/alos-palsar/).

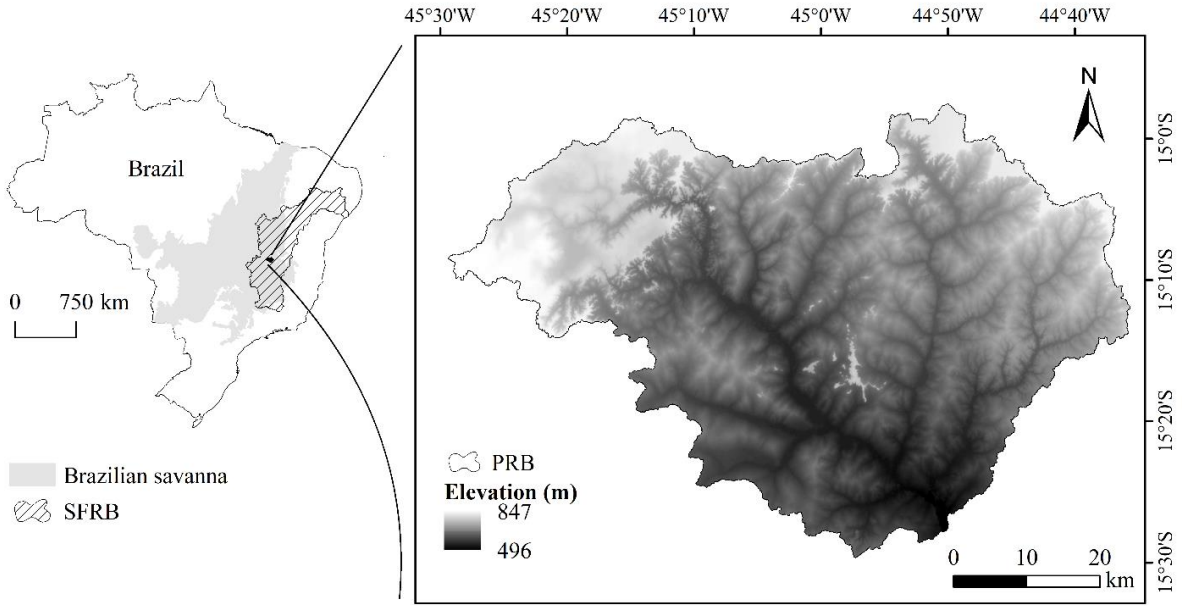

Figure 1. Location of PRB, SFRB, Brazilian savanna, and the basin DEM.

The Aw climate according to the Köppen classification predominates in PRB, consisting of a tropical climate with rainy summers and dry winters. The Thornthwaite climate classification is C1 (dry sub-humid) (MARTINS et al., 2018). The annual average precipitation in the basin is approximately 1085 mm, of which 883.4 mm returns to the atmosphere through evapotranspiration (JUNQUEIRA et al., 2020). The annual average temperature is 23.8 ºC, with a minimum of 17.9 ºC and a maximum of 31.6 ºC.

2.2.SWAT model

SWAT is a hydrological model that operates in a daily step, is physically based, computationally efficient, and capable of continuous simulation for long periods (GASSMAN

et al., 2007). Also, it is a semi-distributed model in which the basin is subdivided into multiple sub-basins and then Hydrological Response Units (HRUs), which consist of regions with the same land use, topography (DEM), and soil type characteristics (ARNOLD et al., 2012). In this study, the PRB was subdivided into 69 sub-basins and 595 HRUs. SWAT is based on the water balance of each of the HRUs, according to Equation 1 (NEITSCH et al., 2011):

$$SW_t = SW_0 + \sum_{i=1}^{t} (R_{day} - Q_{surf} - E_a - w_{seep} - Q_{gw}) \quad (1)$$

where: SW_t is the final soil water content (mm); SW_0 is the initial soil water content on day i (mm); t is the time (days); R_{day} is the amount of precipitation on day i (mm); Q_{surf} is the amount of surface runoff on day i (mm); E_a is the amount of evapotranspiration on day i (mm H2O); w_{seep} is the amount of water entering the vadose zone from the soil profile on day i (mm); Q_{gw} is the amount of return flow on day i (mm).

The surface runoff was calculated using the Curve Number method developed by the Soil Conservation Service of the United States (SCS 1972) and the evapotranspiration was estimated by Penman-Monteith (MONTEITH, 1965; PENMAN, 1956).

SWAT requires soil type, land use, topography, and weather data (precipitation, maximum and minimum temperature, wind speed, solar radiation, and relative humidity) to simulate the hydrological process in a basin. Streamflow data is subsequently required to calibrate and validate the model.

2.3.SWAT model input data

Next, the observed streamflow and precipitation data were obtained from the ANA and weather data from the Brazilian National Institute of Meteorology (INMET) in order to calibrate and validate the SWAT model (Figure 2c). Junqueira et al. (2020) described the data collection and its consistency analyses. All of this information contains daily datasets from June 2000 to December 2018.

Soil type derived from the Minas Gerais State Environmental Foundation (FEAM, 2010) on a scale of 1:650,000 (Figure 2a) and land use maps of 2010 elaborated by IBGE (2018) on a scale of 1:1,000,000 (Figure 2b) were used to generate the HRUs. Furthermore, the DEM (Figure 1) was also used to generate the slope map. Considering the low slope of the basin (5,9% on average), it was divided into four classes: 0-3%, 3-5%, 5-8%, and > 8%.

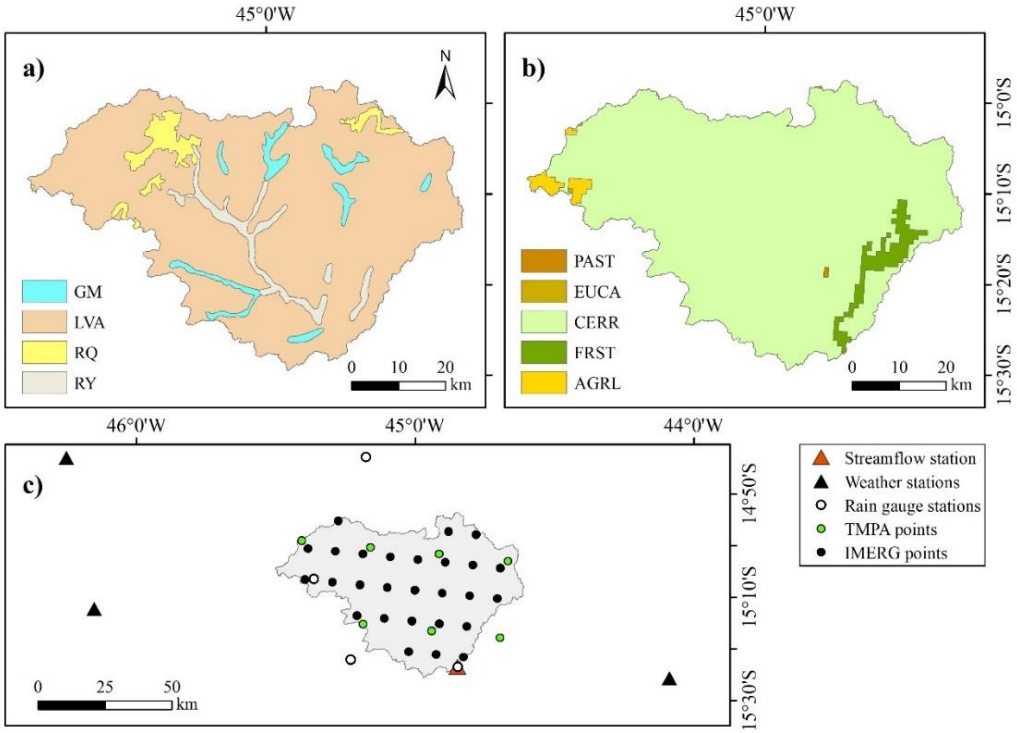

Figure 2. Soil (a) and land use (b) maps and streamflow, weather, and rain gauge stations and TMPA and IMERG points (c).

The predominant soil in PRB is the Red-Yellow Oxisol (LVA), covering 88.3% of the total area, followed by the Fluvic Entisol (RQ, 4.1%), Quartz Entisol (RY, 4.0%), and Melanic Entisol (GM, 3.7%). The predominant land uses are Cerrado (CERR, 95.3%), forest vegetation (FRST, 3.3%), agriculture (AGRL, 1.3%), pasture (PAST, 0.1%), and eucalyptus (EUCA, 0.1%).

The TMPA and IMERG data obtained from NASA (https://disc.gsfc.nasa.gov/) were used to evaluate performance and uncertainties related to remote sensing precipitation data. Thus, their results were compared with those obtained using OP. A brief description of these products is presented below.

2.4.TMPA data

TMPA is an algorithm that is intended to provide the best estimate of quasi-global precipitation (50ºN-S) at relatively fine spatial (0.25º x 0.25º) and temporal resolution (3 hours). Hence, a wide variety of modern satellite-borne precipitation-related sensors are used, mainly on the TRMM board (HUFFMAN et al., 2010).

According to Huffman et al. (2010), the research TMPA is carried out in four steps: i) the microwave precipitation estimates are calibrated and merged; ii) infrared (IR) precipitation

estimates are created using the calibrated microwave precipitation; iii) the microwave and IR estimates are merged; and iv) rain gauge data are incorporated.

In this study, we used the latest TMPA version available (TRMM_3B42_Daily V7) containing daily precipitation from June 2000 to December 2018. This version incorporates relevant changes compared to the previous one (version 6), such as new satellites and uniformly reprocessed input data using current algorithms (Huffman; Bolvin, 2015).

2.5.IMERG data

IMERG is an algorithm developed to intercalibrate, merge, and interpolate satellite microwave precipitation estimates, together with microwave-calibrated IR satellite estimates, rain gauges, and other precipitation estimators for the TRMM and GPM eras (HUFFMAN, GEORGE J et al., 2019).

The IMERG has fine spatial (0.1º x 0.1º) and temporal (half-hour) resolutions between latitudes 60ºN and 60ºS, and is available in three levels: Early; Late; and Final run. The Final run is intended for research applications and has a 4-month delay, with bias correction based on rain gauges (TAN et al., 2017). The process to estimate precipitation in IMERG is similar to TMPA (HUFFMAN et al., 2019). The Final Run Version 06 (GPM_3IMERGDF) was used in this study, with daily precipitation from June 2000 to December 2018.

2.6.TMPA and IMERG rainfall validation

The TMPA and IMERG precipitation data in PRB were validated by comparison with rain gauges. The rain gauge stations were selected and compared using the point-to-pixel approach. This methodology compares the value of the rain gauge point with the pixel value of the TMPA and IMERG corresponding to the point's location (NOGUEIRA; MOREIRA; VOLPATO, 2018). The comparison was carried out on daily and monthly scales for the entire period used in the hydrological modeling (2000-2018) and for the drought period (2014/15 to 2017/18), as related by Junqueira et al. (2020). This analysis was performed in three setups: for the entire year (January to December), rainy period (October to March), and dry period (April to September). The percent bias (PBIAS), Mean Error (ME), Root Mean Square Error (RMSE), and Pearson's correlation coefficient (r) with statistical significance of 5% were used to evaluate the errors of the TMPA and IMERG products, according to equations 2, 3, 4, and 5.

$$\mathrm{PBIAS} = \left[\frac{\sum_{i=1}^{N}(O_i - E_i)}{\sum_{i=1}^{N} O_i}\right].100 \qquad (2)$$

$$ME = \frac{1}{N}\sum_{i=1}^{N}(E_i - O_i) \quad (3)$$

$$RMSE = \sqrt{\frac{\sum_{i=1}^{N}(E_i - O_i)^2}{N}} \quad (4)$$

$$r = \frac{\sum_{i=1}^{N}(O_i - O_m).(E_i - E_m)}{\sqrt{\sum_{i=1}^{N}(O_i - O_m)^2 . \sum_{i=1}^{N}(E_i - E_m)^2}} \quad (5)$$

where: O is the observed rainfall; O_m is the average observed rainfall; E is the estimated rainfall; E_m is the average estimated rainfall; i is the time sequence of observed and simulated pairs; N is the number of observed and simulated pairs.

ME and RMSE values close to zero are related to low errors in precipitation estimation. Positive ME values indicate an overestimation of precipitation, while negative values indicate an underestimation. According to Yapo et al. (1996), PBIAS measures the tendency of the simulated precipitation to be higher or lower than the observed precipitation, where the value zero indicates the ideal situation. The r measures the strength and direction (decreasing or increasing, depending on the sign) of a linear relationship between the estimated and OP (AHLGREN; JARNEVING; ROUSSEAU, 2003). The closer to 1, the greater the similarity between the two-time series.

The cumulative precipitation curve and the average monthly precipitation for OP, TMPA, and IMERG from June 2000 to December 2018 were additionally performed. These analyses allow us to evaluate the temporal behavior of the remote sensing precipitation products concerning the OP, verifying the occurrence of overestimation/underestimation of precipitation by these products and identifying in which periods this occurs.

2.7.Calibration, validation, sensitivity, and uncertainty of the SWAT model

The SWAT-CUP software package with the SUFI-2 algorithm was used for calibration, validation, sensitivity, and uncertainty analysis. This algorithm maps all uncertainties regarding

parameters (expressed as uniform distributions or ranges) and attempts to capture most of the measured data within the 95% (95PPU) prediction uncertainty of the model in an iterative process (ABBASPOUR et al., 2015). The 95PPU is calculated at levels of 2.5% and 97.5% of the cumulative distribution of output variables obtained using Latin hypercube sampling (ABBASPOUR et al., 2007). According to Abbaspour (2015), SUFI-2 seeks to cover most of the measured data with the smallest band of uncertainty possible.

Traditional statistics, such as Nash-Sutcliffe efficiency (NSE), are not adequate when outputs are expressed as uncertainty bands (ARNOLD et al., 2012). Therefore, Abbaspour (2015) suggests the use of p-factor, which is a result of the percentage of the measured data covered by the 95PPU range and is responsible for accounting for the degree of uncertainty; and r-factor, which is the mean thickness of the 95PPU band divided by the standard deviation of the measured data. Abbaspour et al. (2015) recommend an r-factor of less than 1.5 and a p-factor greater than 0.7. When the latter is closer to 1, the better the model simulation regarding uncertainty.

Sensitivity analysis, calibration, and uncertainty analysis were initially performed for the SWAT inputted with OP. The parameters adopted in the sensitivity analysis were previously selected from previous studies and literature reviews. Thus, 19 parameters were evaluated using the Global Sensitivity method available in SWAT-CUP (ABBASPOUR, 2015), and those which presented the highest sensitivity were used in the calibration. The calibration procedure was performed automatically in SWAT-CUP using SUFI-2 from 2004 to 2018. The parameters were fit using two iterations with 600 simulations each and NSE as the objective function.

The best value and final range of the parameters obtained in the calibration of the OP setup were used to validate the SWAT inputted with TMPA and IMERG from 2004 to 2018. This procedure was adopted to evaluate the performance and uncertainty of TMPA and IMERG in the streamflow simulation in the Brazilian savanna and SFRB environments. The period from June 2000 to December 2003 was used to warm-up the model in all configurations.

2.8.Model performance analysis

Three statistical indexes were used to analyze the model performance in calibration and validation: PBIAS (Equation 2), NSE (NASH; SUTCLIFFE, 1970), and its logarithmic version (LNSE), according to equations 6 and 7:

$$NSE = 1 - \left[\frac{\sum_{i=1}^{N} (Qo_i - Qs_i)^2}{\sum_{i=1}^{N} (Qo_i - Qom_i)^2} \right] \quad (6)$$

$$LNSE = 1 - \left\{ \frac{\sum_{i=1}^{N}\left[\log(Qo_i) - \log(Qs_i)\right]^2}{\sum_{i=1}^{N}\left[\log(Qo_i) - \log(Qom_i)\right]^2} \right\} \quad (7)$$

where: *Qo* is observed streamflow; *Qs* is simulated streamflow; *Qom* is average observed streamflow.

According to Moriasi et al. (2007), the NSE indicates how well the graph of the observed data concerning the simulations fits a 1:1 line, and its value varies from -∞ to 1, with the latter being the ideal value. These authors developed a general performance rating for NSE and PBIAS to evaluate the model during the calibration and validation in a monthly time step, as observed in Table 1. The same classification of NSE was used for LNSE.

Table 1. General performance ratings for recommended statistics for a monthly time step.

Performance rating	NSE	PBIAS (%)
Very good	0.75 < NSE ≤ 1.00	PBIAS < ± 10
Good	0.65 < NSE ≤ 0.75	± 10 ≤ PBIAS < ± 15
Satisfactory	0.50 < NSE ≤ 0.65	± 15 ≤ PBIAS < ± 25
Unsatisfactory	NSE ≤ 0.50	PBIAS ≥ ± 25

3. RESULTS AND DISCUSSION

3.1.TMPA and IMERG precipitation validation

Figure 3a shows the average basin precipitation (based on the Thiessen polygon methodology) accumulated for OP, TMPA, and IMERG. The remote sensing precipitation products overestimated precipitation, especially in the 2010s; however, IMERG showed closer results to the observed data.

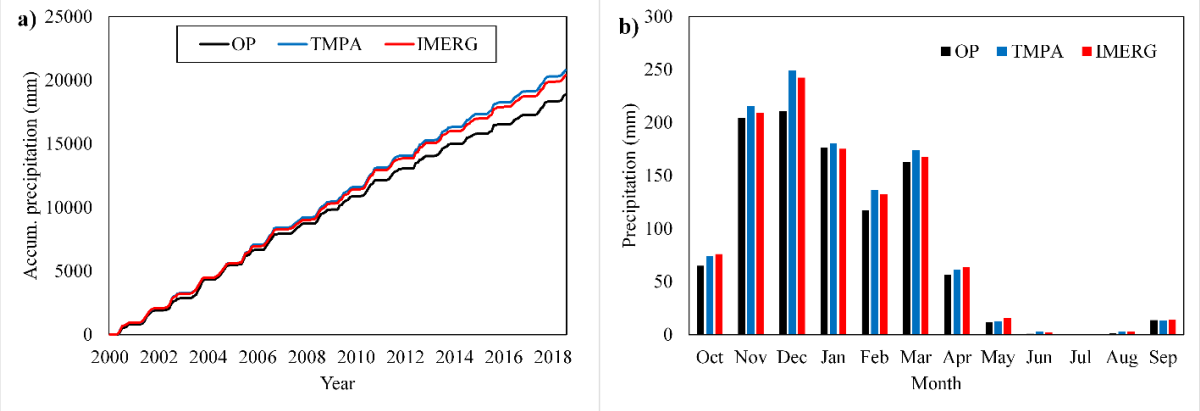

Figure 3. Accumulated precipitation (a) and average monthly precipitation (b) for OP, TMPA, and IMERG.

Similar behavior among the OP, TMPA, and IMERG precipitation data is observed in Figure 3b, i.e., TMPA and IMERG were able to reproduce the seasonality of precipitation in PRB. However, both remote sensing precipitation data overestimate the OP. This result is confirmed by the scatter plots of observed and simulated precipitation (Figure 4) and the average of statistical results related to the precipitation estimation accuracy by TMPA and IMERG in PRB for the total (June 2000 to December 2018) and drought (2014/15 to 2017/18) periods (Table 2).

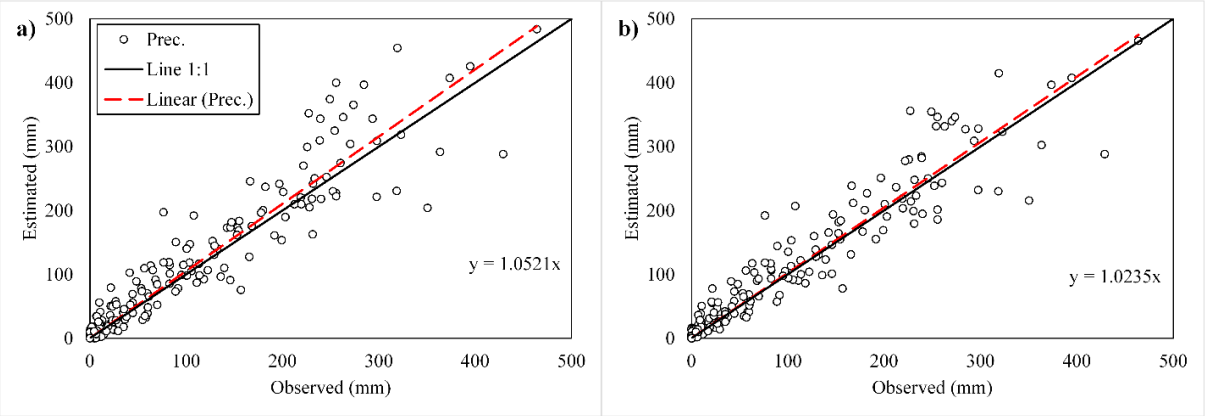

Figure 4. Scatter plots of the observed and estimated precipitation (Prec.) with linear trend line (Linear (Prec.)) by TMPA (a) and IMERG (b) for PRB.

Table 2. Statistical results for TMPA and IMERG precipitation validation for the total and drought periods on daily and monthly time scales, considering the entire year (January to December), wet period (October to March), and dry period (April to September).

Index	TMPA						IMERG					
	Total period			Drought period			Total period			Drought period		
	Entire year	Wet	Dry	Entire year	Wet	Dry	Entire year	Wet	Dry	Entire year	Wet	Dry
ME*	0.20	0.35	0.06	0.54	0.96	0.13	0.16	0.26	0.07	0.45	0.81	0.10
RMSE*	9.76	13.15	4.14	8.93	12.18	3.28	9.50	12.86	3.80	8.67	11.91	2.92
PBIAS (%)*	-7.9	-7.5	12.8	-29.8	28.8	46.0	-6.33	-5.7	14.6	-25.1	24.6	34.7
r*	0.41	0.37	0.27	0.42	0.40	0.28	0.45	0.41	0.37	0.45	0.42	0.32
ME**	5.66	9.75	1.85	15.93	29.45	4.11	4.62	7.33	2.13	13.08	24.57	3.18
RMSE**	58.76	81.16	20.49	44.06	62.19	14.20	56.98	78.59	20.23	43.88	62.44	12.11
PBIAS (%)**	-7.7	-7.4	12.7	-29.1	27.8	46.0	-6.3	-5.6	14.5	-24.2	23.6	34.7
r**	0.88	0.79	0.82	0.92	0.89	0.84	0.88	0.79	0.82	0.91	0.87	0.83

ME and PBIAS showed an overestimation of precipitation for TMPA and IMERG in the PRB for all situations. Similar results were found by Oliveira et al. (2014) for the Brazilian

savanna and by Almeida et al. (2020) in the Itapemirim river basin, Southeastern Brazil, both using TMPA, and by Gadelha et al. (2019) using IMERG in Southeastern Brazil.

The ME in the seasonal analysis was lower for the dry season for daily and monthly time scales; however, the average monthly precipitation in this period is much lower than the entire year and the rainy period. Thus, the PBIAS indicates greater bias (in absolute values) during the dry period than the other periods for TMPA and IMERG. Salles et al. (2019) and Almeida et al. (2020) also found higher errors of remote sensing precipitation data during the dry season in Brazilian regions.

The overestimation of precipitation expressed by the ME and PBIAS during the drought period (2014/15 to 2017/18) was greater (in absolute values) for the TMPA and the IMERG in relation to the total period. The precipitation overestimation was even higher during the dry period, where the PBIAS reached a value of -46.0% for the TMPA and -34.7% for the IMERG for both time scales.

Despite the better performance of IMERG during the drought period and dry season, there is greater difficulty for the two products (IMERG and TMPA) in estimating precipitation during periods of water scarcity. However, Santos et al. (2017) report that drought analysis using TRMM-derived precipitation data showed satisfactory results in the upper SFRB. Therefore, it is recommended to perform a thorough analysis before using these data in studies involving drought periods.

The TMPA and IMERG errors were low and the r values indicate strong similarity between the observed and estimated precipitation for the entire year in a monthly time scale, which corroborates the values found in other studies in Brazil (ALMEIDA et al., 2020; GADELHA et al., 2019; NOGUEIRA; MOREIRA; VOLPATO, 2018; OLIVEIRA et al., 2014; ROZANTE et al., 2018). The daily r results show a reduction in the accuracy of satellite precipitation estimates at shorter time scales, as also stated by Guo and Liu (2016) in China and by Salles et al. (2019) in Brazil's Central Plateau region. Considering the seasonal behavior, the RMSE during the rainy period was higher than for the entire year and dry periods, since the average monthly precipitation is higher during the rainy period.

IMERG generally presented the best performance for the daily and monthly time scales, which in addition to presenting better statistical coefficients than TMPA, presented estimated values which were closer to the observed ones, as shown in the scatter plot (Figures 4a and 4b), as also found by Salles et al. (2019) and by Amorim et al. (2020) in other Brazilian regions. This result can be explained by the wider frequency range used by the sensors on board the GPM, giving greater accuracy in the estimates of heavy, moderate, and light precipitations

(HOU et al., 2014; HUFFMAN et al., 2019). In this sense, IMERG is an adequate substitute for TMPA for studies, mainly for monthly time scales in the Brazilian savanna and SFRB environments, as also observed by Serrão et al. (2016) in the Amazon basin.

3.2.Parameter sensitivity and calibration analysis of SWAT model

Next, ten parameters based on the sensitivity analysis results were considered for SWAT calibration and validation (Table 3). A predominance of groundwater-related parameters was observed since the baseflow accounts for 80% of the streamflow in this basin. This behavior is associated with the high infiltration capacity of the basin, influenced by the low average slope (5.9%), a predominance of Oxisol, and preserved vegetation (JUNQUEIRA et al., 2020). In a catchment with a low slope in Germany, Guse et al. (2014) also observed that dominance of the baseflow resulted in the most sensitive parameters.

Table 3. Parameters used to calibrate the SWAT model with OP and their initial and final ranges, and best parameters (BP).

Parameters	**Initial range**		**Final range**		**BP**
r_CN2.mgt	-0.10	0.10	-0.04	0.08	0.03
v_ALPHA_BF.gw	0.0050	0.0100	0.0050	0.0077	0.0052
a_GW_DELAY.gw (days)	0.00	60.00	27.72	60.00	34.63
a_GWQMN.gw (mm)	0	2000	357	1453	880
v_CH_K2.rte ($mm.h^{-1}$)	0.00	20.00	9.92	20.00	15.73
v_GW_REVAP.gw	0.020	0.200	0.089	0.200	0.190
r_SLSUBBSN.hru (m)	0.00	1.00	0.44	1.00	0.87
v_RCHRG_DP.gw	0.000	0.200	0.001	0.134	0.050
v_CH_K1.sub ($mm.h^{-1}$)	0.00	20.00	8.17	20.00	11.44
v_CH_N2.rte	0.00	0.30	0.11	0.30	0.26

Note: r = relative; v = replace; and a = absolute.

3.3.Uncertainty and performance analysis

Figure 5 presents the simulated streamflow using the best parameters and 95PPU for calibration with OP and validation with TMPA and IMERG from 2004 to 2018, as well as the basin-scale precipitation of each product obtained by the area-weighted procedure and the scatter plots of observed and simulated streamflows with OP, TMPA, and IMERG setups. Moreover, Table 4 presents the results of p-factor, r-factor, NSE, LNSE, and PBIAS for the hydrological modeling with the three precipitation products.

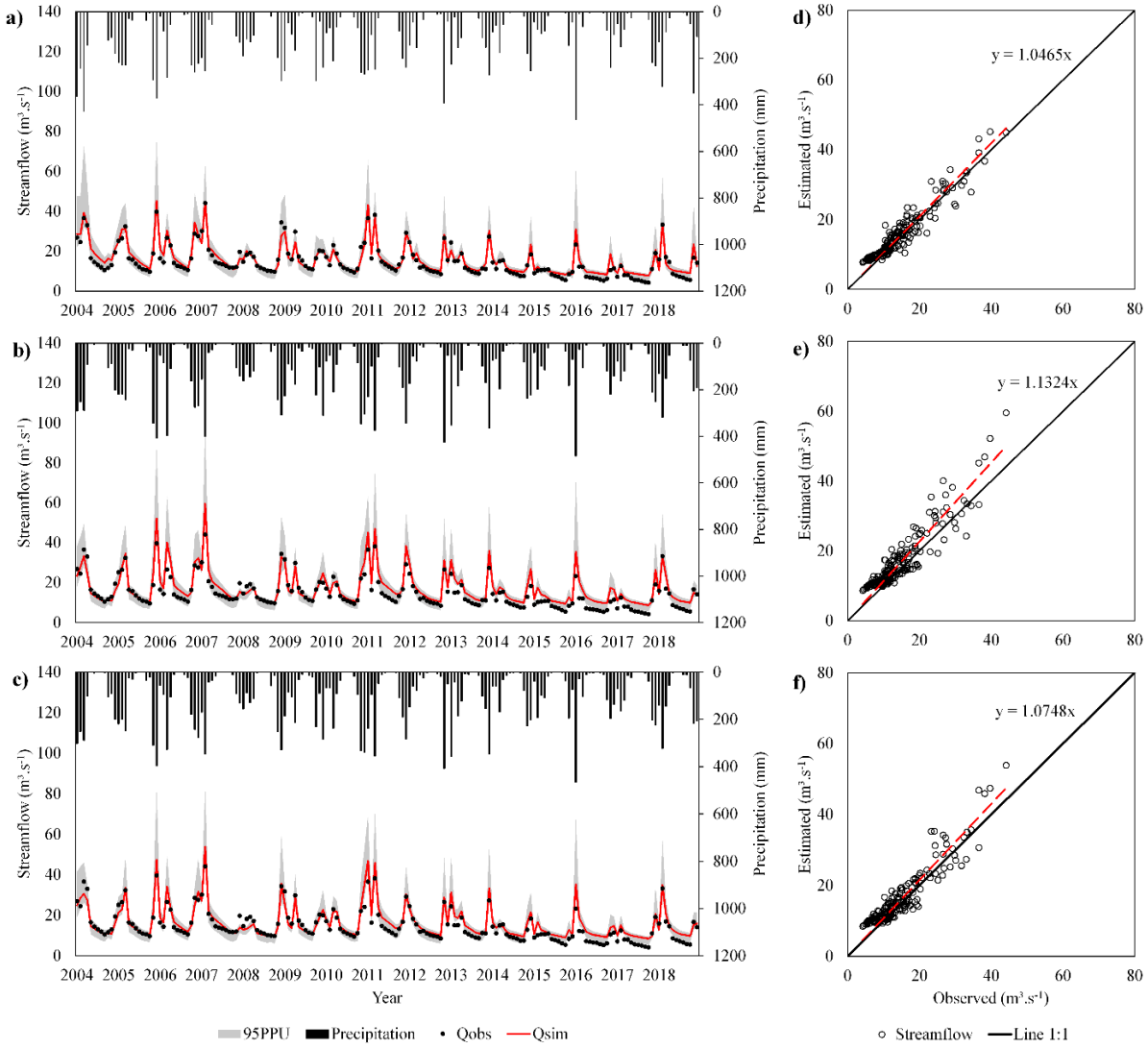

Figure 5. Average precipitation, observed (Qobs) and simulated (Qsim) monthly streamflow, uncertainty band (95PPU), and scatter plots of the observed and simulated streamflows during the for OP (a and d), TMPA (b and e), and IMERG (c and f) in PRB.

Table 4. Results of uncertainty and performance analysis of SWAT for the calibration with OP and validation with TMPA and IMERG in PRB.

Precipitation input data	p-factor	r-factor	NSE	LNSE	PBIAS (%)
OP	0.94	1.05	0.88	0.83	-7.6
TMPA	0.76	1.16	0.71	0.68	-16.0
IMERG	0.79	1.09	0.81	0.75	-10.2

Similar behavior could be detected when comparing observed and simulated streamflows using OP, TMPA, and IMERG setups (Figure 5). Zubieta et al. (2017) also observed a similar behavior in the Peruvian-Ecuadorian Amazon basin between observed and

simulated streamflow. Moreover, the simulated streamflow was able to capture the temporal variability of precipitation, coinciding with the wet and dry periods.

95PPU covers most of the simulated streamflow (Figure 5), which can be explained by the p-factor being higher than 0.70 in all the cases (Table 4). R-factor is lower than 1.5 for all hydrological modeling setups, as recommended by Abbaspour et al. (2015), although the uncertainty band in the peaks is higher. Silva et al. (2018) also found greater uncertainty during extreme events in the upper SFRB using only OP, especially for peak streamflow prediction.

According to Li et al. (2018), sparse rain gauges are one of the factors responsible for model uncertainty. In addition, rain gauges provide information for a small area and are extrapolated to the spatial scale of several km², introducing many uncertainties (GYASI-AGYEI, 2020). Nevertheless, although it used only four rain gauges, the hydrological modeling setup using OP presented less uncertainty estimation than TMPA and IMERG. On the other hand, Meira Neto et al. (2018) and Amorim et al. (2020) found lower uncertainty of hydrological modeling with remote sensing products in the Ribeirão da Onça basin and Serra da Mesa Hydropower Plant, respectively. The influence of a low rain gauge density was softened due to the low spatial variability of precipitation on a monthly scale in PRB. Furthermore, the higher uncertainty associated with the precipitation estimation by remote sensing products is transferred to the accuracy of model predictions (MICHAELIDES et al., 2009), increasing the uncertainty of the hydrological modeling with TMPA and IMERG compared to the OP.

IMERG presented lower uncertainty than TMPA regarding hydrological modeling with the remote sensing products, as expressed by the higher p-factor and lower r-factor. In addition to the better spatial resolution, IMERG uses data from more modern and accurate sensors than TMPA, such as the GPM (HOU et al., 2014), which reduces the uncertainty in precipitation estimation and consequently in hydrological modeling.

The OP setup presented satisfactory results regarding performance, in which the NSE and LNSE classified as “very good”. PBIAS also shows an adequate performance, classified as “very good”, although an overestimation of the simulated streamflow was observed, mainly in the recession period. SWAT presented difficulty in simulating the streamflow in the recession period from 2015 to 2018, in which (according to Junqueira et al., 2020) there was the incidence of intense hydrological drought, causing changes in the hydrological behavior of the PRB.

The performance of hydrological modeling is reduced during validation. This occurred due to the associated error in the precipitation estimation by TMPA and IMERG. This result is a reflection of the higher overestimation of remote sensing precipitation data during the drought

event (2014/15 to 2017/18), especially during the dry period (April to September), which caused overestimation of the simulated streamflow with these products to be higher than the OP setup (Table 2).

Greater overestimation of the simulated streamflow rate with the TMPA setup is observed in analyzing the scatter plot for the OP (Figure 5d), TMPA (Figure 5e), and IMERG (Figure 5f) setups, while the OP setup showed simulated values closer to those observed, especially in the higher streamflow months.

The IMERG setup generally performed better than the TMPA setup, with NSE classified as "very good" and PBIAS as "good", while the TMPA setup showed NSE classified as "good" and PBIAS as "satisfactory" (Table 4). On the other hand, Amorim et al. (2020) report better streamflow simulation with TMPA than IMERG at Serra da Mesa Hydropower Plant. Also, the IMERG setup presented higher LNSE than the TMPA setup, which indicates better accuracy of the IMERG in the streamflow simulation during the recession period.

Despite the better performance of OP setup, IMERG can be an adequate alternative for hydrological modeling studies and water resource management, especially for regions with scarce temporal and spatial conventional precipitation data (GADELHA et al., 2019; ZUBIETA et al., 2017), such as the Brazilian savanna region and Amazon basin region. Also, the use of IMERG has provided accurate performance worldwide, such as Jiang and Bauer-Gottwein (2019) in five different climatic regions of China, Le et al. (2020) in Vietnam basins, and Zubieta et al. (2017) in Andean-Amazon regions.

4. CONCLUSIONS

TMPA and IMERG presented satisfactory accuracy in estimating monthly precipitation, with low errors and strong similarity between the observed and estimated precipitation. ME and PBIAS indicated an overestimation of precipitation from these products, especially during the drought event and dry period.

The uncertainty analysis obtained with SUFI-2 showed reduced uncertainty when using OP, TMPA, and IMERG setups, with a p-factor higher than 0.70 and r-factor lower than 1.50 in all cases. The OP setup showed the lowest uncertainty among the three setups. Regarding remote sensing products, the IMERG setup showed lower uncertainty than the TMPA setup.

All hydrological modeling setups presented satisfactory results in the performance analysis, with NSE and LNSE higher than 0.50 and PBIAS ranging from ± 25. However, there was an overestimation of the streamflow from 2015 to 2018 during the recession period with

all three setups, mainly due to the occurrence of hydrological drought in that period. The OP setup showed better performance, followed by the IMERG setup.

Therefore, IMERG is a suitable alternative for hydrological modeling and ecological and water resource management in regions with scarce temporal and spatial precipitation datasets, such as the Brazilian savanna and SFRB.

REFERENCES

ABBASPOUR, K. C. et al. Modelling hydrology and water quality in the pre-alpine/alpine Thur watershed using SWAT. **Journal of Hydrology**, v. 333, n. 2–4, p. 413–430, 2007.

ABBASPOUR, K. C. **SWAT-CUP: SWAT Calibration and Uncertainty Programs**, 2015.

ABBASPOUR, K. C. et al. A continental-scale hydrology and water quality model for Europe: Calibration and uncertainty of a high-resolution large-scale SWAT model. **Journal of Hydrology**, v. 524, p. 733–752, 2015.

AHLGREN, P.; JARNEVING, B.; ROUSSEAU, R. Requirements for a cocitation similarity measure, with special reference to Pearson's correlation coefficient. **Journal of the American Society for Information Science and Technology**, v. 54, n. 6, p. 550–560, 2003.

ALMEIDA, K. N. et al. Performance analysis of TRMM satellite in precipitation estimation for the Itapemirim River basin, Espirito Santo state, Brazil. **Theoretical and Applied Climatology**, v. 2, n. 2012, 12 Mei 2020.

AMORIM, J. S. et al. Evaluation of Satellite Precipitation Products for Hydrological Modeling in the Brazilian Cerrado Biome. **Water**, v. 12, n. 2571, p. 1–19, 2020.

ARNOLD, J. G. et al. SWAT: Model use, calibration, and validation. **Transactions of the ASABE**, v. 55, n. 4, p. 1491–1508, 2012.

BRAZILIAN INSTITUTE OF GEOGRAPHY AND STATISTICS (IBGE). **Mapa de Cobertura e Uso da Terra do Brasil 2010**, 2018. Disponível em: <https://www.ibge.gov.br/geociencias/informacoes-ambientais/cobertura-e-uso-da-terra/15831-cobertura-e-uso-da-terra-do-brasil.html?edicao=16023&t=sobre>

CALDEIRA, T. L. et al. LASH hydrological model: An analysis focused on spatial discretization. **Catena**, v. 173, p. 183–193, Feb 2019.

DEVI, G. K.; GANASRI, B. P.; DWARAKISH, G. S. A Review on Hydrological Models. **Aquatic Procedia**, v. 4, p. 1001–1007, 2015.

ELGAMAL, A.; REGGIANI, P.; JONOSKI, A. Impact analysis of satellite rainfall products on flow simulations in the Magdalena River Basin, Colombia. **Journal of Hydrology: Regional Studies**, v. 9, p. 85–103, 2017.

GADELHA, A. N. et al. Grid box-level evaluation of IMERG over Brazil at various space and time scales. **Atmospheric Research**, v. 218, p. 231–244, 2019.

GASSMAN, P. W. et al. The soil and water assessment tool: historical development, applications, and future research directions. **Transactions of the ASABE**, v. 50, n. 4, p. 1211–1250, 2007.

GUO, R.; LIU, Y. Evaluation of satellite precipitation products with rain gauge data at different scales: Implications for hydrological applications. **Water**, v. 8, n. 7, 2016.

GUSE, B.; REUSSER, D. E.; FOHRER, N. How to improve the representation of hydrological processes in SWAT for a lowland catchment – temporal analysis of parameter sensitivity and model performance. **Hydrological Processes**, v. 28, n. 4, p. 2651–2670, 2014.

GYASI-AGYEI, Y. Identification of the Optimum Rain Gauge Network Density for Hydrological Modelling Based on Radar Rainfall Analysis. **Water**, v. 12, n. 7, p. 1906, 3 Jul 2020.

HOU, A. Y. et al. The global precipitation measurement mission. **Bulletin of the American Meteorological Society**, v. 95, n. 5, p. 701–722, 2014.

HUFFMAN, G. J. et al. The TRMM Multisatellite Precipitation Analysis (TMPA): Quasi-Global, Multiyear, Combined-Sensor Precipitation Estimates at Fine Scales. **Journal of Hydrometeorology**, v. 8, n. 1, p. 38–55, 2006.

HUFFMAN, G. J. et al. The TRMM Multi-Satellite Precipitation Analysis (TMPA). **Satellite Rainfall Applications for Surface Hydrology**, p. 3–22, 2010.

HUFFMAN, G. J. et al. **NASA Global Precipitation Measurement (GPM) Integrated Multi-satellitE Retrievals for GPM (IMERG)NASA/GSFC Code**, 2019.

HUFFMAN, G. J.; BOLVIN, D. T. TRMM and other data precipitation data set documentation. **NASA,** Greenbelt**,** 2015.

JIANG, L.; BAUER-GOTTWEIN, P. How do GPM IMERG precipitation estimates perform as hydrological model forcing? Evaluation for 300 catchments across Mainland China. **Journal of Hydrology**, v. 572, p. 486–500, 2019.

JUNQUEIRA, R. et al. Hydrological Response to Drought Occurrences in a Brazilian Savanna Basin. **Resources**, v. 9, n. 10, p. 123, 16 Oct. 2020.

KLINK, C. A.; MACHADO, R. B. Conservation of the Brazilian Cerrado. **Conservation Biology**, v. 19, n. 3, p. 707–713, 2005.

LE, M. H. et al. Adequacy of Satellite-derived Precipitation Estimate for Hydrological Modeling in Vietnam Basins. **Journal of Hydrology**, v. 586, n. February, 2020.

LI, D. et al. Adequacy of TRMM satellite rainfall data in driving the SWAT modeling of Tiaoxi catchment (Taihu lake basin, China). **Journal of Hydrology**, v. 556, p. 1139–1152, 2018.

MARTINS, F. B. et al. Classificação climática de Köppen e de Thornthwaite para Minas Gerais: cenário atual e projeções futuras. **Revista Brasileira de Climatologia**, v. 1, p. 149–164, 8 Nov 2018.

MEIRA NETO, A. A. et al. Improving streamflow prediction using uncertainty analysis and Bayesian model averaging. **Journal of Hydrologic Engineering**, v. 23, n. 5, p. 1–9, 2018.

MICHAELIDES, S. et al. Precipitation: Measurement, remote sensing, climatology and modeling. Atmospheric Research, v. 94, n. 4, p. 512–533, 2009.

MINAS GERAIS STATE ENVIRONMENTAL FOUNDATION (FEAM). **Mapa de solos do Estado de Minas Gerais**, 2010.

MOKHTARI, E. H.; REMINI, B.; HAMOUDI, S. A. Modelling of the rain-flow by hydrological modelling software system HEC-HMS - watershed's case of wadi Cheliff-Ghrib, Algeria. **Journal of Water and Land Development**, v. 30, n. 1, p. 87–100, 1 Sep 2016.

MONTEITH, J. L. Evaporation and environment. **Symposia of the society for experimental biology**, p. 205–234, 1965.

MORIASI, D. N. et al. Model Evaluation Guidelines for Systematic Quantification of Accuracy in Watershed Simulations. **Transactions of the ASABE**, v. 50, n. 3, p. 885–900, 2007.

MYERS, N. et al. Biodiversity hotspots for conservation priorities. Nature, v. 403, n. 6772, p. 853–858, Feb 2000.

NASH, J. E.; SUTCLIFFE, J. V. River flow forecasting through conceptual models part I - A discussion of principles. Journal of Hydrology, v. 10, n. 3, p. 282–290, 1970.

NEITSCH, S. L. et al. **Soil & Water Assessment Tool Theoretical Documentation: Version 2009**. Texas: [s.n.].

NOGUEIRA, S. M. C.; MOREIRA, M. A.; VOLPATO, M. M. L. Evaluating precipitation estimates from Eta, TRMM and CHRIPS data in the south-southeast region of Minas Gerais state-Brazil. **Remote Sensing**, v. 10, n. 2, p. 313–329, 2018.

NUNES, Y. R. F. et al. Pandeiros: o Pantanal Mineiro. MG. **Biota**, v. 2, n. 2, p. 4–17, 2009.

OLIVEIRA, P. T. S. et al. Trends in water balance components across the Brazilian Cerrado. **Water Resources Research**, v. 50, n. 9, p. 7100–7114, Sep 2014.

PENMAN, H. L. Evaporation: An introductory survey. **Netherlands Journal of Agricultural Sciences**, 1956.

REBOITA, M. S. et al. Regimes de precipitação na América do Sul: uma revisão bibliográfica. **Revista Brasileira de Meteorologia**, v. 25, n. 2, p. 185–204, Jun 2010.

ROZANTE, J. R. et al. Evaluation of TRMM/GPM Blended Daily Products over Brazil. **Remote Sensing**, v. 10, n. 6, p. 1–17, 2018.

SALLES, L. et al. Seasonal effect on spatial and temporal consistency of the new GPM-based IMERG-v5 and GSMaP-v7 satellite precipitation estimates in Brazil's Central Plateau region. **Water**, v. 11, n. 4, 2019.

SANTOS, C. A. G. et al. Drought assessment using a TRMM-derived standardized precipitation index for the upper São Francisco River basin, Brazil. **Environmental Monitoring and Assessment**, v. 189, n. 6, 2017.

SANTOS, U. et al. Fish fauna of the Pandeiros River, a region of environmental protection for fish species in Minas Gerais state, Brazil. **Check List**, v. 11, n. 1, p. 1507, 1 Jan 2015.

SCHIASSI, M. C. E. V. et al. Fruits from the Brazilian Cerrado region: Physico-chemical characterization, bioactive compounds, antioxidant activities, and sensory evaluation. **Food Chemistry**, v. 245, p. 305–311, 2018.

SERRÃO, E. A. O. et al. Avaliação estatística entre as estimativas de precipitação da constelação GPM com TRMM: uma análise a bacia hidrográfica do rio Solimões. **Revista Brasileira de Climatologia**, v. 18, p. 361–376, 2016.

SILVA, R. M. DA et al. Hydrological simulation in a tropical humid basin in the cerrado biome using the SWAT model. **Hydrology Research**, v. 49, n. 3, p. 908–923, 2018.

SOIL CONSERVATION SERVICE (SCS). **National engineering handbook, section 4, hydrology.** [s.l.] USDA, 1972.

SOUZA, C. M. et al. Reconstructing Three Decades of Land Use and Land Cover Changes in Brazilian Biomes with Landsat Archive and Earth Engine. **Remote Sensing**, v. 12, n. 17, p. 2735, 25 Aug 2020.

TAN, J. et al. Performance of IMERG as a function of spatiotemporal scale. **Journal of Hydrometeorology**, v. 18, n. 2, p. 307–319, 2017.

TORRES, M. D. O. et al. Economic impacts of regional water scarcity in the São Francisco river Basin, Brazil: An application of a linked hydro-economic model. **Environment and Development Economics**, v. 17, n. 2, p. 227–248, 2012.

WANG, Z. et al. Evaluation of the GPM IMERG satellite-based precipitation products and the hydrological utility. **Atmospheric Research**, v. 196, p. 151–163, Nov 2017.

WMO - WORLD METEOROLOGICAL ORGANIZATION. **Guide to Hydrological Practices**. In: 6th. ed. Geneva 2, Switzerland: WMO, 2008. v. Ip. 296.

YAPO, P. O.; GUPTA, H. V.; SOROOSHIAN, S. Automatic calibration of conceptual rainfall-runoff models: sensitivity to calibration data. **Journal of Hydrology**, v. 181, n. 1, p. 23–48, 1996.

ZUBIETA, R. et al. Hydrological modeling of the Peruvian-Ecuadorian Amazon Basin using GPM-IMERG satellite-based precipitation dataset. **Hydrology and Earth System Sciences**, v. 21, n. 7, p. 3543–3555, 2017.

ARTIGO 3 - Hydrological retrospective and historical droughts analysis in a Brazilian savanna basin

ABSTRACT

Analyzing historical droughts is essential to improve the assessment of future hydrological risks and understanding the effects of climate variability on the streamflow. However, prolonged and consistent hydrological time series are scarce in the Brazilian savanna region. This study aimed to analyze the performance of climate reanalysis products in precipitation estimation, hydrological modeling, and historical drought analysis in a Brazilian savanna basin. For this purpose, precipitation data from the twentieth-century atmospheric model ensemble (ERA-20CM) and the land component of the fifth generation of European ReAnalysis (ERA5-Land) with bias correction were used in this study. The weather variables were obtained from the Climatic Research Unit (CRU) and the hydrological modeling was performed using the Soil and Water Assessment Tool (SWAT). The Standardized Streamflow Index (SSI) was used to calculate hydrological drought in the basin. Overall, ERA5-Land performed satisfactorily in precipitation estimation, mainly on monthly time scale (r = 0.89, RMSE = 56.1 mm, and KGE = 0.86), hydrological modeling (NSE = 0.53, LNSE = 0.63, PBIAS = 5.5%, and KGE = 0.76), and drought prediction (five of six observed events). However, the ERA-20CM ensemble members showed unsatisfactory performance in all analyses. Therefore, hydrological drought was performed with ERA5-Land from 1950 to 2018. An increase in the number of drought months and a reduction of wet months has been observed in recent decades.

Keywords: bias correction; ERA-20CM; ERA5-Land; historical drought; Hydrological Retrospective; SWAT.

1. INTRODUCTION

Brazilian savanna is one of the world's 25 biodiversity hotspots (MYERS et al., 2000) and plays a fundamental hydrological role in Brazil and South America (OLIVEIRA et al., 2014). However, an increase in deforestation (SOUZA et al., 2020) and air temperature (HOFMANN et al., 2021) has been observed in the last decades, compromising multiple uses of water and the environment in this biome. Also, recent studies indicate a reduction in precipitation and streamflow by the end of the century in the Brazilian savanna (OLIVEIRA et al., 2019; RODRIGUES et al., 2019).

Analyzing past extreme events, such as droughts, is essential to improve the assessment of future hydrological risks, as well as understanding the effects of climate variability (CORREA et al., 2017). Managing the impacts of the deficit on the hydrological system is currently one of the main concerns of water resource managers across the globe (KIM; KWON; HAN, 2018; SMITH et al., 2019). However, long historical records of hydrometeorological data are required to estimate the likelihood of droughts and assist the drought risk management (BARKER et al., 2019; KIM; KWON; HAN, 2018). These records are scarce in Brazil, presenting gaps in observed data that limit their use in hydrological studies (GADELHA et al., 2019; ROZANTE et al., 2018; XAVIER; KING; SCANLON, 2016).

To overcome the lack of historical hydrometeorological data, recent studies have sought to produce climate reanalysis, a consistent reprocessing of archived weather observations using modern forecasting systems (DEE et al., 2014). These datasets provide continuous estimates of weather variables for any terrestrial location worldwide extended over several decades (AUERBACH et al., 2016). Contrasting with ground measured data, reanalysis is uniform in time and space and provides spanned weather elements (IPCC, 2013). The climate reanalysis has presented satisfactory results worldwide (GAO et al., 2016; TAREK; BRISSETTE; ARSENAULT, 2020). However, its quality varies according to the region since the same product may present different performances according to the study region (KIM; HAN, 2019). Therefore, more studies are needed to evaluate its applicability in different climate regions, especially in Brazil, where the number of hydrological studies using climate reanalysis products is small.

When associated with hydrological models, the climate reanalysis allows the simulation of long and consistent hydrometeorological variables, among them streamflow series. This process is known as Hydrological Retrospective (HR). According to Auerbach et al. (2016), HR may be necessary for applications focused on seasonal and interannual variability relevant to water supply risk assessment or ecological studies. Some studies have adopted this

methodology and achieved satisfactory results (CORREA et al., 2017; JAJARMIZADEH et al., 2016; UNIYAL et al., 2019).

In this context, this study aimed to i) validate different precipitation products of climate reanalysis in the Pandeiros river basin (PRB), representative of the Brazilian savanna; ii) analyze the performance of these products in hydrological modeling; iii) test the simulated streamflow based on reanalysis products in predicting the occurrence of droughts; and iv) perform HR and historical drought analysis in the basin.

2. MATERIAL AND METHODS

2.1.Study area

The PRB, delimited from the "Usina do Pandeiros Montante" streamflow station, has an area of 3220 km² and is completely inserted in the Brazilian savanna (IBGE, 2019). Its altitude varies from 496 to 897 m, with an average of 677 m and an average slope of 5.9 %. Figure 1 presents the PRB location, the streamflow station, and the Digital Elevation Model (DEM) ALOS (Advanced Land Observing Satellite) PALSAR (Phased Array L-band Synthetic Aperture Radar), with a spatial resolution of 12.5 m.

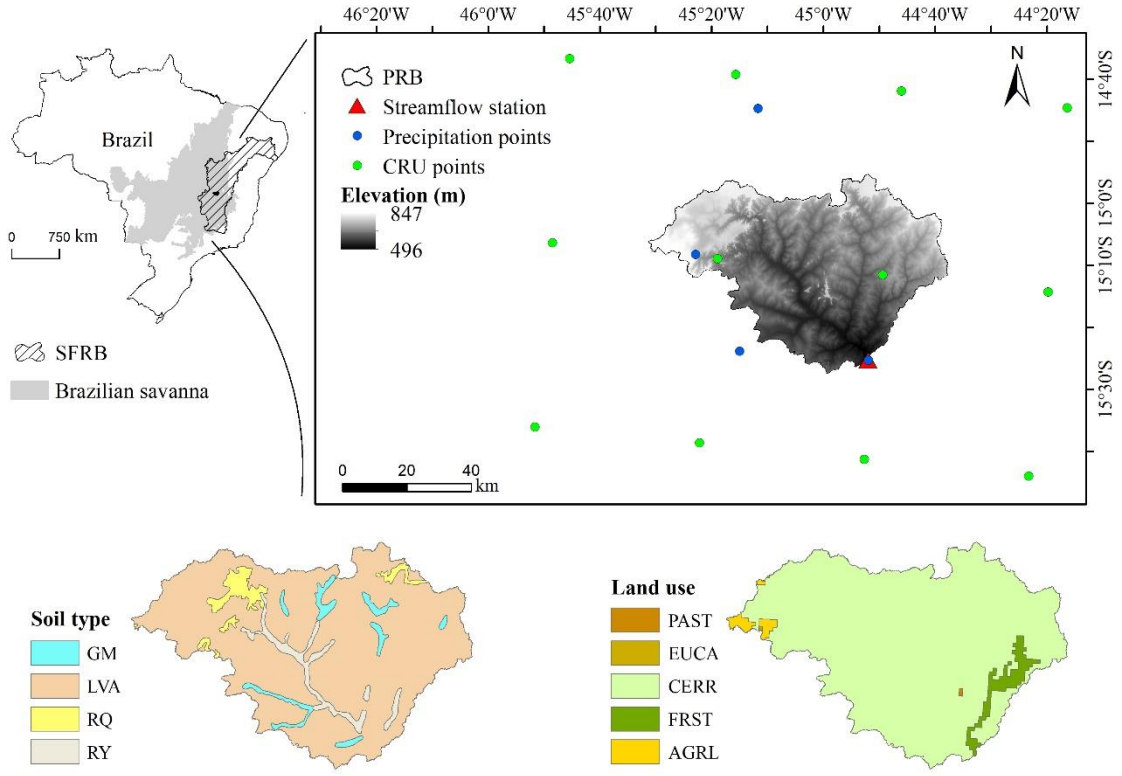

Figure 1. Location of PRB and its DEM, hydrometeorological data, and soil and land use maps.

PRB is strategically for the reproduction and development of the ichthyofauna of the São Francisco River midstream (NUNES et al., 2009). To protect the growth and reproduction of native fish species, the Pandeiros River Environmental Protection Area was created in 1995 through State Law nº 11,901, the largest unit for sustainable use in Minas Gerais State (SANTOS et al., 2015).

The Köppen climate type for PRB is tropical, with predominant precipitation in summer and dry winter (Aw). According to the Thornthwaite climate classification, the climate is defined as dry sub-humid (C1) (MARTINS et al., 2018). The annual temperature varies from 17.9 ºC to 31.6 ºC, with an average of 23.8 ºC.

The average annual precipitation in PRB is 1085 mm, of which 92% occurs during the rainy period (October to March), and evapotranspiration corresponds to 81.4% of rainfall (JUNQUEIRA et al., 2020b). The precipitation in the Brazilian savanna is significantly influenced by the South Atlantic Convergence Zone (SACZ), which is characterized by the coupling of the convergent winds and moisture to transient vortices from higher latitudes and remains quasi-stationary for several days, mainly in the austral summer (December to February) (AMBRIZZI; FERRAZ, 2015; PRADO et al., 2021). Also, other climatic phenomena, such as the El Niño-Southern Oscillation (ENSO), can influence precipitation in the basin (JUNQUEIRA et al., 2020b).

2.2.SWAT model

The Soil and Water Assessment Tool (SWAT) (ARNOLD et al., 1998) is a physically-based hydrological model developed to simulate and predict the impacts of management on water, sediment, and agricultural chemicals in basins over long periods (NEITSCH et al., 2011). In this model, the basin is divided into multiple sub-basins, subdivided into Hydrological Response Units (HRUs), which are territorial units with similar hydrological behavior (GASSMAN et al., 2007). SWAT is based on the water balance in each of the HRUs, according to Equation 1 (NEITSCH et al., 2011).

$$SW_t = SW_0 + \sum_{i=1}^{t} (R_{day} - Q_{surf} - E_a - w_{seep} - Q_{gw}) \quad (1)$$

where: SW_t is the final soil water content (mm); SW_0 is the initial soil water content on day i (mm); t is the time (days); R_{day} is the amount of precipitation on day i (mm); Q_{surf} is the amount of surface runoff on day i (mm); Ea is the amount of evapotranspiration on day i (mm H2O);

w_{seep} is the amount of water entering the vadose zone from the soil profile on day i (mm); Q_{gw} is the amount of return flow on day *i* (mm).

In this study, the Curve Number (CN) method (SCS, 1972) was used to estimate the surface runoff from HRUs, and the Penman-Monteith (MONTEITH, 1965; PENMAN, 1956), to estimate the evapotranspiration in the basin. The variable storage routing method (WILLIAMS, 1969) was adopted to routing the water through the channel network.

2.3.SWAT model input data

To calibrate and validate SWAT, daily streamflow was obtained from the Brazilian National Water Agency (ANA) from 1981 to 2018. The weather variables (mean, minimum, and maximum temperatures, and vapor pressure) were obtained from the Climatic Research Unit (CRU) Time Series (TS) version 4.04 from 1901 to 2018 at a spatial resolution of 0.5º (HARRIS et al., 2020).

As the wind speed is not available in CRU TS v. 4.04 and has low monthly variability (ALLEN et al., 2006), it was obtained from the monthly climatological normal for the period 1961-1990 from CRU CL version 2.0 (NEW et al., 2002), at the same points as CRU TS v. 4.04, and replicated for the entire period (1901-2018). This product provides wind speed data at 10 m in height, which was converted to 1.7 m (HALTINER; MARTIN, 1957). Solar radiation (derived from Hargreaves methodology) and relative humidity were estimated according to Allen et al. (2006) methodology. The location of hydrometeorological variables and maps of soil type and land use are in Figure 1.

To generate the HRUs, soil type (FEAM, 2010) on a scale of 1:650,000 and land use maps (IBGE, 2018) on a scale of 1:1,000,000 were used. The DEM (Figure 1) was used to generate the slope map, which was divided into four classes: 0-3 %, 3-5 %, 5-8 %, and > 8 %. The Red-Yellow Oxisol (LVA) is the predominant soil unit in PRB (88.3 % of the basin's area), followed by the Fluvic Entisol (RQ, 4.1 %), Quartz Entisol (RY, 4.0 %), and Melanic Entisol (GM, 3.7 %). Cerrado is the predominant land use (CERR, 96.3 %), followed by agriculture (AGRL, 2.0 %), forest vegetation (FRST, 1.7 %), and pasture (PAST, 0.1 %).

2.4.Reanalysis data

2.4.1. ERA-20CM

The twentieth-century atmospheric model ensemble (ERA-20CM) is an ensemble of ten atmospheric model integrations that provide data from 1900 to 2010. Its resolution is T159 (approximately 125 km in grid-point space) in the spectral horizon, using 91 levels in the

vertical from the surface up to 1 Pa (approximately 80 km altitude), and a time step of one hour (HERSBACH et al., 2015; POLI et al., 2016).

According to Hersbach et al. (2015), ERA-20CM is a variation of the atmosphere and ocean-wave forecast model components of Cy38r1, daily sea surface temperature (SST) and sea ice cover are prescribed by an ensemble of ten realizations (HadISST2.1). These realizations are a biased reflection of the estimates and uncertainties in the observed sources. The forcing terms in the model radiation scheme follow Coupled Model Intercomparison Project Phase 5 recommendations. The forcing terms incorporate both long-term climate evolution and the periodical occurrence of events, such as the El Niño-Southern Oscillations and volcanic eruptions.

In this study, we select the ten ERA-20CM ensemble members (Ens0 to Ens9) with precipitation data every 3 hours, accumulated for a daily scale, and a 0.125°×0.125° grid from January 1900 to December 2010 (HERSBACH et al., 2013, 2015). The values of the ten ERA-20CM ensemble members were averaged (AE) for further analysis.

2.4.2. ERA5-Land

The land component of the fifth generation of European ReAnalysis (ERA5-Land) is a reanalysis dataset that produces precipitation and 52 other variables describing, globally, the water and energy cycle over land, with a temporal resolution of 1 hour and spatial resolution of 9 km. This dataset is available from January 1950 to the present (with up to a 3-month lag) (MUÑOZ-SABATER, 2019, 2021; MUÑOZ-SABATER et al., 2021).

The land surface model used in the ERA5-Land production is the Carbon Hydrology-Tiled ECMWF Scheme for Surface Exchanges over Land (CHTESSEL) from the model cycle Cy45r1. The ERA5-Land does not assimilate observations directly; however, atmospheric observations (air temperature, specific humidity, wind speed, and surface pressure) are added as atmospheric forcing and corrected using a daily lapse rate correction derived from ERA5 (MUÑOZ-SABATER et al., 2021). According to Muñoz Sabater (2019), these forcings are essential so that the model estimates do not deviate from the real pattern.

This study uses the accumulated hourly precipitation data, which was converted to a daily time scale from January 1950 to December 2018 (MUÑOZ-SABATER, 2019, 2021).

2.5.Bias correction

Several methodologies have been developed to remove the bias of the precipitation outputs from climatic models, among which the linear scaling (LSC) (LENDERINK;

BUISHAND; VAN DEURSEN, 2007) stands out due to its simplicity and efficiency (CORREA et al., 2019). This method is based on the difference between observed precipitation (OP) and estimated precipitation, corrected with a factor based on the long-term monthly average ratio (TEUTSCHBEIN; SEIBERT, 2012), according to Equation 2.

$$P^{*}_{rean} = P_{rean} \times \left[\frac{\mu_m(P_{obs})}{\mu_m(P_{rean,obs})} \right] \quad (2)$$

where: P^{*}_{rean} is the final value of precipitation with bias correction; P_{rean} is the precipitation without bias correction; P_{obs} is the observed precipitation; $P_{rean,obs}$ is the precipitation without bias correction for the period when observed data are available; μ_m is the average parameter of the normal distribution for month *m*.

This study applied the bias correction to the ten ERA-20CM ensemble members, the AE, and the ERA5-Land.

2.6.Calibration, validation, and uncertainty analysis

The SWAT-CUP software package with the SUFI-2 algorithm was used for calibration, validation, and uncertainty analysis. According to Abbaspour et al. (2015), this algorithm seeks all uncertainties (parameter, conceptual model, input, etc.) on the parameters and tries to envelop most of the observations within the 95 % prediction uncertainty (95PPU) of the model. The 95PPU is calculated at the 2.5 % and 97.5 % levels of the cumulative distribution of an output variable using Latin hypercube sampling.

In this study, the calibration (2004-2011) was carried out with OP of four rain gauge stations from ANA (station codes 1545006, 1445000, 1545005, and 1544032) and CRU climate data, with the warm-up period from June 2000 to December 2003. It used two iterations of 600 simulations each and Nash-Sutcliffe efficiency (NSE) as the objective function. The best set parameters and the final range obtained in the calibration were replicated in the validation phase with OP and CRU setup from January 2012 to December 2018. Afterward, the validation of the hydrological simulation with the ten ERA-20CM ensemble members, AE, and ERA5-Land with bias correction and CRU climate data was conducted with the best parameters obtained in the calibration phase from 1981 to 2010.

To quantify the uncertainty during the calibration and validation phases with OP and CRU data, two statistics were used: p-factor, which relates to the percentage of observed data enveloped by the modeling result, the 95PPU; and r-factor, which is associated with the thickness of the 95PPU envelop (ABBASPOUR, 2015). Abbaspour et al. (2015) highlighted

that there should be a balance between these two indices; however, p-factor >0.7 and r-factor <1.5 for discharge are recommended.

2.7.Performance of precipitation and hydrological modeling

To analyze the quality of estimated precipitation data and identify the reanalysis product that most adequately represents the past climatic conditions, the ten ERA-20CM ensemble members, AE, and ERA5-Land were compared with the OP on a daily and monthly time scales through the point-to-pixel approach, using the most extended as possible the same period between the reanalysis and OP products. This methodology compares the rain gauge values with the corresponding pixel value of reanalysis products (NOGUEIRA; MOREIRA; VOLPATO, 2018). For this purpose, the Pearson correlation coefficient (r), Root Mean Square Error (RMSE), and Kling-Gupta efficiency (KGE) were used (Table 1).

Table 1. Statistical metrics that will be used to evaluate the performance of precipitation and hydrological modeling.

Statistical metrics	Equation	Ideal value	Unit
Pearson correlation coefficient	$r = \frac{\sum_{i=1}^{N}(O_i - O_m)\times(E_i - E_m)}{\sqrt{\sum_{i=1}^{N}(O_i - O_m)^2 \times \sum_{i=1}^{N}(E_i - E_m)^2}}$	1	-
Root Mean Square Error	$RMSE = \sqrt{\frac{\sum_{i=1}^{N}(E_i - O_i)^2}{N}}$	0	mm
Kling-Gupta efficiency	$KGE = 1 - \sqrt{(r-1)^2 + (\beta-1)^2 + (\gamma-1)^2}$ $\beta = \frac{E_m}{O_m} \qquad \gamma = \frac{\sigma_E/E_m}{\sigma_O/O_m}$	1	-
Percent bias	$PBIAS = \left[\frac{\sum_{i=1}^{N}(O_i - E_i)}{\sum_{i=1}^{N} O_i}\right] \times 100$	0	%
Nash-Sutcliffe efficiency	$NSE = 1 - \left[\frac{\sum_{i=1}^{N}(O_i - E_i)^2}{\sum_{i=1}^{N}(O_i - E_m)^2}\right]$	1	-
Logarithmic Nash-Sutcliffe efficiency	$LNSE = 1 - \left\{\frac{\sum_{i=1}^{N}[\log(O_i) - \log(E_i)]^2}{\sum_{i=1}^{N}[\log(O_i) - \log(E_m)]^2}\right\}$	1	-

Note: E and O are the estimated and observed variables, respectively; Em and Om are the averages of the estimated and observed variables, respectively; σE and σO are the standard deviations of the estimated and observed variables, respectively; i is the time sequence of observed and simulated pairs; N is the number of observed and simulated pairs.

KGE, percent bias (PBIAS), NSE, and its logarithmic version (LNSE) (Table 1) were used in this study to analyze the performance of best fit in the hydrological modeling. Moriasi et al. (2007) developed an overall performance rating for NSE and PBIAS to evaluate the model during the calibration and validation in a monthly time step: “very good” (NSE > 0.75; PBIAS < ± 10); “good” (0.65 < NSE ≤ 0.75; ± 10 ≤ PBIAS < ± 15); “satisfactory” (0.50 < NSE ≤ 0.65; ± 15 ≤ PBIAS < ± 25); and “unsatisfactory” (NSE ≤ 0.50; PBIAS ≥ ± 25). Because of the similarities, the same classification of NSE was used for the LNSE. KGE values above 0.6 are generally considered good (TAREK; BRISSETTE; ARSENAULT, 2020).

2.8. Hydrological drought analysis

The Standardized Streamflow Index (SSI) is a hydrological drought index, helpful in making comparisons over a wide variety of river regimes and flow characteristics (VICENTE-SERRANO et al., 2012). In this study, the SSI was used to validate the hydrological drought with simulated streamflow (from 1981 to 2010) and then calculate the historical drought with the simulation that provided the best streamflow estimates.

To calculate the SSI, the mean annual observed and simulated streamflow, considering the hydrological year (October to September). In this historical series, the Gamma probability density function (PDF) was fitted. Then, the inverse normal distribution was used to obtain the respective "z" value for each non-exceeded probability prior estimated by Gamma PFD. The adherence of the Gamma PDF was tested with the Kolmogorov-Smirnov test.

The coefficient of correlation (r) between observed and simulated SSI was calculated ($\alpha = 0.05$). This analysis assists in understanding which product has better performance in simulating SSI, either drought or wet events, in PRB.

Finally, the SSI was classified according to Svoboda et al. (2002), the same classification adopted by the National Oceanic and Atmospheric Administration of the United States (NOAA), which divides drought into four levels: “moderate drought” – D1 ($-0.8 \geq SSI > -1.3$); “severe drought” – D2 ($-1.3 \geq SSI > -1.6$); “extreme drought” – D3 ($-1.6 \geq SSI > -2.0$); and “exceptional drought” – D4 ($SSI \leq -2.0$). Additionally, this classification includes a fifth category, D0 ($-0.5 \geq SSI > -0.8$), which designates those areas experiencing either "abnormally dry" conditions that may precede a drought or that portend persistent impacts following a drought event.

The reanalysis product that presents the best performance in the validation of hydrological modeling and best hydrological drought estimation was used to develop the HR and historical drought analysis on the monthly time scale.

The Run Theory (YEVJEVICH, 1967) characterizes the droughts' severity and duration. In this methodology, drought events are grouped independently, and the duration is obtained by the number of years that the event persisted below a threshold. In contrast, the severity is a result of the sum of the drought index of all the months, in absolute values ("S = "-" " ∑_"i=1" ^"D" ▒"SSI" , where S is the severity, and D is the duration).

Sklar (1959) introduced the bivariate copula function to model the dependence structure among the two main drought characteristics, severity, and duration. For this analysis, the threshold for characterizing drought events was −0.5. The exponential and log-normal distributions are used to model the drought duration and severity, respectively. Afterward, the two-dimensional copula was employed to jointly analyze drought duration and intensity. Among the several copula families available, the Frank (1979) family was used in this study because it has presented satisfactory results in Brazil (ALMEIDA; BARBOSA, 2020; ROCHA JÚNIOR et al., 2020).

3. RESULTS AND DISCUSSION

3.1.Precipitation evaluation

Table 2 presents the average statistical results on daily and monthly time scales related to the accuracy of the ten ERA-20CM ensemble members, AE, and ERA5-Land with bias correction regarding observed precipitation (OP) in PRB. The reanalysis products presented a better performance on a monthly scale, mainly due to higher r and KGE values, which agrees with the results obtained by Gehne et al. (2016) with reanalysis products on a global scale.

Table 2. Statistical results for the ten ERA-20CM ensemble members, the AE, and the ERA5-Land on a daily (*) and monthly (**) time scales in the PRB.

Statistic	ERA-20CM ensemble members										AE	ERA5-Land
	Ens 0	Ens 1	Ens 2	Ens 3	Ens 4	Ens5	Ens6	Ens7	Ens8	Ens9		
r*	0.14	0.17	0.17	0.15	0.15	0.16	0.17	0.19	0.18	0.17	0.30	0.43
RMSE*	10.9	10.6	10.5	10.9	10.7	10.8	10.6	10.4	10.5	10.6	9.1	9.1
KGE*	0.09	0.12	0.11	0.09	0.08	0.11	0.10	0.14	0.11	0.12	0.06	0.36
r**	0.64	0.70	0.64	0.67	0.65	0.62	0.66	0.67	0.68	0.68	0.78	0.89
RMSE**	99.7	90.7	98.8	96.0	95.3	101.4	96.0	94.7	92.2	92.2	75.3	56.1
KGE**	0.64	0.70	0.63	0.66	0.63	0.61	0.65	0.66	0.67	0.67	0.70	0.86

The ERA5-Land presented the best performance, which can be associated with the climate variables used, such as air temperature, air humidity, and pressure, as radiative forcing

that are not used in ERA-20CM (MUÑOZ-SABATER et al., 2021). In addition, ERA5-Land uses a more recent model cycle than ERA-20CM (Cy45r1 from 2018 vs. Cy38r1 from 2012). Cy45r1 showed relevant updates in the dynamic coupling between the ocean, sea ice, and atmosphere compared to previous versions and other appropriate changes (ECMWF, 2018).

AE performed better than the ten ERA-20CM ensemble members, especially on a monthly scale. On the other hand, Kim and Han (2019) found a better performance of other ensemble members in relation to AE in South Korea. There was a slight variation in performance among the ten ERA-20CM ensemble members, with the Ens7 and Ens1 performing better on a daily and monthly scale, respectively. However, Gao et al. (2016) reported that Ens7 and Ens1 did not perform well in China, and each performed worst in two of the eight regions analyzed. Therefore, these members cautiously should be used in hydrological studies in the Brazilian savanna.

3.2.Calibration, validation, and uncertainty analysis

Ten parameters were used in the SWAT calibration and validation with OP and CRU climatological data, selected based on previous studies in the PRB (JUNQUEIRA et al., 2022a). The final range and the best parameters obtained in the calibration (Table 3) agree with the result obtained by Junqueira et al. (2022) in the same basin using OP and observed climatological data from 2004 to 2018. However, there are divergences like RECHG_DP (deep aquifer percolation fraction) and CH_K1 (effective hydraulic conductivity in tributary channel alluvium), which showed best values equal to 0.050 and 11.44 mm.h-1, respectively, in the previous study.

Table 3. Parameters used to calibrate the SWAT model with OP and CRU climatological data and their initial and final ranges, and best parameters (BP).

Parameters	**Initial range**		**Final range**		**BP**
r_CN2.mgt	-0.100	0.100	-0.100	0.002	-0.090
v_ALPHA_BF.gw	0.0050	0.0100	0.0050	0.0078	0.0051
a_GW_DELAY.gw	0.00	60.00	22.72	60.00	50.09
a_GWQMN.gw	0	2000	0	1208	925
v_CH_K2.rte	0.00	20.00	5.92	17.78	14.27
v_GW_REVAP.gw	0.020	0.200	0.109	0.200	0.190
r_SLSUBBSN.hru	0.00	1.00	0.39	1.00	0.78
v_RCHRG_DP.gw	0.000	0.200	0.093	0.200	0.198
v_CH_K1.sub	0.00	20.00	0.00	12.48	2.86
v_CH_N2.rte	0.000	0.300	0.149	0.300	0.259

Figure 2 presents the simulated streamflow in the calibration and validation using the best parameters and the 95PPU with OP and CRU climatological data (from 2004 to 2018) and the scatter plots of observed and simulated streamflow. Besides, Table 4 presents the uncertainty analysis and performance results for the calibration and validation, expressed by the p-factor, r-factor, NSE, LNSE, PBIAS, and KGE.

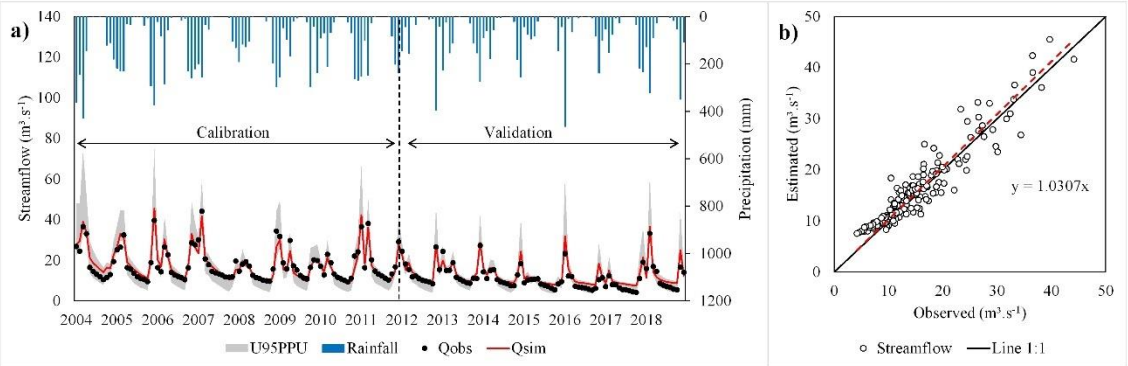

Figure 2. a) Average precipitation, observed (Qobs) and simulated (Qsim) monthly streamflow, and uncertainty band; and b) scatter plots of the observed and simulated streamflow.

Table 4. Results of uncertainty and performance analysis of SWAT for the calibration and validation with OP and CRU climate data.

	p-factor	r-factor	NSE	LNSE	PBIAS (%)	KGE
Calibration	0.98	1.29	0.89	0.88	-1.8	0.94
Validation	0.95	1.24	0.78	0.72	-12.7	0.85

The hydrological modeling showed low uncertainty during the calibration, with a p-factor close to 1 and r-factor less than 1.5, as recommended by Abbaspour et al. (2015). This result is confirmed by Figure 2a, where it is observed that the 95PPU presented a small band covering most of the observed data. Regarding the performance of the hydrological modeling, NSE, LNSE, and PBIAS gave a result classified as "very good", according to Moriasi et al. (2007) classification. Also, the KGE close to 1 indicates a high fit between the simulated and observed data.

In the validation phase, there was a reduction in the r-factor, which caused a reduction in the p-factor. Abbaspour et al. (2015) suggest that there should be a balance between the two factors. Therefore, there is no significant difference between the calibration and validation phases' uncertainty. However, the performance of the hydrological simulation in the validation was worsened with a decrease in NSE, LNE, and KGE and an increase in PBIAS (in absolute values).

According to Junqueira et al. (2020), an intense hydrological drought from 2013 to 2018 affected the basin, reducing the average streamflow rate by more than 50%. This drought can

be related to the most significant overestimation of the simulated streamflow in the validation since the hydrological conditions were distinct during the calibration period. This behavior was also observed in the scatter plot (Figure 2b), where there was an overestimation of the lowest observed streamflow, which occurred during the drought years' recession period. Despite that, there was a satisfactory performance of the hydrological modeling.

3.3.Hydrological validation with reanalysis products

The hydrological modeling validation using precipitation products of climate reanalysis and CRU climate data was performed from 1981 to 2010 (Figure 3). Additionally, Table 5 presents the statistical results of the validation with the different products.

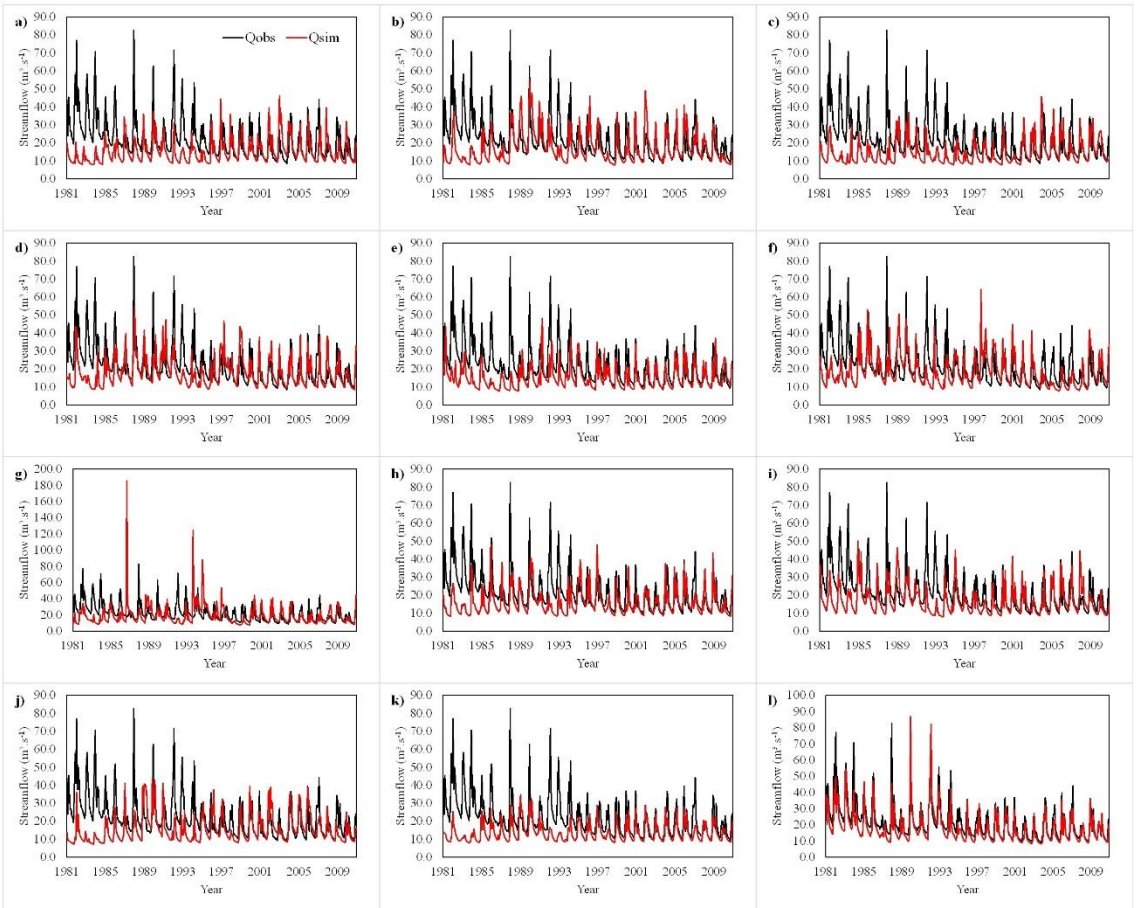

Figure 3. Hydrological validation with the ten ERA-20CM ensemble members (a to j) and AE (k) from the ERA-20CM, and the ERA5-Land (l) from 1981 to 2010 to PRB.

Table 5. Statistical results of hydrological validation with the ten ERA-20CM ensemble members, the AE, and the ERA5-Land from 1981 to 2010 to PRB.

Statistic	ERA-20CM ensemble members										AE	ERA5-Land
	Ens 0	Ens 1	Ens 2	Ens 3	Ens 4	Ens 5	Ens 6	Ens 7	Ens 8	Ens9		
NSE	-0.50	-0.23	-0.51	-0.16	-0.33	-0.21	-1.35	-0.21	-0.09	-0.53	-0.42	0.53
LNSE	-0.96	-0.49	-1.03	-0.27	-0.57	-0.26	-0.67	-0.43	-0.22	-1.08	-0.81	0.63
PBIAS (%)	31.0	22.5	34.8	18.3	31.1	16.9	13.9	28.2	24.9	30.1	38.8	5.5
KGE	0.05	0.29	0.08	0.28	0.15	0.28	0.08	0.24	0.32	0.11	0.09	0.76

All reanalysis products were able to simulate the seasonal behavior of the streamflow (Figure 3); however, some divergences are observed. The ERA5-Land was the only reanalysis product to show satisfactory results. i.e., NSE and LNSE > 0.5 and a “very good” PBIAS (MORIASI et al., 2007). Also, the KGE was greater than 0.6, considered good according to Tarek et al. (2020). This result corroborates with the precipitation validation, where the ERA5-Land presented accumulated precipitation values closer to OP and better statistics on a daily and monthly scales.

Approximately 72.5% of the observed streamflow is covered by the range of simulated streamflow with the ten ERA-20CM ensemble members, with no significant difference between the rainy and dry periods (72.2% and 72.8%, respectively). However, the performance of these products was unsatisfactory, according to Moriasi et al. (2007) and Tarek et al. (2020) classifications. Correa et al. (2017) also found unsatisfactory performance with ERA-20CM applied to hydrological modeling in the Amazon basin. Although they did not show the best result among the ten ERA-20CM ensemble members and AE in precipitation validation, Ens5 and Ens8 performed reasonably well in hydrological modeling, as shown in Table 5.

3.4.Drought analysis

The Kolmogorov-Smirnov test ($\alpha = 0.05$) indicated the suitability of the Gamma PDF in all situations. Therefore, the SSI was calculated for the observed and simulated streamflow, as shown in Figure 4.

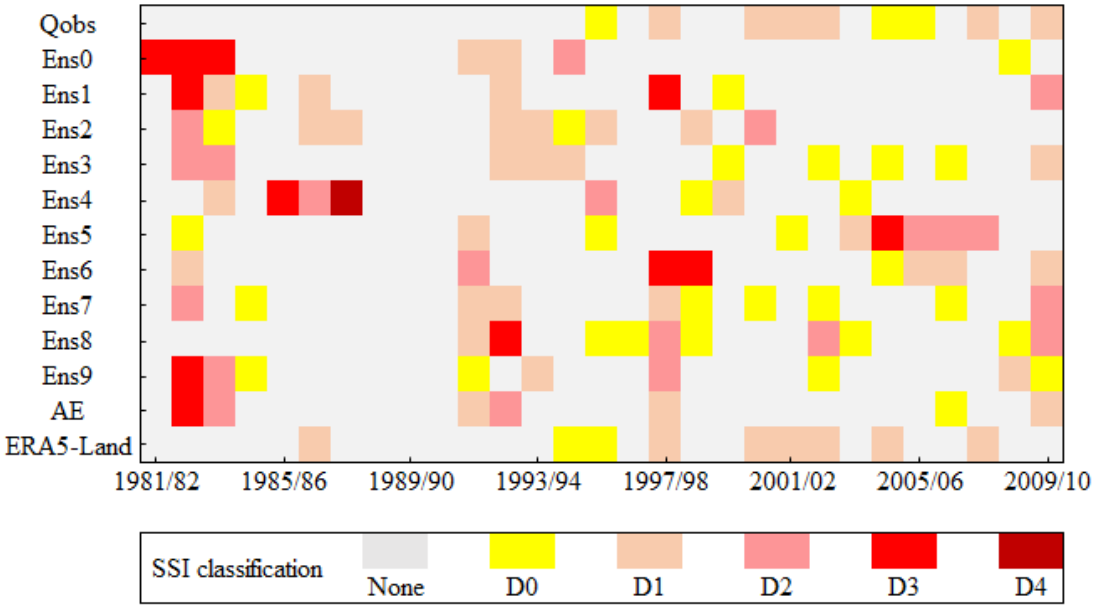

Figure 4. SSI classification for the observed (Qobs) and simulated streamflow with the ten ERA-20CM ensemble members, the AE, and the ERA5-Land from 1981/82 to 2009/10 for the PRB.

The main observed hydrological drought events occurred in 1997/98, 2000/01 to 2002/03, 2007/08, and 2009/10, all in the second half of the time series. In addition, abnormally dry years were observed in 1995/96, 2004/05, and 2005/06, the latter two reflecting the longest and most severe drought (2000/01 to 2002/03) to hit the basin from 1981 to 2010. Although 2003/04 was considered an average year, the SSI was -0.47, close to the D0 class.

ERA5-Land was the reanalysis product that presented the best capacity to represent the hydrological drought occurrence in the basin, reflecting the best performance of this product in precipitation estimation and hydrological modeling. ERA5-Land setup could predict five of the six observed hydrological drought events from 1981 to 2010, all in the same drought classification, representing 83% of the total events.

The longest hydrological drought that affected the basin occurred from 2000/01 to 2002/03, with severity equal to 3.23. The SSI based on the ERA5-Land setup was able to correctly estimate the duration (three years) and severity (3.25) of the drought in this period. On the other hand, the SSI based on ERA-20CM products did not provide an appropriate estimate of the drought in this period.

Among the ten ERA-20CM ensemble members, the one that presented the highest representation of drought events in the basin was the Ens8 setup (which also gave a better performance in hydrological modeling), with 50% of coincidence (1997/98, 2002/03, and 2009/10). However, it overestimated the drought intensity in all of these events. Ens0 and Ens4

setups could not capture any drought events in the basin. On the other hand, Correa et al. (2019), using data assimilation techniques and different approaches for bias correction, report that ERA-20CM was able to capture extreme events in the Amazon basin. AE, which showed better precipitation performance, could not perform a satisfactory hydrological simulation and, consequently, an acceptable simulation, therefore, predicting drought years.

Pearson's correlation coefficient indicates an adequate fit of the estimated SSI based on ERA5-Land to the observed SSI ($r = 0.87$), while the SSI calculated based on the ERA-20CM products showed a low correlation to the observed SSI ($r < 0.2$). This result indicates the better ability of ERA5-Land to simulate dry, wet, and average periods.

Although ERA5-Land has a shorter historical series than ERA-20CM, the performance was superior in all analyses conducted. Moreover, in general, the uncertainty of the model estimates is higher for the older period due to a smaller number of observations available to create an atmospheric forcing of adequate quality (MUÑOZ-SABATER et al., 2021). A similar situation occurs with the CRU data estimate, where the availability of observed data is low at the beginning of the 20th century in Brazil and increases over the years (HARRIS et al., 2020). Thus, ERA5-Land should be considered in hydrological studies that require long precipitation time series in the Brazilian savanna.

3.5.Hydrological retrospective and historical droughts

Based on results obtained in the precipitation products validation, hydrological modeling, and drought analysis, the HR was developed using ERA5-Land precipitation data and CRU climate data from January 1950 to December 2018 (Figure 5a). The inter and intra-annual behavior of the simulated streamflow was similar to the behavior of the basin-scale precipitation, which shows the model's capacity to simulate the streamflow in different meteorological conditions, such as wet and dry periods.

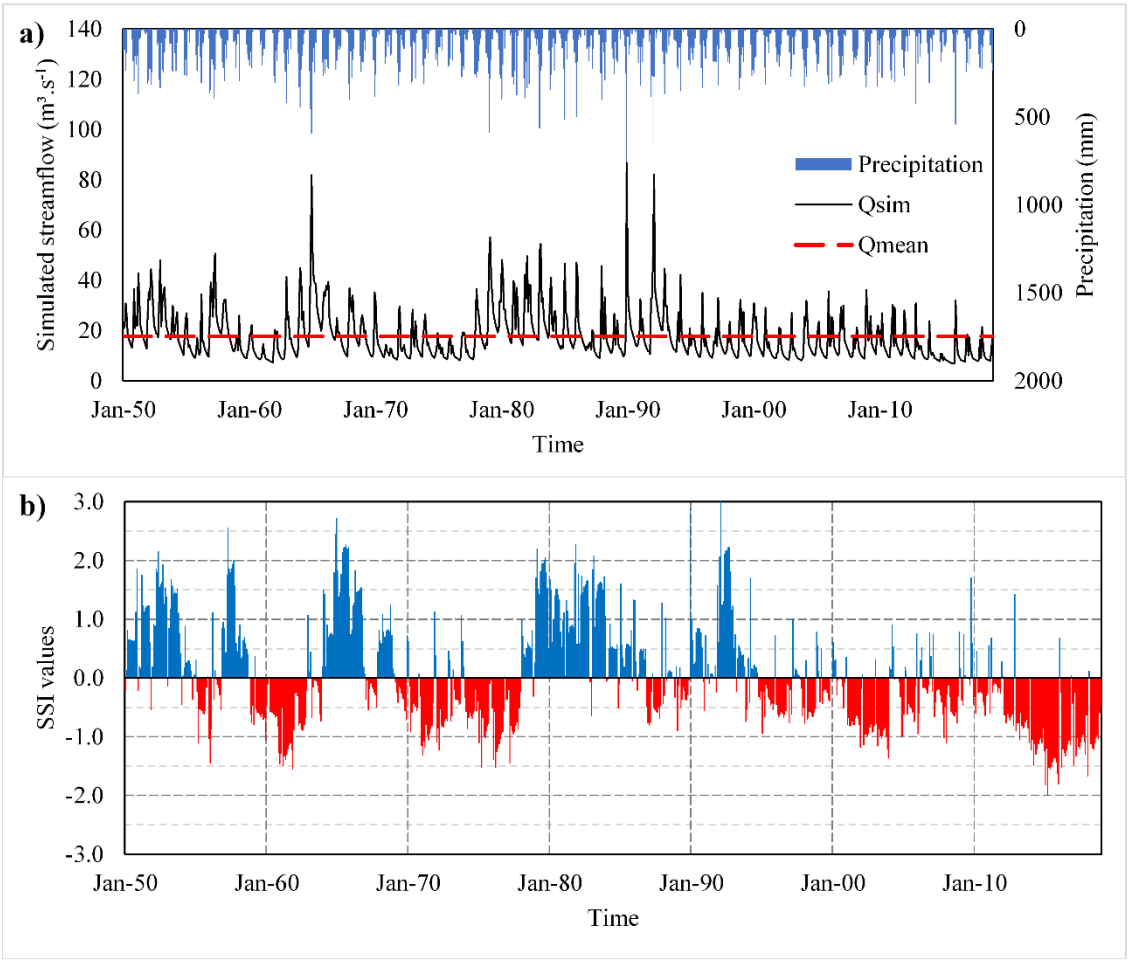

Figure 5. HR (Qsim), mean streamflow (Qmean), and basin-scale precipitation (a) and historical drought results for PRB from January 1950 to December 2018 (b).

The most severe and most extended droughts that hit PRB from 1950 to 2018 occurred in 1958/62, 1970/72, 1974/77, 2001/03, and 2012/18 (Figure 5b), although there were some non-drought months within these events. Other Brazilian regions also have experienced drought events in some of these years, such as the state of Ceará in 1958 and 2012/18 (PONTES FILHO et al., 2020), Northeastern Brazil; São Paulo city in 1962/63 and the metropolitan region of Belo Horizonte in 1970/71 (SILVA; MELLO, 2021), both in Southeastern Brazil; in the Doce river basin in 2000/01 and 2013/17 (JESUS et al., 2020), Southeastern Brazil; and the Tocantins river basin from 2015 to 2017 (JUNQUEIRA et al., 2020a), located in the Brazilian savanna; which confirms the adopted procedure's ability to represent the most relevant droughts.

Overall, 294 months presented SSI values classified as drought or abnormally dry, of which 51.7% occurred in the last third of the period (1996-2018), behavior also observed in other studies of hydrological drought in Brazil (CUARTAS et al., 2022; JESUS et al., 2020; JUNQUEIRA et al., 2022b). Consequently, this period (1996-2018) displayed the lowest

amount of months with SSI ≤ 0.5, only 7.9% of the total. On the other hand, the second third of the period (1973-1995) showed a high incidence of wet months (47.9% of the total) and a low incidence of drought months (20.1%). Therefore, there has been an increase in droughts and a reduction of wet periods (precipitation above average) in recent decades.

Considering only the periods when the SSI was less than −0.5, the longest and most severe drought occurred from January 2014 to December 2015, totaling 24 months of duration and severity equal to 32.57, followed by the drought from April 1960 to December 1961, with a duration of 21 months and severity of 21.77, and by the drought from March 2017 to January 2018 (11 months), with a severity of 12.53. Therefore, there is a strong correlation between drought duration and severity, as observed by (ALMEIDA; BARBOSA, 2020), i.e., the longer the duration of the drought, the greater its severity. This result is confirmed by Pearson's correlation coefficient between drought severity and duration (r = 0.96). A similar analysis was conducted by Shiau (2006) at a rain gauge station in Southern Taiwan, who found a correlation of 0.756.

The copula function was performed to model the dependency structure between the two main drought characteristics, severity, and duration (Figure 6).

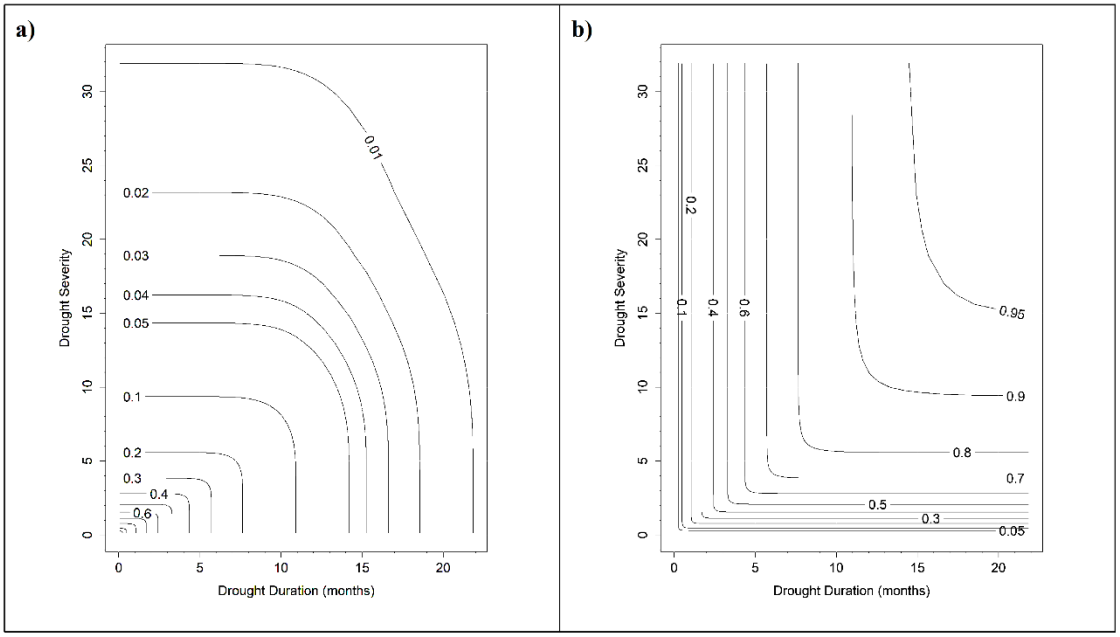

Figure 6. Conditional probability (a) and joint probability (b) of copula analysis.

Figure 6a indicates the probability that the drought's duration and severity exceed certain thresholds simultaneously. On the other hand, the joint probability (Figure 6b) indicates the probability of a given severity occurring related to a given duration. For example, there is a 5% probability that a given drought event will simultaneously exceed 13,5 months in duration

and severity of 10 (Figure 6a). However, when a drought reaches 13,5 months in duration, the probability of its severity equaling 10 is almost 90% (Figure 6b). This result can have a relevant practical application, for example, to recognize a critical condition for a specific water supply system or be used to trigger a drought contingency plan (SHIAU, 2006).

4. CONCLUSIONS

ERA5-Land performed better in the precipitation validation for daily and monthly time scales when compared to ERA-20CM, with superior results in all statistics (r, RMSE, and KGE). Among the ERA-20CM products, AE performed better than the ten ERA-20CM ensemble members, especially on a monthly scale.

In hydrological modeling, ERA5-Land was the only product to show satisfactory performance, following the criteria of Moriasi et al. (2007) and Tarek et al. (2020) (NSE = 0.53, LNSE = 0.63, PBIAS = 5.5%, and KGE = 0.76). On the other hand, the ERA-20CM ensemble members and the AE showed unsatisfactory performance in most statistics. A similar result was obtained in the drought analysis, where ERA5-Land simulated five out of six drought events from 1981 to 2010. Therefore, ERA5-Land was able to simulate past streamflow and hydrological droughts.

The main historical drought events occurred in 1958/62, 1970/72, 1974/77, 2001/03, and 2012/18, with most of the months classified as drought or abnormally dry (51.7% of the total) occurring in the last third of the historical series (1996-2018). Also, there was a reduction in the months with excess precipitation in the final third of the historical series (only 7.9% of the total).

REFERENCES

ABBASPOUR, K. C. et al. A continental-scale hydrology and water quality model for Europe: Calibration and uncertainty of a high-resolution large-scale SWAT model. **Journal of Hydrology**, v. 524, p. 733–752, 2015.

ABBASPOUR, K. C. **SWAT-CUP: SWAT Calibration and Uncertainty Programs**, 2015.

ALLEN, R. G. et al. **FAO Irrigation and Drainage Paper - Crop Evapotranspiration,** Rome, Italy, 2006.

ALMEIDA, R. DE; BARBOSA, P. S. F. Simulation of the occurrence of drought events via copulas. **Revista Brasileira de Recursos Hídricos**, v. 25, p. 1–13, 2020.

AMBRIZZI, T.; FERRAZ, S. E. T. An objective criterion for determining the South Atlantic convergence zone. **Frontiers in Environmental Science**, v. 3, n. APR, p. 1–9, 2015.

ARNOLD, J. G. et al. Large area hydrologic modeling and assessment part I: model development. **Journal of the American Water Resources Association**, v. 34, n. 1, p. 73–89, 1998.

AUERBACH, D. A. et al. Evaluating weather observations and the Climate Forecast System Reanalysis as inputs for hydrologic modelling in the tropics. **Hydrological Processes**, v. 30, n. 19, p. 3466–3477, 15 Sep 2016.

BARKER, L. J. et al. Historic hydrological droughts 1891–2015: systematic characterisation for a diverse set of catchments across the UK. **Hydrology and Earth System Sciences**, v. 23, n. 11, p. 4583–4602, 15 Nov 2019.

BRAZILIAN INSTITUTE OF GEOGRAPHY AND STATISTICS (IBGE). **Mapa de Cobertura e Uso da Terra do Brasil 2010, 2018.** Disponível em: <https://www.ibge.gov.br/geociencias/informacoes-ambientais/cobertura-e-uso-da-terra/15831-cobertura-e-uso-da-terra-do-brasil.html?edicao=16023&t=sobre>

BRAZILIAN INSTITUTE OF GEOGRAPHY AND STATISTICS (IBGE). **Biomas e Sistema Costeiro-Marinho do Brasil - 1:250.000**, 2019.

CORREA, S. W. et al. Multi-decadal Hydrological Retrospective: Case study of Amazon floods and droughts. **Journal of Hydrology**, v. 549, p. 667–684, 2017.

CORREA, S. W. et al. Hydrological reanalysis across the 20th century: A case study of the Amazon Basin. **Journal of Hydrology**, v. 570, p. 755–773, 2019.

CUARTAS, L. A. et al. Recent Hydrological Droughts in Brazil and Their Impact on Hydropower Generation. **Water**, v. 14, n. 4, p. 601, 16 Feb 2022.

DEE, D. P. et al. Toward a consistent reanalysis of the climate system. **Bulletin of the American Meteorological Society,** v. 95, n. 8, p. 1235–1248, 2014.

ECMWF. **IFS Documentation CY45R1**. Reading, England: ECMWF, 2018.

FRANK, M. J. On the simultaneous associativity of F(x, y) and x+y−F(x, y). **Aequationes Mathematicae**, v. 19, n. 1, p. 194–226, Des 1979.

GADELHA, A. N. et al. Grid box-level evaluation of IMERG over Brazil at various space and time scales. **Atmospheric Research**, v. 218, p. 231–244, 2019.

GAO, L. et al. A first evaluation of ERA-20CM over China. **Monthly Weather Review**, v. 144, n. 1, p. 45–57, 2016.

GASSMAN, P. W. et al. The soil and water assessment tool: historical development, applications, and future research directions. **Transactions of the ASABE**, v. 50, n. 4, p. 1211–1250, 2007.

GEHNE, M. et al. Comparison of global precipitation estimates across a range of temporal and spatial scales. **Journal of Climate**, v. 29, n. 21, p. 7773–7795, 2016.

HALTINER, G. J.; MARTIN, F. L. **Dynamic and physical meteorology.** McGraw-Hill Book Company, 1957.

HARRIS, I. et al. Version 4 of the CRU TS monthly high-resolution gridded multivariate climate dataset. **Scientific Data**, v. 7, n. 1, p. 109, 3 Des 2020.

HERSBACH, H. et al. ERA-20CM: a twentieth century atmospheric model ensemble. **Report**, p. 46, 2013.

HERSBACH, H. et al. ERA-20CM: a twentieth-century atmospheric model ensemble. **Quarterly Journal of the Royal Meteorological Society**, v. 141, n. 691, p. 2350–2375, 2015.

HOFMANN, G. S. et al. The Brazilian Cerrado is becoming hotter and drier. **Global Change Biology,** v. 27, n. 17, p. 4060–4073, 2021.

IPCC. **Climate Change 2013: The Physical Science Basis. Contribution of Working Group I to the Fifth Assessment Report of the Intergovernmental Panel on Climate Change**. Cambridge, United Kingdom and New York, NY, USA.

JAJARMIZADEH, M. et al. Prediction of Surface Flow by Forcing of Climate Forecast System Reanalysis Data. **Water Resources Management**, v. 30, n. 8, p. 2627–2640, 2016.

JESUS, E. T. et al. Meteorological and hydrological drought from 1987 to 2017 in Doce River Basin, Southeastern Brazil. **Revista Brasileira de Recursos Hídricos**, v. 25, p. 1–12, 2020.

JUNQUEIRA, R. et al. Drought severity indexes for the Tocantins River Basin, Brazil. **Theoretical and Applied Climatology**, v. 140, p. 1–17, 3 Mei 2020a.

JUNQUEIRA, R. et al. Hydrological Response to Drought Occurrences in a Brazilian Savanna Basin. **Resources**, v. 9, n. 10, p. 123, 16 Okt 2020b.

JUNQUEIRA, R. et al. Hydrological modeling using remote sensing precipitation data in a Brazilian savanna basin. **Journal of South American Earth Sciences**, v. 115, n. March, p. 103773, Mrt 2022a.

JUNQUEIRA, R. et al. Drought occurrences and impacts on the upper Grande river basin, Brazil. **Meteorology and Atmospheric Physics**, v. 134, n. 3, p. 45, 12 Jun 2022b.

KIM, D.-I.; HAN, D. Evaluation of ERA-20cm reanalysis dataset over South Korea. **Journal of Hydro-Environment Research**, v. 23, n. January, p. 10–24, 2019.

KIM, D.-I.; KWON, H.; HAN, D. Exploring the Long-Term Reanalysis of Precipitation and the Contribution of Bias Correction to the Reduction of Uncertainty over South Korea : A Composite Gamma-Pareto Distribution Approach to the Bias Correction. **Hydrology and Earth System Sciences**, February, p. 1–53, 2018.

LENDERINK, G.; BUISHAND, A.; VAN DEURSEN, W. Estimates of future discharges of the river Rhine using two scenario methodologies: direct versus delta approach. **Hydrology and Earth System Sciences**, v. 11, n. 3, p. 1145–1159, 3 Mei 2007.

MARTINS, F. B. et al. Classificação climática de Köppen e de Thornthwaite para Minas Gerais: cenário atual e projeções futuras. **Revista Brasileira de Climatologia**, v. 1, p. 149–164, 8 Nov 2018.

MINAS GERAIS STATE ENVIRONMENTAL FOUNDATION (FEAM). **Mapa de solos do Estado de Minas Gerais**, 2010.

MONTEITH, J. L. Evaporation and environment. **Symposia of the society for experimental biology**, p. 205–234, 1965.

MORIASI, D. N. et al. Model Evaluation Guidelines for Systematic Quantification of Accuracy in Watershed Simulations. **Transactions of the ASABE**, v. 50, n. 3, p. 885–900, 2007.

MUÑOZ-SABATER, J. **ERA5-Land hourly data from 1981 to presentCopernicus Climate Change Service (C3S) Climate Data Store (CDS)**, 2019. Disponível em: <https://cds.climate.copernicus.eu/cdsapp#!/dataset/10.24381/cds.e2161bac?tab=overview>. Acesso em: 14 jul. 2021

MUÑOZ-SABATER, J. **ERA5-Land hourly data from 1950 to 1980Copernicus Climate Change Service (C3S) Climate Data Store (CDS)**, 2021. Disponível em: <https://cds.climate.copernicus.eu/cdsapp#!/dataset/reanalysis-era5-land?tab=overview>

MUÑOZ-SABATER, J. et al. ERA5-Land: a state-of-the-art global reanalysis dataset for land applications. **Earth System Science Data,** v. 13, n. 9, p. 4349–4383, 7 Sep 2021.

MYERS, N. et al. Biodiversity hotspots for conservation priorities. **Nature**, v. 403, n. 6772, p. 853–858, Feb 2000.

NEITSCH, S. L. et al. **Soil & Water Assessment Tool Theoretical Documentation: Version 2009.** Texas.

NEW, M. et al. A high-resolution data set of surface climate over global land areas. **Climate Research**, v. 21, n. 1, p. 1–25, 2002.

NOGUEIRA, S. M. C.; MOREIRA, M. A.; VOLPATO, M. M. L. Evaluating precipitation estimates from Eta, TRMM and CHRIPS data in the south-southeast region of Minas Gerais state-Brazil. **Remote Sensing**, v. 10, n. 2, p. 313–329, 2018.

NUNES, Y. R. F. et al. Pandeiros: o Pantanal Mineiro. MG.Biota, v. 2, n. 2, p. 4–17, 2009.

OLIVEIRA, P. T. S. et al. Trends in water balance components across the Brazilian Cerrado. **Water Resources Research**, v. 50, n. 9, p. 7100–7114, Sep 2014.

OLIVEIRA, V. A. et al. Modeling the effects of climate change on hydrology and sediment load in a headwater basin in the Brazilian Cerrado biome. **Ecological Engineering**, v. 133, p. 20–31, Aug 2019.

PENMAN, H. L. Evaporation: An introductory survey. **Netherlands Journal of Agricultural Sciences**, 1956.

POLI, P. et al. ERA-20C: An atmospheric reanalysis of the twentieth century. **Journal of Climate**, v. 29, n. 11, p. 4083–4097, 2016.

PONTES FILHO, J. D. et al. Copula-Based Multivariate Frequency Analysis of the 2012–2018 Drought in Northeast Brazil. **Water**, v. 12, n. 3, p. 834, 16 Mrt 2020.

PRADO, L. F. et al. Changes in summer precipitation variability in central Brazil over the past eight decades. **International Journal of Climatology**, v. 41, n. 8, p. 4171–4186, 2021.

ROCHA JÚNIOR, R. L. et al. Bivariate assessment of drought return periods and frequency in brazilian northeast using joint distribution by copula method. **Geosciences**, v. 10, n. 4, p. 135, 2020.

RODRIGUES, J. A. M. et al. Climate change impacts under representative concentration pathway scenarios on streamflow and droughts of basins in the Brazilian Cerrado biome. **International Journal of Climatology**, p. 1–16, 28 Okt 2019.

ROZANTE, J. R. et al. Evaluation of TRMM/GPM Blended Daily Products over Brazil. **Remote Sensing**, v. 10, n. 6, p. 1–17, 2018.

SANTOS, U. et al. Fish fauna of the Pandeiros River, a region of environmental protection for fish species in Minas Gerais state, Brazil. **Check List**, v. 11, n. 1, p. 1507, 1 Jan 2015.

SHIAU, J. T. Fitting Drought Duration and Severity with Two-Dimensional Copulas. **Water Resources Management**, v. 20, n. 5, p. 795–815, 27 Okt 2006.

SILVA, VI. O.; MELLO, C. R. Meteorological droughts in part of southeastern Brazil: Understanding the last 100 years. **Anais da Academia Brasileira de Ciências**, v. 93, n. suppl 4, p. 1–17, 2021.

SKLAR, A. Fonctions de repartition a ‘n dimensions et leur marges. **Publications de Institut de Statistique Université de Paris**, 1959.

SMITH, K. A. et al. A multi-objective ensemble approach to hydrological modelling in the UK: an application to historic drought reconstruction. **Hydrology and Earth System Sciences**, v. 23, n. 8, p. 3247–3268, 8 Aug 2019.

SOIL CONSERVATION SERVICE (SCS). **National engineering handbook, section 4, hydrology**. USDA, 1972.

SOUZA, C. M. et al. Reconstructing Three Decades of Land Use and Land Cover Changes in Brazilian Biomes with Landsat Archive and Earth Engine. **Remote Sensing**, v. 12, n. 17, p. 2735, 25 Aug 2020.

SVOBODA, M. et al. The drought monitor. **Bulletin of the American Meteorological Society**, v. 83, n. 8, p. 1181–1190, Aug 2002.

TAREK, M.; BRISSETTE, F. P.; ARSENAULT, R. Evaluation of the ERA5 reanalysis as a potential reference dataset for hydrological modelling over North America. **Hydrology and Earth System Sciences**, v. 24, n. 5, p. 2527–2544, 2020.

TEUTSCHBEIN, C.; SEIBERT, J. Bias correction of regional climate model simulations for hydrological climate-change impact studies : Review and evaluation of different methods. **Journal of Hydrology**, v. 456–457, p. 12–29, 2012.

UNIYAL, B. et al. Simulation of regional irrigation requirement with SWAT in different agro-climatic zones driven by observed climate and two reanalysis datasets. **Science of The Total Environment**, v. 649, p. 846–865, 2019.

VICENTE-SERRANO, S. M. et al. Accurate Computation of a Streamflow Drought Index. **Journal of Hydrologic Engineering**, v. 17, n. 2, p. 318–332, Feb 2012.

WILLIAMS, J. R. Flood Routing With Variable Travel Time or Variable Storage Coefficients. **Transactions of the ASAE**, v. 12, n. 1, p. 100–103, 1969.

XAVIER, A. C.; KING, C. W.; SCANLON, B. R. Daily gridded meteorological variables in Brazil (1980–2013). **International Journal of Climatology**, v. 36, n. 6, p. 2644–2659, 2016.

YEVJEVICH, V. M. Objective approach to definitions and investigations of continental hydrologic droughts. **Hydrology papers (Colorado State University)**, p. 25, 1967.

CONSIDERAÇÕES FINAIS

A BHRP apresenta uma elevada importância ecológica para a bacia do rio São Francisco e para o bioma Cerrado, uma vez que a reprodução e desenvolvimento de diversas espécies de peixe nativos acontecem no interior dessa bacia. Diante disso, em 1995 foi criada a Área de Preservação Ambiental de Pandeiros, com o intuito de preservar a fauna e a flora da região. Portanto, estudos hidrológicos na BHRP podem melhorar o entendimento do comportamento hidrológico e auxiliar em uma melhor gestão dos recursos hídricos na região.

Os resultados da presente tese foram subdivididos em três artigos. No Artigo 1 objetivou-se caracterizar o comportamento hidrológico e a ocorrência de secas meteorológica e hidrológica na BHRP. A precipitação média anual na bacia foi 1085 mm, sendo que 81,4% retorna à atmosfera por meio da evapotranspiração e 14,9% é utilizado na recarga dos aquíferos. Destaca-se ainda que a bacia possui uma elevada capacidade de regularização natural, com SY7,10 igual a 33% do SYmean e coeficiente de depleção próximo a zero (α = 0,0073). Foi observado uma maior duração da seca hidrológica em relação à meteorológica. Esse comportamento pode ser explicado por uma redução no armazenamento de água subterrânea provocado pela redução da precipitação e aumento da temperatura, uma vez que o escoamento subterrâneo é responsável por 80% do escoamento total na bacia (BFI = 0,8).

No Artigo 2 foi avaliada a qualidade de dois produtos de precipitação por satélite (TMPA e IMERG) e sua aplicabilidade para a modelagem hidrológica da BHRP. A análise da qualidade do TMPA e do IMERG foi realizada com base em dados observados pela metodologia point-to-pixel em escala diária e mensal. Foram obtidos melhores resultados para o IMERG, com PBIAS igual a 6,3%, r de 0,45 (diário) e 0,88 (mensal), e RMSE de 9,5 mm (diário) e 57 mm (mensal). Na modelagem hidrológica com o SWAT, o IMERG apresentou melhor desempenho (NSE = 0,81, LNSE = 0,75 e PBIAS = -10,2%) e menor incerteza (p-fator = 0,79 e r fator = 1,09) em relação ao TMPA (NSE = 0,71, LNSE = 0,68, PBIAS = -16,0%, p-fator = 0,76 e r fator = 1,16). Dessa forma, conclui-se que o IMERG é uma alternativa adequada para o desenvolvimento de estudos hidrológicos na BHRP.

Embora o IMERG seja um dos principais produtos de precipitação baseados em sensores remotos, principalmente após a descontinuidade do TMPA a partir de 2019, sugere-se que estudos futuros investiguem outros produtos de precipitação por satélite, como o Precipitation Estimation from Remotely Sensed Information using Artificial Neural Networks - Climate Data Record (PERSIANN-CDR), e também grids de dados interpolados, como o de Xavier et al. (2016) (https://doi.org/10.1002/joc.4518), os quais também fornecem dados pluviométricos com resolução espacial e temporal adequados para estudos hidrológicos.

No Artigo 3 foi estudada a qualidade da estimativa da precipitação por dois produtos de reanálise climática: o ERA-20CM e o ERA5-Land, sendo que este último proporcionou desempenho superior em escala diária (r = 0,43, RMSE = 9,1 mm.dia-1 e KGE = 0,36) e mensal (r = 0,89, RMSE = 56,1 mm.mês-1 e KGE = 0,86). Os produtos de reanálise climática foram validados para a simulação hidrológica na BHRP utilizando o SWAT no período de 1981 a 2010. Apenas o ERA5-Land apresentou desempenho adequado na simulação da vazão no período de validação, tendo sido obtido NSE = 0,53 e PBIAS = 5,5%. Por fim, foi feita a validação da seca utilizando o SSI calculado com base em dados observados e simulados de vazão, onde o ERA5-Land apresentou melhor desempenho na predição das secas (cinco de seis eventos observados).

A retrospectiva hidrológica foi realizada de 1950 a 2018, utilizando o ERA5-Land como dado pluviométrico de entrada, bem como a análise de secas históricas na bacia. A análise dos dados de vazão simulados para o período de 1950 a 2018 mostrou um prognóstico de aumento na frequência de meses secos e redução de meses úmidos nas últimas décadas, o que também foi observado em outros estudos no Brasil utilizando dados observados, o que comprova a capacidade da metodologia adotada na predição das secas.

Embora as reanálises climáticas sejam uma importante alternativa para estudos hidrológicos em regiões com baixa densidade e séries históricas curtas de dados pluviométricos observados, esses produtos apresentam algumas limitações. Uma das principais limitações está relacionada à maior incerteza na estimativa da precipitação para períodos mais distantes. Dessa forma, a validação das reanálises climáticas para todo o período analisado é recomendada, porém, esbarra na indisponibilidade de dados observacionais. Diante desta constatação, recomenda-se a elaboração de estudos futuros em bacias hidrográficas com disponibilidade de observações que possibilitem validar as reanálises para todo o período estudado, o que possibilitaria conclusões mais abrangentes sobre a assertividade desses produtos.

Além disso, foram utilizados dados climáticos do CRU que, embora sejam baseados em dados observados, os mesmos fornecem esses dados em escala mensal, diferentemente do SWAT que requer dados em escala diária. Embora essa metodologia esteja respaldada na literatura, recomenda-se para estudos futuros a utilização de dados meteorológicos diários, caso estes estejam disponíveis.

Por fim, existe também a limitação relacionada ao uso do solo, o qual é mantido fixo ao longo do período de modelagem hidrológica. No entanto, essa limitação é minimizada na BHRP, uma vez que a bacia está inserida em uma Área de Preservação Ambiental. Conclui-se que, diante das limitações identificadas e aqui descritas, o desenvolvimento de pesquisas que

possibilitem o aperfeiçoamento da retrospectiva hidrológica é de grande relevância para a ciência hidrológica, com vistas à modelagem de bacias no período prévio ao início do monitoramento, ou mesmo, para bacias não monitoradas.